VALIDATION OF NEW APPROACHES FOR MEASURING UV INACTIVATION KINETICS OF ENTERIC ADENOVIRUSES IN WATER

by

NING DING ©

A thesis submitted to the Faculty of Graduate Studies and Research in partial fulfillment
of the requirements for the degree of MASTER OF SCIENCE
in
ENVIRONMENTAL SCIENCE

DEPARTMENT OF CIVIL AND ENVIRONMENTAL ENGINEERING

EDMONTON, ALBERTA
SPRING, 2008

Library and
Archives Canada

Published Heritage
Branch

395 Wellington Street
Ottawa ON K1A 0N4
Canada

Bibliothèque et
Archives Canada

Direction du
Patrimoine de l'édition

395, rue Wellington
Ottawa ON K1A 0N4
Canada

Your file Votre référence
ISBN: 978-0-494-45802-0
Our file Notre référence
ISBN: 978-0-494-45802-0

NOTICE:
The author has granted a non-exclusive license allowing Library and Archives Canada to reproduce, publish, archive, preserve, conserve, communicate to the public by telecommunication or on the Internet, loan, distribute and sell theses worldwide, for commercial or non-commercial purposes, in microform, paper, electronic and/or any other formats.

The author retains copyright ownership and moral rights in this thesis. Neither the thesis nor substantial extracts from it may be printed or otherwise reproduced without the author's permission.

AVIS:
L'auteur a accordé une licence non exclusive permettant à la Bibliothèque et Archives Canada de reproduire, publier, archiver, sauvegarder, conserver, transmettre au public par télécommunication ou par l'Internet, prêter, distribuer et vendre des thèses partout dans le monde, à des fins commerciales ou autres, sur support microforme, papier, électronique et/ou autres formats.

L'auteur conserve la propriété du droit d'auteur et des droits moraux qui protège cette thèse. Ni la thèse ni des extraits substantiels de celle-ci ne doivent être imprimés ou autrement reproduits sans son autorisation.

In compliance with the Canadian Privacy Act some supporting forms may have been removed from this thesis.

While these forms may be included in the document page count, their removal does not represent any loss of content from the thesis.

Conformément à la loi canadienne sur la protection de la vie privée, quelques formulaires secondaires ont été enlevés de cette thèse.

Bien que ces formulaires aient inclus dans la pagination, il n'y aura aucun contenu manquant.

Canada

ABSTRACT

Enteric adenoviruses have been found in water and wastewater and induce gastroenteric illness. There is no standard method to analyze UV inactivation of enteric adenoviruses. Cytopathic effect (CPE) based traditional cell culture infectivity assay has been used and accepted in most studies. In this study, it was demonstrated that the method of cell culture integrated with real-time quantitative RT-PCR was capable to analyze UV inactivation of adenovirus 41. The methods of direct real-time quantitative PCR/RT-PCR, and cell culture integrated with real-time quantitative PCR were not reliable to analyze UV inactivation of adenovirus 41. Real-time quantitative RT-PCR was able to give the quantitative results without additional gel electrophoresis. RT-CES™ could not reliably quantify the UV inactivation of adenovirus 41 on experiment conditions tested. The results suggest that cell culture integrated with real-time quantitative RT-PCR could substitute CPE based infectivity assay for analysis UV inactivation of enteric adenoviruses.

DEDICATION

To my dearest mother for her never stopped spiritual support, sincere love, and constant encouragement.

ACKNOWLEDGEMENTS

I would like to express my sincere gratitude to my supervisor Dr. Stephen A. Craik, for his professional guidance, support, feedback and encouragement throughout the course of the project.

I am grateful to my co-supervisor Dr. Xiaoli Lilly Pang who gave immensely technical support on molecular part of the project. Without her knowledgeable guidance, all the work would not progress smoothly.

I would also like to thank my graduate supervisor Dr. Daryl M. McCartney, for his valuable suggestions on thesis writing.

The technical assistance provided by Kimberly Martin is greatly appreciated. Many thanks to Li Xie who gave generous help on the use of RT-CES™ system. My appreciation also goes to Min Cao, for her friendship, advice and encouragement. Special thanks to Dr. Bonita Lee, for her theoretical and technical assistance. Thanks to my company Qingsheng Ke, Heejin Kang, for sharing information and opinions.

The funding of this project has been provided by Alberta Ingenuity Center for Water Research, the Natural Science and Research Council (NSERC). This is a collaborative project between Department of Civil and Environmental Engineering in University of Alberta and Alberta Provincial Laboratory for Public Health.

Table of Contents

CHAPTER 1 INTRODUCTION **1**

1.1 BACKGROUND 1

1.2 RESEARCH OBJECTIVES 5

1.3 SCIENTIFIC HYPOTHESIS 6

1.4 OVERVIEW OF THE STUDY 7

1.5 ORGANIZATION OF THE THESIS 8

CHAPTER 2 LITERATURE REVIEW **10**

2.1 BACKGROUND OF ENTERIC ADENOVIRUSES 10

2.1.1 Structure and the Cell Entry Mechanisms *10*

2.1.2 Health Effects *11*

2.2 CELL CULTURE 12

2.3 ANALYTICAL METHODS 15

2.3.1 Infectivity Assays *16*

2.3.2 Molecular Techniques *18*

2.3.3 Real-time Cell Electronic Sensing (RT-CES^{TM}) System *26*

2.4 UV DISINFECTION 27

2.4.1 History and Regulations *27*

2.4.2 The Germicidal Nature of UV *29*

2.4.3 Mechanisms of Microbial Inactivation by UV *30*

2.4.4 UV Collimated Beam Apparatus *32*

2.4.5 Determination of UV Dose *34*

2.4.6 Inactivation of Enteric Adenoviruses *36*

2.5 CONCLUSION 40

CHAPTER 3 CELL CULTURE OF AD41 ON HEP-2 AND A549 CELLS ANALYZED WITH REAL-TIME QUANTITATIVE RT-PCR **43**

3.1 INTRODUCTION 43

3.2 MATERIALS AND METHODS 44

3.2.1 Cells and Viruses *44*

3.2.2 Virus Propagation 44
3.2.3 Assay of Adenovirus 41 46
3.3 RESULTS AND DISCUSSIONS 48
3.3.1 Clinical Stool Samples Cultured on Hep-2 and A549 Cells 48
3.3.2 Cell Culture (stool sample VC6536) and Virus Passage on Hep-2 Cells 51
3.3.3 Comparison of mRNA and DNA in the Supernatant 54
3.3.4 Consistency of Taqman® RT-PCR 55
3.4 CONCLUSION 57
CHAPTER 4 COMPARISON OF MOLECULAR METHODS TO THE CPE BASED CELL CULTURE INFECTIVITY ASSAYS FOR DETERMINING UV INACTIVATION OF AD41 59
4.1 INTRODUCTION 59
4.2 MATERIALS AND METHODS 63
4.2.1 Cell Culture 63
4.2.2 Virus Purification 65
4.2.3 UV Exposure 66
4.2.4 Exposure Time and Fluence Rate Determination and Control 68
4.2.5 Set-up of UV Inactivation of Ad41 Experiments 70
4.2.6 Assay of Ad41 after UV Inactivation 70
4.3 RESULTS 73
4.3.1 UV Inactivation Measured by cell culture CPE Based TCID$_{50}$ 73
4.3.2 UV Inactivation Measured by Direct Taqman® PCR and RT-PCR 76
4.3.3 UV Inactivation of Ad41 Measured by Integrated Cell Culture Taqman® PCR or RT-PCR 80
4.3.4 Comparison of Cell Culture CPE Based Infectivity Assay and Molecular Methods for Measuring Ad41 Inactivation by UV 83
4.4 DISCUSSION 86
4.4.1 UV Inactivation of Ad41 86
4.4.2 Correlation between CPE based Cell Culture Infectivity Assay and Direct Taqman® PCR/RT-PCR 91

4.4.3 Correlation between CPE based Cell Culture Infectivity Assay and Integrated Cell Culture Real-time Quantitative RT-PCR *92*
4.4.4 Comparison of UV Inactivation of Purified and Unpurified Ad41 .... *93*
4.5 CONCLUSION 94

CHAPTER 5 DETECTION OF UV INACTIVATION OF AD41 WITH RT-CES^{TM} SYSTEM **97**

5.1 INTRODUCTION 97
5.2 MATERIALS AND METHODS 97
5.2.1 RT-CES^{TM} System *97*
5.2.2 Cell Index (CI) *100*
5.2.3 Cell Culture and Cell Count *100*
5.2.4 Cell Quantification *102*
5.2.5 Sample loading *103*
5.3 RESULTS AND DISCUSSION 103
5.3.1 Propagation of Ad41 on HEK293 Cells *103*
5.3.2 Propagation of Ad41 on Hep-2 Cells *110*
5.4 CONCLUSIONS AND RECOMMENDATIONS 111

CHAPTER 6 CONCLUSIONS AND RECOMMENDATIONS **113**

6.1 CONCLUSIONS 113
6.2 RECOMMENDATIONS 115

REFERENCES **117**

APPENDIX A **122**

APPENDIX B **131**

APPENDIX C **153**

List of Tables

Table 3.1 Sequences and location of primers and probes for detection of enteric adenovirus by Taqman® PCR 47

Table 3.2 Condition of stool samples cultured on Hep-2 and A549 cell lines 51

Table 3.3 Ct (threshold cycle) value of cell cultures 53

Table 3.4 Comparison of viral mRNA, viral DNA and residual DNA after digestion in supernatant 55

Table 3.5 RT-PCR results of three measurements 56

Table 4.1 UV inactivation of purified and unpurified Ad41 detected by cell culture CPE based $TCID_{50}$ 74

Table 4.2 Ad41 initial titers before UV exposure in each experiment 75

Table 4.3 Calculation of UV inactivation of Ad41 analyzed by direct Taqman® RT-PCR 79

Table 4.4 Calculation of UV inactivation of Ad41 at UV dose of 80 mJ/cm^2 analyzed by direct Taqman® RT-PCR 80

Table 4.5 Experimental procedures and analysis methods in previous studies and this study on UV inactivation of enteric adenovirus 89

Table B-1 CPE track of 11 clinical stool samples cultured on Hep-2 cell line. 131

Table B-2 CPE track of 11 clinical stool samples cultured on A549 cell line. 131

Table B-3 CPE track of 10 stool samples blind passage on Hep-2 cell line. 132

Table B-4 CPE track of 9 stool samples blind passage on A549 cell line. 132

Table B-5 CPE track of 8 stool samples 2nd blind passage on Hep-2 cells. 132

Table B-6 CPE track of 8 stool samples 2nd blind passage on A549 cells 133

Table B-7 The titer of Ad41 of non-UV exposure negative control under 40 mJ/cm^2 134

Table B-8 The titer of Ad41 of non-UV exposure negative control under 320 mJ/cm^2 134

Table B-9 The titer of Ad41 under exposure of UV dose of 40 mJ/cm^2 134

Table B-10 The titer of Ad41 under exposure of UV dose of 80 mJ/cm^2 135

Table B-11 The titer of Ad41 under exposure of UV dose of 160 mJ/cm^2 135

Table B-12 The titer of Ad41 under exposure of UV dose of 320 mJ/cm^2............ 135

Table B-13 Inactivation of Ad41 under UV dose of 40, 80, 160 and 320 mJ/cm^2 . 136

Table B-14 The titer of Ad41 of non-UV exposure negative control 136

Table B-15 The titer of Ad41 under exposure of UV dose of 40 mJ/cm^2............... 137

Table B-16 The titer of Ad41 under exposure of UV dose of 80 mJ/cm^2............... 137

Table B-17 The titer of Ad41 under exposure of UV dose of 160 mJ/cm^2............. 137

Table B-18 The titer of Ad41 under exposure of UV dose of 320 mJ/cm^2............. 138

Table B-19 Inactivation of Ad41 under UV dose of 40, 80, 160 and 320 mJ/cm^2 . 138

Table B-20 The titer of Ad41 of non-UV exposure negative control under 40 mJ/cm^2 139

Table B-21 The titer of Ad41 of non-UV exposure negative control under 320 mJ/cm^2 139

Table B-22 The titer of Ad41 under exposure of UV dose of 40 mJ/cm^2............... 139

Table B-23 The titer of Ad41 under exposure of UV dose of 80 mJ/cm^2............... 140

Table B-24 The titer of Ad41 under exposure of UV dose of 160 mJ/cm^2............. 140

Table B-25 The titer of Ad41 under exposure of UV dose of 320 mJ/cm^2............. 140

Table B-26 Inactivation of Ad41 under UV dose of 40, 80, 160 and 320 mJ/cm^2 . 141

Table B-27 The titer of Ad41 of non-UV exposure negative control 142

Table B-28 The titer of Ad41 under exposure of UV dose of 40 mJ/cm^2............... 142

Table B-29 The titer of Ad41 under exposure of UV dose of 80 mJ/cm^2............... 142

Table B-30 The titer of Ad41 under exposure of UV dose of 160 mJ/cm^2............. 143

Table B-31 The titer of Ad41 under exposure of UV dose of 320 mJ/cm^2............. 143

Table B-32 Inactivation of Ad41 under UV dose of 40, 80, 160 and 320 mJ/cm^2 . 144

Table B-33 Titration for the titer of Ad41 used in experiment 1 144

Table B-34 Titration for the titer of Ad41 used in experiment 2 145

Table B-35 Titration for the titer of Ad41 used in experiment 3 145

Table B-36 Titration for the titer of Ad41 used in experiment 4 145

Table B-37 Threshold Ct results for UV inactivated unpurified and purified Ad41 analyzed by direct Taqman® RT-PCR and PCR 146

Table B-38 The logarithm of viral titer results for UV inactivated unpurified and purified Ad41 by direct Taqman® RT-PCR and PCR..................................... 147

Table B-39 Inactivation of unpurified and purified Ad41 analyzed by direct Taqman® RT-PCR and PCR 148

Table B-40 Threshold Ct results for UV inactivated unpurified and purified Ad41 analyzed by integrated cell culture Taqman® RT-PCR and PCR of experiment 1 149

Table B-41 Threshold Ct results for UV inactivated unpurified and purified Ad41 analyzed by integrated cell culture Taqman® RT-PCR and PCR of experiment 2 150

Table B-42 Threshold Ct results for UV inactivated unpurified and purified Ad41 analyzed by integrated cell culture Taqman® RT-PCR and PCR of experiment 3 151

Table B-43 Threshold Ct results for UV inactivated unpurified and purified Ad41 analyzed by integrated cell culture Taqman® RT-PCR and PCR of experiment 4 152

Table C-1 $TCID_{50}$ endpoints determination factors 153

Table C-2 Data for 50% infectivity end point determination 154

Table C-3 Data for ANOVA of direct Taqman® PCR to analyze UV inactivation of Ad41 155

Table C-4 ANOVA of direct Taqman® RT-PCR to analyze UV inactivation of unpurified and purified Ad41 156

Table C-5 ANOVA of direct Taqman® PCR to analyze UV inactivation of unpurified and purified Ad41 156

Table C-6 ANOVA of direct Taqman® PCR to analyze UV inactivation of unpurified and purified Ad41 157

Table C-7 Data for ANOVA of integrated cell culture Taqman® RT-PCR to analyze UV inactivation of unpurified and purified Ad41 158

Table C-8 ANOVA of integrated cell culture Taqman® RT-PCR to analyze UV inactivation of unpurified and purified Ad41 159

Table C-9 Data for ANOVA of integrated cell culture Taqman® RT-PCR to analyze UV inactivation of unpurified and purified Ad41 160

Table C-10 ANOVA of integrated cell culture Taqman® PCR to analyze UV inactivation of unpurified and purified Ad41 161

Table C-11 Data for ANOVA of integrated cell culture Taqman® PCR and cell culture CPE based $TCID_{50}$ to analyze UV inactivation of unpurified and purified Ad41 162

Table C-12 ANOVA of integrated cell culture Taqman® PCR and cell culture CPE based $TCID_{50}$ to analyze UV inactivation of unpurified and purified Ad41 163

Table C-13 Data for ANOVA of integrated cell culture Taqman® RT-PCR and cell culture CPE based $TCID_{50}$ to analyze UV inactivation of unpurified and purified Ad41 164

Table C-14 ANOVA of integrated cell culture Taqman® RT-PCR and cell culture CPE based $TCID_{50}$ to analyze UV inactivation of unpurified and purified Ad41 165

List of Figures

Figure 2.1 Electromagnetic spectrums (USEPA, 2006) 30
Figure 2.2 UV absorbance of nucleotides (Adapted from USEPA, 2006) 31
Figure 2.3 UV absorbance of DNA 31
Figure 2.4 Draft of Bench scale device of UV inactivation experiments 33
Figure 3.1 Flowchart of passage of stool sample VC6536 on Hep-2 and A549 Cells 52
Figure 4.1 Collimated beam apparatus 67
Figure 4.2 UV inactivation of Ad41 versus UV dose response curve tested by cell culture CPE based $TCID_{50}$ 75
Figure 4.3 Standard curve of the viral copies/PCR versus Ct (threshold cycle) of adenovirus for Taqman® PCR. 77
Figure 4.4 UV inactivation of Ad41 as measured by direct Taqman® PCR and RT-PCR. 78
Figure 4.5 UV inactivation of Ad41 as function of UV dose as measured by HEK293 cell culture with Taqman® RT-PCR detection. 82
Figure 4.6 UV inactivation of Ad41 as a function of UV dose as measured by HEK293 cell culture with Taqman® PCR detection. 83
Figure 4.7 Comparison of cell culture with CPE and cell culture integrated with Taqman® RT-PCR for measuring UV inactivation of unpurified Ad41 (raw data in Appendix B, table B-40 to B-43). 84
Figure 4.8 Comparison of cell culture with CPE and cell culture integrated with Taqman® RT-PCR for measuring UV inactivation of purified Ad41 raw data in Appendix B, table B-40 to B-43). 84
Figure 4.9 UV inactivation of enteric adenovirus reported in previous studies and this study. 86
Figure 5.1 RT-CES™ System work station 98
Figure 5.2 E-Plates and cell electronic sensing system 99
Figure 5.3 Hemocytomer counting grid 101

Figure 5.4 Cell Index versus time curve for different sizes of HEK293 cells inoculated into the E-plates. 104
Figure 5.5 Growth of HEK293 cells inoculated with UV exposed Ad41 as monitored by RT-CES™ 105
Figure 5.6 Growth of HEK293 cells inoculated with 10 times diluted UV exposed Ad41 as monitored by RT-CES™. 106
Figure 5.7 Growth of Ad41 infected HEK293 cells with and without PPL adhesion coating on RT-CES™. 108
Figure 5.8 Growth of Hep-2 cells inoculated with different dilutions of Ad41 in RT-CES™. 110
Figure A-1 DFA stained Ad41 infected HEK293 cells 125
Figure A-2 ABI PRISM 7000 Sequence Detection System (Applied Biosystems) 128
Figure A-3 Standard curve 129
Figure A-4 Cycle number versus ΔRn curve 129
Figure C-1 n-score of residuals plot of ANOVA of Direct Taqman® RT-PCR 155
Figure C-2 n-score of residuals plot of ANOVA Direct Taqman® PCR 157
Figure C-3 n-score of residuals Cell culture integrated Taqman® RT-PCR 158
Figure C-4 n-score of residuals Cell culture integrated Taqman® PCR 160
Figure C-5 n-score of residuals Cell culture CPE based $TCID_{50}$ and integrated cell culture Taqman® PCR in detection of UV inactivated purified and unpurified Ad41 163
Figure C-6 n-score of residuals Cell culture CPE based $TCID_{50}$ and integrated cell culture real-time quantitative RT-PCR in detection of UV inactivated purified and unpurified Ad41 165

List of Abbreviations

®	The trademark is registered
ABI	Applied Biosystems
ANOVA	Analysis of variance
ATCC	American Type Culture Collection
Ad40	Adenovirus type 40
Ad41	Adenovirus type 41
bp	Blind passage
CAR	Coxsackie and Adenovirus receptor
CCL	Contaminant candidate list
CI	Cell index
CPE	Cytopathic effects
Ct	Threshold Cycle
DFA	Direct Immunofluorescent Assay
DNA	Deoxyribonucleic Acid
DNase I	Deoxyribonuclease I
ECM	Extracellular matrix
EM	Electron Microscope
FBS	Fetal bovine serum
FCV	Feline calicivirus
FITC	Fluorescein isothiocyanate
FRET	Fluorescence resonance energy transfer
GEC	Genomic equivalent copies
HBS	Horse bovine serum
HDF	Human diploid fibroblasts
HEK	Human embryonic kidney
HEPES	4-(2-hydroxyethyl)-1-piperazineethanesulfonic acid
LT2ESWTR	Long Term 2 Enhanced Surface Water Treatment Rule
MEM	Minimum essential medium

MEM-T	Minimum essential medium containing trypsin
MPN	Most probable number
mRNA	Messenger ribonucleic acid
p	Passage
PBS	Phosphate buffered saline buffer
PCR	Polymerase chain reaction
PLPH	Provincial Laboratory for Public Health
PPL	Poly-L-Lysine
RGD	Arg-Gly-Asp
RT-CES	Real-time cell electronic sensing
RT-PCR	Reverse-transcription polymerase chain reaction
$TCID_{50}$	50% tissue cell culture infective dose
TM	Trademark
USEPA	United States Environmental Protection Agency
UV	Ultraviolet

Units

°C	Degree Celsius
cm	Centimeters
h	Hour
W	Watt
mJ/cm^2	Mill Joule per square centimeters
nm	Nanometer
%	Percent
h	Hour
mL	Milliliter
cm^{-1}	Per square centimeter
µg/mL	Microgram per milliliter
IU	Infectious Unit
µL	Micro liter
U/µL	Proteinase unit per micro liter
min	minute
s	Second
µm	Micro meter
× g	Times gravity
mL/min	Milliliter per minute
mm	Millimeter
rpm	Centrifuge rotor speed
log	Logarithm
mW/cm^2	Mill watt per square centimeters
cm^2	square centimeters

Chapter 1 Introduction

1.1 Background

During the 1990s and early 2000s, the drinking water industry in North America placed significant emphasis on development of disinfection criteria. Because of improvement of water treatment technologies and the use of water quality indicators, the number of reported waterborne outbreaks has declined over the past hundred years. In spite of the decline, waterborne outbreaks still occur. It is reported that 10% of the waterborne outbreaks in the United Stated are associated with viruses. However, the proportion is estimated to be higher. A large percentage of waterborne outbreaks in the United States are not etiologically known and are suspected to be originated from viruses (Fout 2003).

Enteric viruses are ubiquitous agents, mostly inducing silent infections (Carter 2005). They are drawn from a variety of virus families, ranging 10-fold in diameter and 20-fold in terms of genome size and complexity. Enteric viruses present a special challenge to water treatment processes because they survive well in the environment once released from an infected host and are thus found in municipal wastewaters, surface water and groundwater. They are not completely removed by conventional filtration processes due to their small size, and they are more resistant to disinfection than bacterial indicators. Both US and Alberta regulations have set standards that state that water treatment processes should be able to provide 99.99% removal or inactivation of enteric viruses by ensuring adequate disinfection and/or physical removal.

Adenoviruses are non-enveloped, icosohedral, double-stranded deoxyribonucleic acid (DNA) viruses (80-110 nm in diameter). Human adenoviruses are classified into six species (A-F). Adenovirus 40 and 41 (species F) are included in enteric adenoviruses which are important etiological agents of pediatric gastroenteritis (Ko et al. 2005a), and have been perceived to be the most prevalent adenovirus in water system (Jothikumar et al. 2005). Enteric adenoviruses are reported to cause 5-20% of the infant and child acute gastroenteritis in developing countries and pose a high pathogenic opportunity in immunization compromised patients, thus have been placed on the United States Environmental Protection Agency (USEPA) contaminant candidate list (CCL) (Meng and Gerba 1996; USEPA 1998). Transmission of enteric adenoviruses in drinking water has been documented. In addition, enteric adenoviruses have been detected in surface water, wastewater and UV-irradiated wastewater (Baxter et al. 2007).

Identification and quantification of enteric adenovirus methods can be achieved by viral culture based infectivity assays, molecular techniques and methods that integrate these techniques. Infectivity methods involve inoculating the viral sample onto host cells and then allowing virus replication to progress to the point that visible signs of cell infection occur. Usually these visible signs are cytopathic effects (CPE). CPE refers to degenerative changes in cells associated with the multiplication of certain viruses. However, because adenovirus 40 and 41 grow slowly in cell culture, it usually takes up to 7-10 days to produce CPE. Sometimes, they do not produce clear and consistent CPE (Ko et al. 2005a). Molecular methods such as PCR, RT-PCR, and probe hybridization have been used to detect adenoviruses because of their rapidity, sensitivity and specificity. However, there are a number of limitations of conventional nucleic acid amplification techniques. Detection by PCR indicates only the presence of nucleic acid which includes viral DNA with and without infectious ability. It may not provide any information on infectivity, which is of primary interest for evaluating risks to public health (Ko et al. 2005a). It has been shown that the ratio of adenovirus 41 viral particles to infectious units is high ($\sim 10^5$) (Brown et al. 1992), thus it is difficult to estimate virus infectivity by PCR. Integrated methods combine cell culture infectivity assays with molecular methods, and thus are able to detect viruses that do not produce CPE. These methods are able to detect specific serotypes and enable post-assay genotyping of infectious viruses (Yates et al. 2006). To avoid false positive determination of adenovirus 41 infectivity, messenger ribonucleic acid (mRNA) extracted from infected cells can be detected by application of RT-PCR following cell culture. This approach reflects viral infectivity because only infectious adenovirus can enter cells and transcribe mRNA during replication (Ko et al. 2003; Ko et al. 2005a).

Although the number of published research studies on viral inactivation has increased in recent years, significant knowledge gaps exist. For many enteric viruses, inactivation by traditional disinfectants, such as chlorine and monochloramine, and alternative disinfectants, such as ultraviolet (UV), is not well characterized. One of the reasons for this knowledge gap is that many human enteric viruses are not easily cultured in the laboratory and traditional cell culture assays based on observation of cytopathic effects (CPE) are difficult and time consuming.

UV disinfection has become more popular in recent years in drinking water treatment due to its capability to inactivate chlorine resistant pathogens such as *Cryptosporidium* and *Giardia* at comparatively low UV doses and short UV exposure times (Craik et al. 2001). UV dose is defined as the total radiant energy of all wavelengths passing from all directions through an infinitesimally small sphere of cross-sectional area d*A*, divided by d*A* (Bolton 2001). UV does not inactivate microorganisms by chemical reaction; therefore, it does not result in the formation of disinfection by-products as do other chemical disinfectants such as chlorine and ozone (USEPA 1999). Germicidal UV is absorbed by nucleic acids of microorganisms, which causes formation of photoproducts such as thymine dimers on the same nucleic acid strand (Ko et al. 2005b). It has been shown that adenoviral particles irradiated by UV are not capable of producing infectious progeny; however, repair of UV-induced DNA lesions occurs sometimes (Rainbow and Mak 1973). If damage is not repaired, DNA replication is blocked and the microorganism is inactivated (Ko et al. 2005b). Most viruses are more resistant to UV than are bacteria and protozoans. Enteric adenoviruses are even more UV-resistant than are other viruses (Ko et al. 2005b; Meng and Gerba 1996). Adenovirus 40 and 41 have been found to require UV doses of at least 120 mJ/cm^2 and possibly as much as 200 mJ/cm^2 to yield 4-log inactivation (Thurston-Enriquez et al. 2003a). Therefore, the USEPA has adopted a UV dose table value of 186 mJ/cm^2 for a 4-log inactivation credit in the Long Term 2 Enhanced Surface Water Treatment Rule (LT2ESWTR). The purpose of LT2ESWTR is to reduce illness linked with the contaminant *Cryptosporidium* and other disease-causing microorganisms in drinking water.

1.2 Research Objectives

The overall objective of the proposed research was to develop efficient analytical procedures for studying the kinetics of inactivation of newly emerging enteric viruses using conventional and alternative disinfectants. Real-time PCR was used in this study. Compared to conventional PCR, it shows the increase in the amount of DNA as it is amplified. This research concentrated on adenovirus 41 (Ad41) which is a type of enteric adenovirus presented in water and wastewater. UV was used in this study for inactivation experiments due to its advantages over chemical disinfectants in water and wastewater treatment. The specific goals of the research were:

a) To determine the correlation between traditional cell culture infectivity assays based on observation of CPE and direct real-time quantitative Polymerase Chain Reaction (PCR), direct real-time quantitative Reverse-Transcriptase (RT)-PCR, cell culture integrated with real-time quantitative PCR and RT-PCR in UV inactivation of Ad41.

b) To determine if a Real-Time Cell Electronic Sensing (RT-CES^{TM}) System is efficient and effective for monitoring dynamic cellular response before and after viral inoculation and can, therefore, be used as an indicator of viral infectivity in UV inactivation experiments.

1.3 Scientific Hypothesis

When germicidal UV is absorbed by Ad41, photoproducts which inhibit DNA replication are formed on the nucleic acid strand. If this damage is not repaired, viral replication is blocked and Ad41 is inactivated. Cell culture CPE observation based $TCID_{50}$ for viruses quantification is widely accepted because it reflects the infectivity of viruses; however it is laborious and not consistent due to different condition of cells and analyst bias. Molecular tests such as PCR and RT-PCR are more rapid, less labor intensive and less subjective. However, if these methods can accurately reflect virus infectivity after UV inactivation is still a research question. The hypothesis of this study is that cell culture integrated with real-time quantitative PCR/RT-PCR is able to reflect infectivity of Ad41 quantitatively after UV inactivation. Real-time RT-PCR tests the level of mRNA which is supposed to indicate the presence of infectious Ad41. Ad41 is a double stranded DNA virus, the presence of mRNA during cultivation would be indicative of viral replication. Because only infectious viruses can enter cells and reproduce mRNA. Cell culture with PCR assay may not be informative on infectivity because it has the potential to detect DNA of inactivated and thus non-infective viruses. Direct PCR was used in some studies to detect adenoviruses in environmental samples but were also doubted to be infectivity informative after UV inactivation of Ad41. In this study, analysis of UV inactivated Ad41 by direct real-time quantitative PCR and RT-PCR were also performed as comparison with traditional CPE infectivity assays.

1.4 Overview of the Study

The origins of Ad41 for this study were either clinical stool samples from the Alberta Provincial Laboratory for Public Health (PLPH) or Tak Strain from American Type Culture Collection (ATCC). It is widely reported that Ad41 is fastidious and grows poorly in conventional cell cultures that are suitable for growth of other serotypes of adenovirus. Thus it is crucial to choose an efficient cell line to propagate a large amount of Ad41 which is required in this study. Based on previous hands-on experience and literature review, it was known that the HEK293 (Graham293) cell line is an efficient culture system that can produce up to 10^{10} infectious particles/mL of Ad41 and, thus, the HEK293 cell line was adopted in this study. Hep-2 and A549 cells were also reported previously to support propagation of Ad41. This study investigated different Ad41 strains with infection on several cell lines. The infection titer of viral stocks was estimated by 50% tissue cell culture infective dose ($TCID_{50}$) analysis from observation of CPE on inoculated cell cultures since this is the traditional approach.

The UV exposure of Ad41 was carried out using a collimated beam UV apparatus, with a 10 W low pressure mercury arc lamp. The viruses were exposed to monochromatic UV at 254 nm. UV doses of 40, 80, 160 and 320 mJ/cm^2 were applied at pH 7, 25° C. Viral infectivity before and after UV exposure, and thus the level of inactivation, was determined by cell culture integrated with real-time quantitative RT-PCR, cell culture integrated with real-time quantitative PCR, direct quantitative PCR, direct quantitative RT-PCR, and cell culture CPE observation based TCID$_{50}$. The presence of infectious viral particles was also measured in terms of Cell Index (CI) which reflects cell adhesion in the RT-CES™ system.

1.5 Organization of the Thesis

The thesis is organized into six chapters. Chapter 1 provides the background of UV inactivation of enteric adenoviruses, the scientific hypothesis, objective and overview of the study. Chapter 2 reviews relevant literature on Ad41 culture, UV inactivation, analytical approaches for determining Ad41 infectivity after inactivation, and the application of RT-CES™. Chapter 3 describes the experiments and results on propagation of the isolates of Ad41 from stool samples on Hep-2 and A549 cells. Chapter 4 compares traditional cell culture based on CPE observation infectivity assay with integrated cell culture quantitative RT-PCR/PCR and direct quantitative PCR/RT-PCR, and discusses the effect of virus purification in UV inactivation.

Chapter 5 investigates the use of RT-CES^{TM} for determination of Ad41 infectivity.

Chapter 6 summarizes the findings of the thesis and proposed recommendations.

Chapter 2 Literature Review

Chapter 2 reviews relevant literature on structure and health effect of enteric adenoviruses; the selection of cell lines for culturing Ad41; viral infectivity determination methods including cytopathic effects (CPE) and molecular techniques such as PCR and RT-PCR; the theory and application of Real-Time Cell Electronic Sensing (RT-CES^{TM}) system; and UV inactivation of enteric adenoviruses.

2.1 Background of Enteric Adenoviruses

2.1.1 Structure and the Cell Entry Mechanisms

Adenoviruses are non-enveloped, double-stranded DNA viruses, infecting all vertebrate classes. They display a characteristic, icosahedral capsid architecture in which 240 subunits of the trimetric hexon protein form the facets and 12 copies of the penton. Those comprise the pentameric penton base protein and the externally projecting trimeric fiber, and form the vertices (Seiradake and Cusack 2005). The human adenoviruses serotypes are divided into 6 subgroups (A to F) on the basis of hemagglutination properties. Serotype 40 and 41 (group F) induce gastroenteric illness and these are shed in large numbers from infected cells (Carter 2005).

Adenovirus cell entry has been characterized as a two-step process. First, the fiber head domain binds to a primary cellular receptor, such as coxsackie and adenovirus receptor (CAR) in the case of serotype A and C to F. In a second step, the penton base binds to cellular integrins, triggering internalization via endocytosis. Integrin binding is mediated by an Arg-Gly-Asp (RGD) motif in the penton base that is conserved in all human adenovirus serotypes except Ad40 and Ad41. Ad40 and Ad41 do not use integrins for cell entry and may use an alternative mechanism for facilitating endocytosis. Different from other adenoviruses, enteric adenoviruses process two different fiber proteins, a long fiber which has been shown to bind CAR and a short one that does not bind CAR. It is possible that the absence of an RGD motif in the penton base and the unusual presence of a second fiber are related to the special ability of these viruses to infect cells in the human gastric system (Seiradake and Cusack 2005).

2.1.2 Health Effects

Adenoviruses 40 and 41 have been found to account for 5-20% of gastroenteritis in US hospital admissions for diarrhea, mainly in children below 2 years. The relatively large numbers of enteric adenoviruses infections that were found among infants suggests that infants may be especially likely to become infected when exposed to an enteric adenovirus (Brandt et al. 1985). Incubation lasts 3-10 days and the illness lasts a week (Carter 2005). These viruses have often been found in infant diarrhea stools and thus called enteric adenoviruses. Although not induced outbreaks, Enteric adenoviruses were found in water and wastewater.

2.2 Cell Culture

The reason that adenovirus 40 and 41 have attracted considerable attention is not only that they are important etiological agents of infantile gastroenteritis but also that they are fastidious and difficult to grow in cell culture. In 1973, an adenovirus (strain Tak) was isolated in cultured Hela cells from an infant with gastroenteritis living in the Netherlands. A number of untypable adenoviruses strains which were isolated from children with diarrhea and vomiting from the Netherlands and North-West Germany have been grown in cynomolgus monkey kidney cells and Hela cells since 1979. These viruses were difficult to isolate in the cell culture mentioned, and could not be passaged in either primary human embryonic kidney (HEK) cells or in human embryonic diploid fibroblast (HDF) cells (Dejong et al. 1983).

Adenovirus 40 and 41 failed to replicate *in vitro* on human embryonic kidney (HEK) and human diploid fibroblasts (HDF) cells. CPE was observed and infectious viruses were recovered for not more than one or two passages in these cells (Dejong et al. 1983). Adenovirus 41 is reported to be able to isolate and propagate with varying success in several cell lines which include Chang conjuctival cells, Hep-2 cells, HeLa cells, HEK293 (Graham 293) cells, cynomolgus monkey kidney (CMK) cells, PLC/PRF/5 cells and HT-29 cells (Brown 1985; Brown et al. 1984; Dejong et al. 1983; Kidd and Madeley 1981; Meng and Gerba 1996; Perronhenry et al. 1988; Pieniazek et al. 1989; Uhnoo et al. 1984). Growth depends on the virus strain, cell type, subline and batch, and other unknown factors (Dejong et al. 1983).

Strain serotype is believed to affect viral growth. Two strains (Dugan and Munster 3415 for Ad40, Tak and Glasgow 22354 for Ad41) of each serotype of Ad40 and Ad41 were used for comparison in one study (Dejong et al. 1983). The time of appearance of CPE was related to the number of viruses in the inoculum. Some strains could not be serially propagated in certain cell lines, and some strains could propagate well in certain cell lines. For example, strain Tak showed CPE on tCMK cells for one or two passage only, however, it grew with increasing yields in HeLa, HEK293 (Graham293) (an Ad5-transformed HEK cell line) and HDF cells. In contrast, strain Dugan grew less readily in these human cell lines but showed adaptation on tCMK cells. From the results of this study, the HEK293 cell line seems to be sensitive to both Ad40 and Ad41. Strain Tak was shown to grow well on Hep-2 cells also. The growth of Ad41 in Hep-2, HeLa, human intestine (HI407), and HEK293 cell lines was compared in one study (Pieniazek 1989). Ad41 prepared and passaged three times in Hep-2 (p11, p12, p13), HeLa (p1, p2, p3), and HI407 (p1, p2, p3) cells could successfully infect these cells as well as HEK293. Maximum CPE was observed between 3 and 9 days after infection. However, Ad41 isolated from Hep-2 (p10), HEK293 (p1) was unable to infect Hep-2, HeLa, or HI407 cells, as shown by lack of CPE. CPE on Ad41 Hep-2 infected cells was visualized later (at 8-9 days) than CPE seen with infected HEK293, HeLa, or HI407 cells (at 3-5 days), however, there was no substantial difference in the dynamics of propagation of Ad41 in Hep-2 cells and HEK293 cells. Ad41 could be successfully propagated at least 14 times in Hep-2, but it rapidly lost infectivity when passaged even once in HEK293 cells. The reason is unclear. Therefore, HEK293 cells were recommended by Pieniazek et al. (1989) for assaying CPE of putative Ad41 isolates. Hep-2 or HeLa and HI407 cells were proposed for continuous propagation of Ad41. Perron-Henry et al. (Perron-Henry 1988) reported that 75% of enteric adenoviruses inoculated onto Hep-2 monolayers were positive, and could be passaged in HEK293 cells. This finding contradicted Pieniazek et al. (1989)'s results. It was conceivable that the source of Hep-2 cells and their passage levels affect the susceptibility to infection. In general, HEK293 cells were more efficient than Hep-2 cells for isolating enteric adenovirus from clinical samples (Perronhenry et al. 1988). The HEK293 cell line is more sensitive to infection of enteric adenovirus from sewage samples than is the A549 cell line (He and Jiang 2005). HEK293 cells are more sensitive than HeLa cells for the isolation of enteric adenovirus species. It has been reported that enteric adenoviruses do not readily grow in Hep-2 cells (Brown et al. 1984). Ko et al. (Ko et al. 2003) confirmed that Ad41 can be successfully propagated in HEK293 cell lines. Ad41 is known to infect HEK293 cells in accordance with a single-hit model, which means that only one virus is sufficient to infect HEK293 cells productivity (Tiemessen and Kidd 1990).

There is no standard cell line used for the detection of adenoviruses. It is reported that a rapid loss of Ad41 infectivity with passage in HEK293 has been demonstrated (Pieniazek 1989). The long incubation time may affect cell monolayer integrity, thus making observation of CPE difficult. To manage this problem, samples have been inoculated into suspended cells rather than onto immobilized monolayers

(Thurston-Enriquez et al. 2003b), which may increase assay sensitivity for some enteric viruses though it has not been proven for adenoviruses (Yates et al. 2006). The phenomenon that representative strains of Ad40 and Ad41 show different characteristics at different stages of the replicative cycle and on different cells suggests that the growth of defectiveness is multifactorial.

2.3 Analytical Methods

Obtaining and interpreting data on the effectiveness of treatment methods has been hampered due to lack of standard method for analysis of water samples. Adenovirus detection methods can be categorized into infectivity assay (e.g. production of CPE), molecular techniques, and methods that integrate cell culture with molecular methods (Yates et al. 2006). Infectivity assays are typically quantified by titration of viruses and calculation of the 50% tissue cell culture infective dose ($TCID_{50}$) from CPE absence and presence data. Another method for determining infectivity is the plaque assay in which viral plaque formation on cell cultures is counted instead of CPE observation in $TCID_{50}$. There are various of molecular methods used to detect the viral nucleic acid but these do not necessarily correlate to infectivity. Integrated methods combine cell culture based infectivity assessment with the benefits of molecular methods (Yates et al. 2006).

2.3.1 Infectivity Assays

2.3.1.1 Cytopathic effect (CPE)

Cytopathic effect (CPE) determination in cell culture is one of the most commonly used methods for detecting and quantifying viruses. CPE are observable changes that take place in the host cells as a result of virus replication. Such changes may be observed as changes in morphology, including rounding or formation of giant cells, or formation of a hole in the monolayer due to localized lysis of virus-infected cells (Maier 2000). For Ad40 and Ad41 which do not plaque efficiently, the Most Probable Number (MPN) (Maier 2000) method may be used (Meng and Gerba 1996). MPN is en estimate of microbial density per unit volume water sample, based on probability theory. However, determining their presence is still challenging. It sometimes takes 6-8 weeks to produce CPE and the signs of CPE are often unclear and inconsistent. Dejong et al. (Dejong et al. 1983) indicated that CPE was not always a reliable indicator of virus multiplication. One strain (Glasgow 22345) was passaged consecutively three times in Hep-2 cells without detectable CPE. When passaged to tCMK culture, it took only 10, 8 and 4 days to show CPE for passage 1, 2, and 3, respectively. This meant that the virus replicated in and adapted to the Hep-2 cells. This phenomenon should encourage the attempt of blind passages, preferably on long-lived cell cultures. However, in a small study, 7 out of 39 epidemiologically unrelated stools were shown by electronic microscope (EM) to contain adenovirus particles. But it was not able to tell if those viruses were infectious under EM. They did not produce definite, progressive CPE in any of the HEK293, Hep-2 and tCMK cell cultures tested (Dejong et al. 1983).

Virus quantification is usually accomplished by preparing serial, tenfold dilution of the viruses; an aliquot from each dilution serves as inoculum for susceptible host cells. The titration procedure does not indicate the number of infectious virus particles in the inoculums directly, but provides an estimate of the $TCID_{50}$ which is defined in terms of the highest viral dilution in which the virus affects 50% of the hosts. Because Ad41 does not produce constant and clear CPE, a MPN procedure with at least 4 and preferably a larger number of inoculations are made of each dilution (Leland and French 1988).

To perform the $TCID_{50}$ titration procedure, tubes or flasks are usually prepared containing certain amount of cells in the growth medium. After development of host cells within the tubes or flasks, the growth medium is substituted by maintenance medium. Decimal dilutions of the original viral suspension are added into each tube or flask and they are observed for CPE after a pre-determined time period. For $TCID_{50}$ titration of fastidious viruses such as Ad41, tubes or flasks with large adhesion area may be used (Brown et al. 1992). Viral titer can be calculated by Reed-Muench equation (1938) or the Karber equation (1931) (Leland and French 1988).

2.3.1.2 Plaque assay

The plaque assay was indicated to be more sensitive than CPE observation for adenoviruses detection since the viruses can be detected by plaque formation when there is no evidence of CPE. Plaque assays utilizing cell culture are typically used with wastewater and biosolid samples. However, many viruses, such as Ad40 and Ad41, do not produce plaques efficiently and some will only produce plaques after several passages on a cell line. One of the drawbacks of plaque assaying is the inability to consecutively identify the plaque originating from viral lysis by visual inspection (Gallagher and Margolin 2007). Plaque formation by adenovirus is strictly dependent on the composition of the overlay medium, the amount of cells seeded into the culture flaks, the amount of inoculum added, and the incubation time (Gallagher and Margolin 2007; Wassermann 1962). The plaque assay was compared to real-time PCR for Ad40 analysis in environmental water samples in one study of environmental monitoring and results showed that real-time PCR methods yielded viral counts 3 to 4 orders of magnitude higher than the plaque assay (He and Jiang 2005).

2.3.2 Molecular Techniques

Molecular techniques can detect enteric adenovirus nucleic acid directly from extracts of clinical samples or environmental samples, or they can be integrated with cell culture (Jothikumar et al. 2005). When integrated with cell culture, the molecular method replaces observation of CPE as the method for detecting viral replication on the host cells. Cell culture prior to nucleic acid amplification increases the copy number of infectious viruses, which leads to higher sensitivity and an increased probability of their detection, even if they do not produce CPE (Ko et al. 2003).

Compared to CPE based infectivity assay, molecular techniques especially real-time quantitative PCR/RT-PCR are fast, accurate and labor-saving.

2.3.2.1 Direct molecular test

Standard cell culture methods for detection of human pathogenic viruses are laborious and time-consuming, and require up to a month for confirmation of positive results. For environmental samples, cell culture assays are further complicated by the presence of organic and inorganic materials that are toxic to cells. As a result, molecular techniques have been extensively used to detect enteric viruses from environmental samples since the early 1990s as alternatives to traditional cell culture with CPE detection.

With both concentrated environmental samples and infected cultured cells, viral nucleic acid can be extracted and purified to remove cell debris and inhibitors before being amplified and detected by PCR. A method is based on guanidium thiocyanate extraction and use of silica columns to bind and wash nucleic acids. This method is rapid, easily used and efficiently removing inhibitors. Extraction kits that are able to purify both viral RNA and DNA in a single step are available commercially.

2.3.2.1.1 PCR

Molecular viral detection assays, such as PCR and hybridization, are usually based on the detection of a part of the viral genome that is reproduced to make a large number of copy the gene region within a specific group of viruses. PCR is rapid, sensitive and specific if assays are well designed. Results from PCR can be obtained within 24 h of sampling, compared to days or even weeks of incubation for cell culture assays (Noble et al. 2003). PCR is capable of differentiating specific viruses. PCR primers can be designed to target whole virus orders, or to be specific to a single type of virus. PCR is highly sensitive and is capable of detecting viruses in low numbers when the virus replicates without showing CPE on cell culture. However, unlike cell culture assays, the infectivity of viruses detected by molecular methods is often unknown. In addition, due to its high sensitivity, PCR detection methods also increase the risk of false positives due to contamination. In order to reduce this, stringent quality control measures, such as using aerosol-resistant pipette tips and rigorous decontamination of instruments between experiments, are required. Likewise, false-negative results may also be a problem when inhibitors in environmental samples are present. Another limitation of conventional direct PCR is that it cannot enumerate viruses; it can only indicate presence or absence. Conventional PCR is also labor intensive and time consuming. Ethidium bromide-stained gel electrophoresis or hybridization procedures require open handling of the PCR amplicon which induces a high risk of template carryover contamination (Heim et al. 2003). Conventional PCR has been modified to improve specificity, sensitivity and efficiency but also to quantify the number of viruses detected. Some variations of conventional PCR include nested PCR, multiplex PCR, and real-time quantitative PCR. Nested PCR means that two pairs of PCR primers were used for a single locus. The first pair amplified the locus as seen in any PCR experiment. The second pair of primers (nested primers) bound within the first PCR product and produced a second PCR product that will be shorter than the first one. If wrong locus were amplified by mistake, the probability is very low that it would also be amplified a second time by a second pair of primers. Nested PCR assays for adenoviruses were demonstrated to be more sensitive than the single round conventional PCR, whereas is more easily contaminated (Fong and Lipp 2005).

2.3.2.1.2 Real-time quantitative PCR

Real-time quantitative PCR provides quantitative data on the presence of a certain type of virus in a water sample. Real-time detection of a single type of human adenovirus DNA out of all 51 types has been achieved by using a fluorescence dye such as SYBR Green®, and fluorescence resonance energy transfer probe pairs (Haramoto et al. 2005; Heim et al. 2003; Watanabe et al. 2005). Taqman® is a PCR based assay with laser scanning technology to excite fluorescent dyes present in the specially designed Taqman® probes or SYBR green which emit a fluorescent signal upon binding to double strand DNA molecules. When using specific primers the amount of each PCR product being synthesized can be measured giving either relative or actual measurement of either DNA or mRNA (via RT-PCR). The results are represented as a sigmoidal curve in which the fluorescence is plotted as against the numbers of cycles. Real-time PCR is less time-consuming than conventional PCR because a confirmation step such as gel electrophoresis and additional hybridization are generally not required.

2.3.2.2 Integrated cell culture PCR

Although there are many advantages of PCR based methods, such as high sensitivity, specificity, and efficiency, they still cannot provide accurate information on the viral infectivity which can be detected by cell culture. To address this problem, cell culture has been combined with PCR in several studies. It is demonstrated that the combined methods integrate the reliability of infectivity detection of cell culture and the advantage of PCR based analysis. Integrated cell culture PCR involves inoculating the sample onto cells. After a growth period, the viral DNA is extracted from the cells and analyzed using PCR (Chapron et al. 2000). The integrated method has also been used to detect mRNA from infected cell extracts by RT-PCR (Ko et al. 2003). Real-time quantitative PCR and RT-PCR can quantify adenoviruses following cell culture (Choi and Jiang 2005; He and Jiang 2005; Jiang et al. 2005; Jothikumar et al. 2005; Ko et al. 2005a).

It has been recognized that viral contamination in environmental samples is sometimes underestimated since no single cell culture system can be used for all human enteric viruses. Therefore, Chapron et al. (2000) used an integrated cell culture (ICC)-RT-PCR procedure coupled with nested PCR to detect human astroviruses and adenovirus 40 and 41. A 48.3% percent of samples were positive for adenovirus 40 and 41 when ICC-RT-PCR-nested PCR was used with BGMK cell line for viral amplification. No sample concentrate was positive if only RT-PCR was performed. These researchers demonstrated the effectiveness of ICC-RT-PCR-nested

PCR technique compared to the CPE method for viral detection. Ad41 may not be detected if other monitoring methods are not applied other than CPE based MPN method. In addition, another advantage of PCR over CPE that was demonstrated is its' increased specificity. Integrated cell culture PCR assay combines cell culture and molecular detection of viral genomic nucleic acid, which leads to higher sensitivity and an increased probability of their detection. Nevertheless, this method has the potential to detect nucleic acid of inactivated viruses that may have been in the sample which was inoculated into cell cultures. This could result in false-positive detection from samples containing no infectious viruses. In other words, it provides no information on virus infectivity, and information on infectivity is required for determining human health risk.

A cell culture PCR assay based on a combination of A549 and BGMK cell lines and molecular identification was used to monitor infectious adenoviruses and enteroviruses in river water in one study (Lee et al. 2004). Results indicated that though the method is a useful method for detection of enteric viruses in water samples, the viral level can be underestimated because only some of the enteric viruses present in the sample may reproduce in a single cell line.

For adenoviruses detection, Ko et al. (Ko et al. 2003) indicated that only infectious adenoviruses could enter cells and transcribe mRNA during replication, thus they developed and verified a molecular method by which to detect viable adenoviruses in environmental samples based on a RT-PCR assay of viral mRNA in cell culture. Since infectious enteric adenoviruses (Ad40 and Ad41) did not produce clear CPE on some cell lines, this method was particularly applicable to quantitative detection of these viruses. It was based on RT-PCR amplification of viral mRNA. The results showed that mRNA RT-PCR assay of Ad41 required more incubation time and had a lower sensitivity than that of Ad2, but with a heminested PCR assay, it was possible to detect mRNA from cells infected with only 5 infectious units (IU) of Ad41 as early as three days. As demonstrated by Chapron et al. (2000), heminested PCR increased both specificity and sensitivity. However, this method required combining cell culture with mRNA RT-PCR, followed by nested PCR. This was time consuming and might lead to PCR product laboratory contamination due to the need to open post-PCR tubes in order to perform nested PCR. In addition, it required at least 3-5 days of cell culture incubation and very low numbers of adenoviruses in samples could be detected by their ability to produce mRNA.

Because of the drawbacks of mRNA RT-PCR developed by Ko et al. (2003) described above, an integrated cell culture (ICC)-Taqman® RT-PCR method for rapid and sensitive detection of mRNA by infectious adenoviruses was developed, without resorting to nested PCR (Ko et al. 2005a). The results show the sensitivity of detecting infectious Ad41 by Taqman® real-time RT-PCR in two different genomic regions. Compared to the fiber gene, the hexon gene RT-PCR has better sensitivity in detection of Ad41 after treated with free chlorine. In a previous study (Jothikumar et al. 2005) discussed in the following, however, a fiber gene assay was found to equally successfully detect and identify low levels of Ad40 and Ad41 as hexon gene. This may due to difference in expression of the hexon and fiber genes, or due to a more pronounced effect of free chlorine in causing DNA damage in the fiber gene region versus the hexon gene. Using the hexon gene mRNA Taqman® RT-PCR method, the detection time of mRNA extracted from cell culture infected with 10^6 IU of Ad41 was as early as 6 h post-infection. By the same method, when cells were infected with 5000 and 500 IU of Ad41, hexon mRNA was detected as early as 1 day post-infection; for inoculation of 5 and 50 IU, hexon mRNA was detected after 3 days of infection. The sensitivity of this method for detecting Ad41 was comparable to or better than that of hexon gene of the nested PCR assay.

Jothikumar et al. (2005) produced a broadly reactive real-time PCR assay for detection of all human adenovirus species, and a specific, discriminatory and sensitive real-time PCR assay for Ad40 and Ad41, using a Taqman® probe targeting a conserved region of the hexon gene. The sensitivity of the Taqman® PCR assay for Ad40 and Ad41 was determined by genomic equivalent copies (GEC). Specific regions of the genome were amplified and cloned, and the plasmid was used as GEC. The sensitivity of another real-time PCR assay using fluorescence resonance energy transfer (FRET) PCR probes that target the adenovirus fiber gene was also determined by GEC. This study found out that the sensitivity of the FRET PCR assay for determination of Ad41 from the fiber gene region was equivalent to the sensitivity of the hexon-based Taqman® assay. In addition, the FRET PCR assay was shown to be highly sensitive for Ad40 and Ad41, indicating that the method could be used to differentiate Ad40 and Ad41. FRET PCR also can be used in conjunction with a broadly reactive Taqman® assay to determine whether adenovirus-positive samples contain these serotypes.

Jiang et al. (Jiang et al. 2005) applied real-time quantitative PCR for detection of enteric adenovirus 40 in environmental waters. This method is specific to human fecal source contaminated water. However, the efficiency of amplification was reduced in presence of PCR inhibitors. In addition, the quantitative ability was limited only to the samples with relatively higher concentration of viruses.

2.3.3 Real-time Cell Electronic Sensing (RT-CES™) System

A real-time cell electronic sensing (RT-CES™) system is used for label-free, dynamic measurement of cell response to cytotoxicants. Cells are grown in a special culture plates with an electrocircuit underneath. Upon the application of an electrical field, ions undergo field-directed movement and concentration gradient-driven diffusion, which leads to frequency-dependent impedance dispersion. The presence of cells leads to an increase in the electrode impedance. Cell viability, cell number, cell morphology, and cell adhesion can all affect the measurement of electrode impedance that is reflected by cell index (CI) on the RT-CES™ system (Xing et al. 2005).

Xing et al. (2005) applied this system to detect environmental toxicants, such as arsenic, mercury, and sodium dichromate. Compared with previous sensor electrodes, this system allows for dynamic monitoring of living cells in response to different toxicants. Solly et al. (2004) applied RT-CES™ for cell-based assays. Results show that the cell growth rate measured by this system was comparable to actual cell numbers counted manually. In addition, cell proliferation, cytotoxity, cytoprotection, cell growth inhibition, and apoptosis data generated by RT-CES™ correlated with those determined by the classic methods. The conclusion is that the RT-CES™ system is a useful tool for label-free detection of certain cell-based parameters.

Cellular interaction with and adhesion on different biological surfaces is a dynamic and integrated process requiring the participation of specialized cell receptors, structural proteins, signaling proteins, and a cellular cytoskeleton. Atienza et al. (2005) use RT-CES™ system to dynamically and quantitatively monitor the specific interaction of fibroblasts with extracellular matrix proteins and with standard polylysine adhesion techniques. This study indicated that RT-CES™ system is fairly sensitive and accurate in detecting attached cells with coating medium.

2.4 UV Disinfection

2.4.1 History and Regulations

The first application of a UV disinfection process in drinking water treatment was in 1910 in Marseille, France. However, general application was hampered because of high cost, poor equipment reliability, maintenance problems and the introduction of chlorination, though UV was still used in small drinking water systems. Relative to UV, chlorine addition was cheaper, more reliable and produced a disinfectant residual that could be measured. With the increasing information on the production of by-products during chlorination and ozonation in 1970s; there was renewed interest in the application of UV as a disinfectant in municipal water treatment plants. Low-pressure UV which usually produces 254 nm UVC output produces almost no by-products; and unlike chemical disinfectants, the biological stability of water is not affected by low-pressure UV lamps. Since 1980s, UV disinfection has been widely applied in drinking water in Europe. Until the discovery of the high efficacy of UV against *Cryptosporidium* and *Giardia* in 1998 did UV come to be an important disinfection process in US and Europe (Hijnen et al. 2006).

Tap water may account for 14-40% of gastrointestinal illness, thus ensuring its safety is vital. The USEPA requires that water treatment plants provide 4-log reduction of viruses in drinking water. Filtration is able to achieve an initial 1-log reduction with a further 3-log achieved by active disinfection (e.g. chlorine, chlorine dioxide, ozone or UV). On January 5th 2006, the USEPA promulgated the Long Term 2 Enhanced Surface Water Treatment Rule (LT2ESWTR). Adenoviruses were identified to be one of the most UV-resistant groups of viruses currently known and were thus used as the benchmark for all waterborne pathogenic microorganisms (Yates et al. 2006). Literature reports indicate that UV doses of less than 30 mJ/cm^2 were generally sufficient for 3-log inactivation of several waterborne viruses, including hepatitis A virus, rotavirus, and poliovirus; vegetative bacteria can be inactivated by one tenth to a quarter of the UV dose required for viruses. Adenoviruses have been found to require at least 120 mJ/cm^2 and possibly as much as 200 mJ/cm^2 for a 4-log inactivation. Therefore, the USEPA adopted a delivered dose of 186 mJ/cm^2 for a 4-log inactivation credit in the LT2ESWTR (Yates et al. 2006). Most public water systems use chemical disinfectants like chlorine for virus inactivation, thus increasing of UV dose does not affect most large surface water system. One exception may be that surface water systems that contemplate using UV disinfection because of short free chlorine contact time. The other exception is the effect on some other water providers who are using groundwater which is not subject to LT2ESWTR. However, LT2ESWTR dose requirement might become the default requirement for them under some states which do not have their specified requirements. Recent research on UV inactivation of adenoviruses, is discussed in the following sections. The review focuses especially on Ad40 and Ad41, since these strains are most resistant to UV and are enteric strains that are likely to be found in water or wastewater.

2.4.2 The Germicidal Nature of UV

Ultraviolet rays have shorter wavelength than visible light. A wavelength, the distance between the crests of two waves, is often measured in units called nanometers. Ultraviolet wavelengths range from 100 to 400 nm and lie between X-rays and visible light (Figure 2.1).

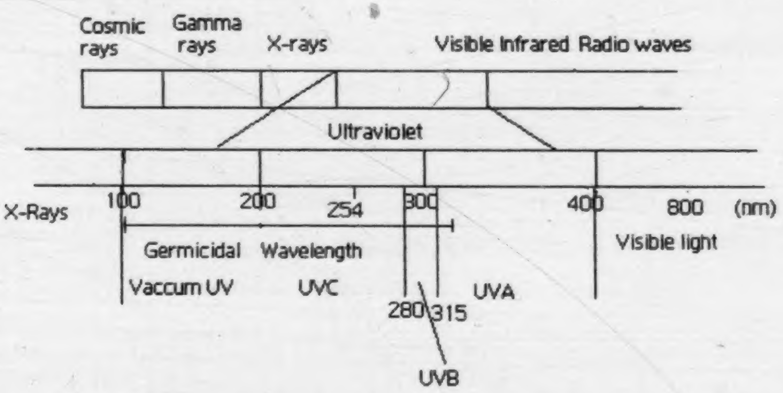

Figure 2.1 Electromagnetic spectrums (USEPA, 2006)

Ultraviolet rays with wavelengths shorter than 300 nm are extremely effective in killing microorganisms. The most effective sterilizing range for UV is with the UVC bandwidth between 200 and 280 nm. This range is called germicidal bandwidth. It deactivates the DNA of bacteria, viruses and other pathogens thus destroys their ability to multiply and cause disease.

2.4.3 Mechanisms of Microbial Inactivation by UV

Ultraviolet photons are absorbed by the DNA or the RNA of a microorganism exposed to UV light. DNA and RNA consist of single or double stranded polymers comprising building blocks called nucleotides which are classified as either purines (adenine and guanine) or pyrimidines (thymine and cytosine) in DNA, or purines (adenine and guanine) or pyrimidines (uracil and cytosine) in RNA. As shown in figure 2.2, the absorption UV of photons by nucleotides happens at wavelength between 200 and 300 nm. DNA absorption of UV light is a combination of absorption by all bases and the absorbance peak of DNA is around 260 nm (Figure 2.3).

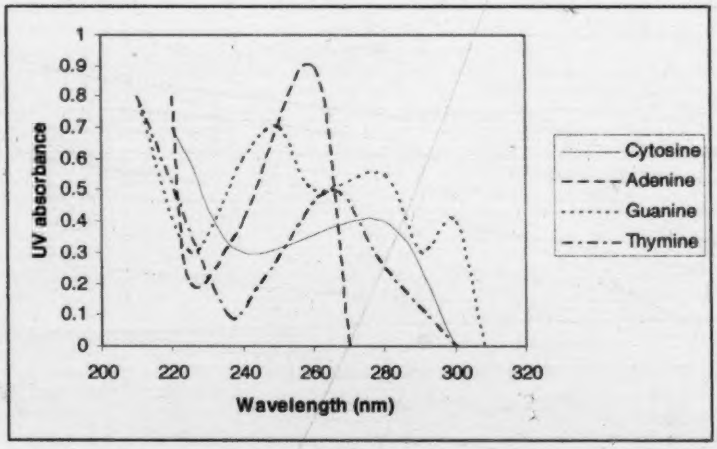

Figure 2.2 UV absorbance of nucleotides (Adapted from USEPA, 2006)

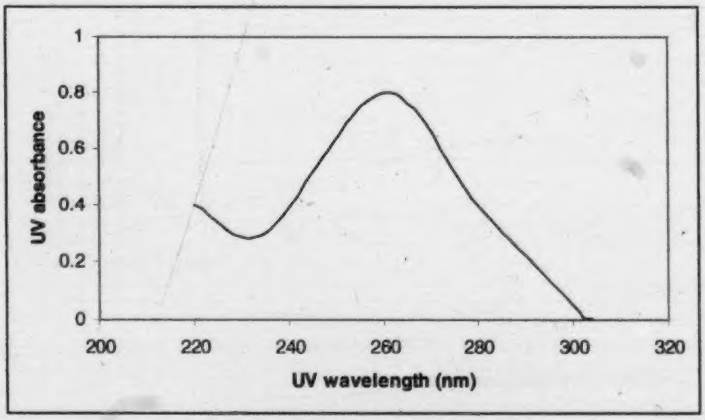

Figure 2.3 UV absorbance of DNA

All purines and pyrimidines strongly absorb UV, however, the rate of UV-induced damage is greater with pyrimidines (Jagger 1966). There are three types of damage which contribute to microorganism inactivation. First, UV inactivation causes a photochemical reaction in which a chemical dimer is formed between the two bases. The dimer inhibits the formation of new DNA (or RNA) chains in the process of cell replication (mytosis) thus resulting in the inactivation (inability to replicate) of the affected microorganisms. This is the most common damage resulting from UV inactivation. Second, pyrimidine (6-4) pyrimidone photoproducts, which are similar to pyrimidine dimers and form on same sites, are formed during UV exposure. Pyrimidine (6-4) pyrimidone photoproducts are highly mutagenic. Third, protein-DNA cross links, which are covalent bonds between a protein and a DNA strand, are formed during UV inactivation. They may be important for the inactivation of certain microorganisms.

2.4.4 UV Collimated Beam Apparatus

In most UV disinfection studies, a low-pressure UV lamp was utilized. When atoms are raised to an excited state, they emit only in very narrow spectrum lines with virtually no emission between the lines. A low-pressure mercury lamp is a very common lamp of this type. With a quartz sleeve, the principle emission is usually at 253.7 nm (Bolton 2001). To determine the UV inactivation of microorganisms, a bench-scale collimated beam apparatus is often used. A collimated beam directs the UV onto a horizontal surface either through a cylindrical tube or through successive apertures. Although there are no standardized designs of collimated beam apparatus, there are a number of components that should be considered essential in the design. These include the lamp located in an enclosure, the shutter, the window, the power supply, the collimating tube, the platform, the vessel containing the microorganism suspension and the stirrer. A shutter, usually located beneath the lamp, controls the duration of the UV exposure and the dose. Because the output of many UV lamps is quite temperature sensitive, it is essential to keep the enclosed lamp thermally stable. A quartz window located beneath the lamp is useful to assure the lamp is not exposed to air drafts when a shutter is opened. It is important to maintain a constant emission of UV emission so that a constant power supply is required. The collimated beam provides a spatially homogeneous irradiation field on a given surface area (Bolton and Linden 2003). A UV dose is determined by monitoring the UV fluence rate with a calibrated radiometer and contact time that the microorganisms are exposed under UV (Hijnen et al. 2006). The platform on which the Petri dish is placed for UV exposure should be thermally stable as well. A stirring motor placed underneath the platform ensures all microorganisms acquire equal UV doses. The most often used lamp is a low pressure mercury lamp which emits about 254 nm monochromatic UV. This corresponds closely to the peak absorbance of DNA and to the peak of the germicidal action spectra of *E. coli* and *Cryptosporidium parvum* (Bolton and Linden 2003).

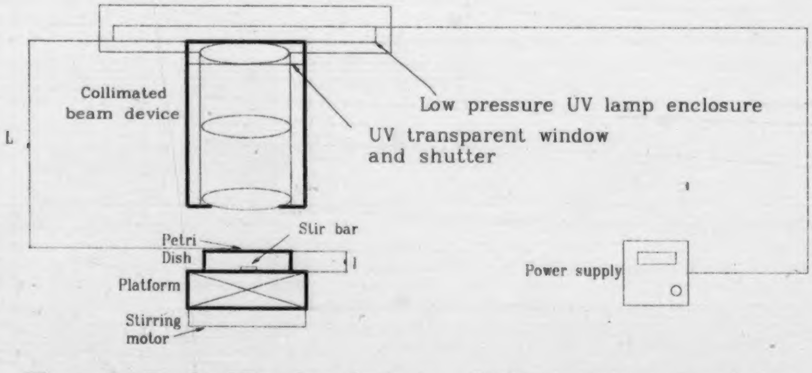

Figure 2.4 Draft of Bench scale device of UV inactivation experiments

2.4.5 Determination of UV Dose

The UV dose is calculated as the product of depth averaged fluence rate in the stirred microorganism suspension and the exposure time. Exposure time can be easily controlled with a shutter and measured with a stop watch for a bench scale collimated beam apparatus with Petri dish setup.

When a low pressure UV lamp is used, the radiometer provides an accurate measurement of the fluence rate at the surface of the water in the Petri dish at the centre of the beam, E_0. Several corrections are required to obtain the *average fluence rate* in the water to which the viruses are exposed. Based on this, the delivered UV dose to a sample can be calculated. There are four factors that need to be considered when using a low-pressure UV lamp; they are the *Reflection Factor*, the *Petri Factor*, the *Water Factor* and the *Divergence Factor*.

Reflection Factor

When the incident beam hits the water surface in Petri dish, a small fraction of the beam is reflected off the interface that separates the media whenever a beam of light passes from one medium to another. For air and water, the fraction reflected is given by the Frensel Law (Meyer-Arendt 1984) and is R = 0.025. The *Reflection Factor* is (1 - R) = 0.975, which represents the fraction of the incidence beam that enters the water.

Petri Factor

The fluence rate of UV light varies over the surface area of the water sample in the Petri dish depending on the design of the apparatus. The *Petri Factor* is the average of the incident fluence rate over the area of the Petri dish to the fluence rate measured at the surface centre of the Petri dish. It is used to correct the fluence rate reading at the surface centre of the Petri dish in order to reflect the average fluence rate over the surface area more accurately. In general, a well designed collimated beam apparatus should be able to deliver a *Petri Factor* of greater than 0.9.

Water factor

It is necessary to account for the decrease in fluence rate arising from absorption as the beam passes through the water if the water absorbs UV at 254 nm for a low-pressure UV lamp. The *Water factor* is defined as

$$\text{Water Factor} = \frac{1-10^{-al}}{al\ln(10)} \qquad \text{Eqn. (1)}$$

Where a = decadic absorption coefficient (cm^{-1}) or absorbance for a 1 cm path length and l = vertical path length (cm) of the water in the Petri dish.

Divergence Factor

Because the beam is never truly collimated, there is divergence in the beam as it passes through the microorganism suspension. For the finite distances of the water samples from the UV lamp, the beam is not perfectly collimated. The *Divergence Factor* corrects for this dispersion.

$$Divergence\ Factor = \frac{L}{(L + l)} \qquad \text{Eqn. (2)}$$

where L is distance from the UV lamp to the surface of the water sample and l is the depth of water sample (Figure 2.4).

Overall, the *Average Irradiance* (E_{avg}) for a low pressure UV lamp in the water is

$$E_{avg} = E_0 \times Petri\ Factor \times Reflection\ Factor \times Water\ Factor \times Divergence\ Factor \qquad \text{Eqn. (3)}$$

where E_0 = radiometer meter reading at the center of the dish and at a vertical position. The average UV dose (H) is

$$H = E_{avg} \times t \qquad \text{Eqn. (4)}$$

where t is the exposure time of water samples.

2.4.6 Inactivation of Enteric Adenoviruses

Meng and Gerba (Meng and Gerba 1996) applied UV to inactivate Ad40 and Ad41 along with poliovirus type 1 and MS-2 as comparisons. UV light was generated using a low-pressure mercury lamp. Ad40 and Ad41 were propagated and assayed in the PLC/PRF/5 cell line. Cell infection was observed for CPE every 3 days for 3 weeks. Results indicate that to achieve 4-log inactivation, 124 mJ/cm^2 and 111.8 mJ/cm^2 UV doses were required for Ad40 and Ad41, respectively. Both Ad40 and Ad41 were much more resistant to UV than poliovirus 1 and MS-2.

However, Thurston-Enriquez et al. (Thurston-Enriquez et al. 2003b) found that Ad40 is even more resistant to UV than what Meng and Gerba (1996) reported. They exposed the virus suspension to a collimated beam of UV from an 8 W low pressure mercury germicidal lamp that emitted nearly monochromatic UV radiation at 253.7 nm. Ad40 and feline calicivirus (FCV) were propagated and assayed in PLC/PRF/5 and CRFK cell lines, respectively. The concentration of viruses was determined by observation of each infected well based on observation of CPE. Results verified that Ad40 was twice as UV-resistant than MS-2, and was several times more UV-resistant than FCV. The UV dose required for 4-log inactivation of Ad40 suspended in buffered-demand-free water was 226 mJ/cm^2 and was 203 mJ/cm^2 for virus suspended in ground water. In comparison, the dose required for 4-log inactivation of Ad40 was 124 mJ/cm^2 in Meng and Gerba's (1996) study. The dose to inactivate Ad40 in the Thurston-Enriquez et al. (Thurston-Enriquez et al. 2003b) study was much higher than that in the Meng and Gerba (Meng and Gerba 1996) study. This difference was suspected due to Ad40 sensitive to freeze-thaw. The protocol used by Meng and Gerba included five freeze-thaw cycles of the virus harvesting whereas only one freeze-thaw cycle was used in the Thurston-Enriquez et al. (Thurston-Enriquez et al. 2003b) study. In addition, the different methods used in virus preparation, water type and experiment design can also produce significant differences in inactivation.

Ko et al. (Ko et al. 2005a) did research on UV inactivation of Ad41 detected by cell culture integrated with RT-PCR. They found that 4-log inactivation of Ad41 required a UV dose of 222 mJ/cm^2, which was close to that reported by Thurston-Enriquez et al. (2003) for Ad40 inactivation, but much higher than the doses reported by Meng and Gerba (1996) for both Ad40 and Ad41 inactivation by UV. The discrepancy could be due to differences in the number of freeze-thaw cycles used to detach and lyse to host cells prior to the PCR analysis. Ko et al. (Ko et al. 2005a) used three freeze-thaw cycles in their work, Thurston-Enriquez et al. (2003) used one freeze-thaw cycle, while Meng and Gerba (1996) used five freeze-thaw cycles. Based on the previous work completed by Thurston-Enriquez et al. (Thurston-Enriquez et al. 2003a), it was demonstrated that enteric adenovirus was sensitive to successive freeze-thaw that might weaken the viral capsid thus increasing the susceptibility to UV. However, this conclusion was speculated by Ko et al. (Ko et al. 2005b), because they did not find any effect of the number of freeze-thaw cycles on UV resistance of Ad41. This suggested that either the number of freeze-thaw cycles did not affect the UV susceptibility of Ad41, or the integrated cell culture RT-PCR method was more sensitive than traditional CPE-based cell culture method in detection of infectious Ad41. Another reason for the differences between studies might be the variability of the infectivity assays of the two viruses based on observation for the appearance of CPE which was used as primary virus detection method in two studies (Meng and Gerba 1996; Thurston-Enriquez et al. 2003a). It is known that Ad40 and Ad41 do not produce consistent CPE; the long incubation time may affect cell monolayer integrity, thereby making observance of CPE difficult. Cell culture integrated RT-PCR for infectivity detection assay may be more reliable.

The study of Baxter et al. (2007) confirmed that at Ad41 is more UV-resistant than Ad2 and Ad5 which are respiratory adenoviruses. A collimated beam apparatus containing two low-pressure UV lamps was used to expose adenoviruses to UV light in this study. At a UV dose of 40 mJ/cm^2, the inactivation was around 1-log for all three adenovirus types studied (Ad41, Ad2 and Ad5). A dose of 120 mJ/cm^2 provided 3-log inactivation of Ad2 and Ad5, but only 2-log inactivation of Ad41 was achieved at this UV dose. These results contradicted with the results of Meng and Gerba (1996) in which Ad2 was more resistant than Ad41. The virus detection method in this study was not only based on CPE due to the limited spread of Ad41 in cell culture (on HEK293 cells). In the study of Baxter et al. (2007), virus detection on the cells was conducted by using an enumeration technique based on immunofluorescent staining of cells with a specific antibody to visualize the presence of newly synthesized viral capsid protein (hexon). Because these proteins were formed only in infected cells, fluorescence emitted from a microplate well indicated adenoviruse infection of the cells. This makes identification of infection on the cells enumeration possible.

Compared to a low-pressure (LP) UV lamp, a medium-pressure (MP) UV lamp can carry much more power, but the emission lines broaden. A MP UV lamp can emit monochromatic UV at a broaden wavelength range, between 220 nm and 300 nm with filters. The data in recent research shows that adenoviruses are relatively resistant to UV at 254 nm compared to other waterborne microorganisms (Yates et al. 2006). LP UV exposure causes damage to the viral DNA in the form of dimers. In the presence of these dimers, the viral genome cannot be replicated. However, once viral genome is in the host cell, these dimers can be repaired by nuclear excision repair, restoring the ability of viral replication (Yates et al. 2006). Linden et al. (Linden 2005) found that UV wavelengths around 220 nm and 228 nm were more effective than was 254 nm UV for inactivation of Ad2. However, 220 nm was not able to efficiently penetrate typical natural water matrixes (Yates et al. 2006). It is demonstrated that both full spectrum MP and any emission below 240 nm filtered MP UV are more efficient than LP UV. However, the life time and germicidal efficiency of LP UV are twice as much as those of MP UV (Bolton 2006). Therefore, LP UV lamp is mostly used in microorganism inactivation in laboratories.

2.5 Conclusion

HEK293 is a cell line that has been demonstrated to support the growth and assay of Ad41. It is a cell line used intensively in *in vitro* tissue cell culture assays for viruses, and for production of recombinant proteins and viruses. However, in washing steps which are conventionally and repeatedly employed in such *in vitro* assays and other manipulations of these cells, the cells are readily detached or are washed away from the plates or dishes in which the studies are performed. Hep-2 is a cell line that has been recommended to continuously propagate Ad41. A549 cell line has also been demonstrated to support the growth of Ad41 it is not as good as Hep-2 and HEK293. However, it really depends on the virus strain for virus propagation on a certain cell line. Based on the characteristics of the above cell lines and their availability, Hep-2, A549 and HEK293 cells were tested for cell culture in this study.

Due to the effect of Ad41 strains on the success of propagation on certain cell lines, both stool isolation of Ad41 from PLPH and Ad41 Strain Tak from ATCC were tested in this study.

Although a diversity of methods have been used to detect viruses in water, a standard analytical method is lacking. It is clear that a standard method is needed for detection of viruses in water, especially for those viruses which are known to cause disease. The traditional cell-culture method based on observation of CPE is time consuming (it often takes several days for observation of CPE) and the signs of CPE are not clear for some viruses such as adenovirus 40 and 41. Detection of the endpoint of infection is difficult. Molecular methods, such PCR and RT-PCR include several alternatives and variations, and the selection of primers and probes is critical. Molecular methods, either PCR or RT-PCR, may potentially be used to quantify the number of infectious viral particles in water samples directly, or may be used as an alternative to CPE to more rapidly and more reliably determine the endpoint of infection on tissue cell cultures. The RT-CES™ offers another potential method for determining the endpoint of virus infection on cell culture. Up to now, there is no information on the use of RT-CES™ for detection of virus infections in cell culture.

Compared to conventional PCR, real-time quantitative PCR is completely automated after sample loading. As a real-time quantitative PCR method, Taqman® PCR avoids the potential of sample contamination that may expose to conventional PCR, especially nested PCR. Furthermore, Taqman® PCR is able to quantitatively detect DNA or cDNA in each viral sample at a very low concentration, thus is more sensitive. The most important is, it gives quantitative results of viral DNA or cDNA copy number without additional analysis steps, thus saves plenty of time and labor.

There are few studies on UV inactivation of enteric adenoviruses despite the fact that these viruses are important waterborne pathogens and are included in the USEPA CCL (Baxter et al. 2007; Ko et al. 2005b; Meng and Gerba 1996; Thurston-Enriquez et al. 2003a). Furthermore, the results of these studies are not in agreement. The results of Thurston-Enriquez et al (2003)'s, Ko et al. (2005)'s and Baxter et al. (2007)'s studies show a significant higher resistance of enteric adenoviruses to 254 nm UV than the UV-resistance reported in Meng and Gerba (1996)'s study. There are many likely reasons but the lack of consistent and reliable analytical methods should be the most important one. Because of the recent emerge of virus detection methods such as molecular analysis which might be a potential substitution for traditional CPE-based infectivity detection method, there is an increasing interest in this area.

Chapter 3 Cell Culture of Ad41 on Hep-2 and A549 Cells Analyzed with Real-time Quantitative RT-PCR

3.1 Introduction

It was reported that Ad41 can be grown on both Hep-2 and A549 cells. Hep-2 cells were recommended for continuous propagation of Ad41 (Pieniazek 1989). Ad41 can also be grown on the A549 cell line (Hashimoto et al. 1991). The objective of cell culture research in this chapter is to determine the best cell line to propagate isolates of Ad41 for the entire study. Based on the availability of cells and Ad41 strains, isolates from stool samples obtained from the Provincial Laboratory for Public Health (PLPH) were grown on Hep-2 and A549 cells. The viral copy number was tested by Taqman® RT-PCR to verify the advantage of this method over traditional CPE method. HEK293 cells which was also reported to support the growth of Ad41 was not applied in the first stage because it was not available in PLPH. Purchase order of HEK293 cells and Ad41 TAK strain from ATCC has been made since the cell culture with Hep-2 and A549 cells started.

3.2 Materials and Methods

3.2.1 Cells and Viruses

3.2.1.1 Hep-2, A549 cells and clinical stool samples

Stool samples were obtained from children with gastroenteritis, provided by the PLPH. The stool sample was demonstrated to be Ad41 positive by both Taqman® PCR (Pang et al. 2005) and electron microscopy (EM). Hep-2 and A549 cells were originally obtained from ATCC and were passaged in the Diagnostic Department in PLPH (Appendix A, 2.1). The Hep-2 cells used in this study were from passage 271 to 289, and A549 cells used in this study were from passage 50 to 62.

3.2.2 Virus Propagation

3.2.2.1 Infection

Hep-2 and A549 cells were ready for inoculation when the growth of the monolayers achieved 70% confluence in 25 cm^2 regular culture flasks, at 37°C, 5% CO_2. Monolayers were rinsed twice with serum-free minimum essential medium (MEM) before the clarified stool extract was added into the serum-free MEM containing 5 µg/mL crystalline trypsin (Sigma chemicals) (MEM-T) (Appendix A, 1.1). Stool suspensions were absorbed for 1 h in an incubator at 37°C, 5% CO_2. Control cultures were mock-infected with MEM-T. Inoculants were removed after absorption; the monolayer was rinsed, covered with fresh maintenance medium and incubated at 37°C, 5% CO_2 to propagate viruses.

3.2.2.2 Propagation and Harvesting

Cultures were examined by placing the flaks under a microscope daily for CPE (cells rounded up and detached) until CPE was observed or 7 days elapsed, whichever came first. Infected cells were disrupted by 3 cycles of freeze-thaw to release intracellular viruses. The flask was frozen at -70°C and thawed at 25°C. When the flask had thawed to "slush", it was shaken vigorously to dislodge any cells that still stuck to the flask. Gently shaking was continued until large ice chunks were all melted. Cell suspensions were transferred to conical tubes and centrifuged at 1375 × g for 10 minutes at 25°C. The viral supernatant was collected and cell pellet was removed after centrifugation. The supernatant was aliquoted into flat bottom screw cap tubes, parafilm sealed and frozen with liquid nitrogen as Ad41 stock for long term storage.

3.2.2.3 Blind Passage

The medium of the cell cultures which did not show CPE was poured off and collected from the culture flasks. Excess medium was removed with a Pasteur Pipette. Five milliliters of 0.25% trypsin (with phenol red and gentamicin) was added and the flask was rocked to cover the cell monolayer. After 1 min, most the trypsin was poured out but 1 mL was kept in the flask. The flask was incubated for 7-10 min at

25%, 5% CO_2 until all cells were detached from the flask walls. The walls of flasks were tapped to completely dislodge the cells. All the cells were re-suspended in the new maintenance medium (Appendix A, 1.1) and dispersed by pipetting up and down vigorously to break up clumps (about 50 times). The cells and medium were transferred into a new flask and some new maintenance medium was added up to the required volume.

3.2.3 Assay of Adenovirus 41

3.2.3.1 Real-time Quantitative RT-PCR assay

Real-time PCR was used to measure the amount of total nucleic acid in the viral suspensions. Total nucleic acid includes viral DNA and mRNA. To test mRNA only, the DNA was digested and the mRNA was measured using Taqman® RT-PCR. Because Ad41 is a DNA virus, there is much more DNA than mRNA in viral particles. The accurate measurement of mRNA depended on complete removal of DNA in the Ad41 suspension.

3.2.3.1.1 Ad41 specific primers for Taqman® PCR

Enteric adenovirus-specific primers (Hexon) were used to detect hexon gene sequences. They yielded an amplicon of 65 bp DNA amplified by Ad41 specific primers (Table 3.1).

Table 3.1 Sequences and location of primers and probes for detection of enteric adenovirus by Taqman® PCR

Assay	Target	Primer or Probe	Amplicon size (bp)	Sequence (5'-3')	Location *
Taqman -PCR	Hexon gene	eADV-TaqF	65	CCGACCCACGATGTAACCA	371-389
		eADV-TaqR		CGGTCGACTGGCACGAAT	435-418
		eADV-TaqP		Fam-ACAGGTCACAGCGACTGACGCTGC-Tamara	393-416

*GeneBank Access number D13781

3.2.3.1.2 Extraction and Digestion

Total nucleic acid was extracted from the cell culture supernatant using MagaZorb RNA extraction kit (Cortex Biochem, CA, USA) (Appendix A, 2.3). Fifty microliter extraction products were diluted to 500 μL with sterilized water and treated with 5 μL of 122.5 U/μL Deoxyribonuclease I (DNase I) and 50 μL of 10 × DNase buffer to damage viral DNA. DNase I digests single- and double- stranded DNA to oligodeoxyribonucleotides containing 5' phosphate terminal ends. Ribonuclease was reduced to non-detectable level which was confirmed by Taqman® PCR.

3.2.3.1.3 Real-time Quantitative RT-PCR

The RT reaction was performed with a total 20 μL mix (Appnedix A, 2.4) incubated at 42°C for 60 min, 70°C for 15 min and the kept at 4°C with a GeneAmp® PCR System 2700 [Applied Biosystems (ABI), Foster City, USA] (Appendix A, 2.5). PCR amplification was performed using an ABI PRISM 7000 Sequence Detection System (Taqman®). Amplification was performed with steps of 50°C for 2 min, 95°C for 10 min, 45 cycles of denaturation at 95°C for 15 s each, annealing at 60°C for 1 min, and extension at 72°C for 1 min. During thermal cycling, fluorescent emission from each sample was recorded continuously and the ABI Prism 7000 SDS Software v. 1.1 processed the raw fluorescence data to produce threshold cycle (Ct) values for each sample. In Taqman® PCR, the cycle number at which the increase in fluorescence (and therefore cDNA) is exponential is measured. This is shown by the horizontal line in the figure generated by the software v.1.1. The point at which the fluorescence crosses the threshold is called the Ct. A standard curve was then computed from the Ct of the diluted adenovirus standards using SDS software, and absolute quantities for the unknown samples were then extrapolated based on their threshold cycle (Ct) values (Appendix A, 2.8).

3.3 Results and Discussions

3.3.1 Clinical Stool Samples Cultured on Hep-2 and A549 Cells

Eleven Ad41 positive stool samples first demonstrated by sequencing by Taqman® PCR and EM were extracted and inoculated onto both Hep-2 and A549 cells. Hep-2 and A549 cell lines have been reported in the literature to propagate Ad41 (Hashimoto et al. 1991; Perronhenry et al. 1988). Stool samples were obtained from PLPH and diluted in 10% PBS. The diluted stool samples were filtered with 0.22 μm filters.

3.3.1.1 Infectivity assay based on CPE

Hep-2 and A549 cell cultures were inoculated with 200 μL of each PBS diluted stool sample after they had achieved 80-90% confluent growth. The CPE in Hep-2 and A549 cells was characterized by marked rounding and clumping and an appearance of very strong cell aggregates. Eleven stool originated Ad41 samples form PLPH were inoculated onto both Hep-2 and A549 cells. Maximum CPE was observed on 1 sample (VC6536) on infected Hep-2 cells and 2 sample (VC8775, VC7941) on infected A549 cells on day 7 of incubation (Appendix B, Table B-1, B-2). All other cultures that did not show CPE were subject to blind passage. With 7 days incubation, 3 out of 19 samples (VC5774 on A549 cells, VC5774 on Hep-2 cells and VC10488 on Hep-2 cells) shown CPE (Appendix B, Table B-3, B-4). However, Hep-2 cells grown fast; it was hard to distinguish cells overgrown from CPE sometimes. When the cells were overgrown, they were aggregated into small clusters and clumped; most of the cells were detached. This phenomenon was similar to CPE of Ad41 infected Hep-2 cells. Therefore, the 6 cultures [VC6536 on Hep-2 cells, VC8775 on A549 cells, VC7941 on A549 cells, VC5774 on A549 cells (blind passage (bp) 1), AC5774 on Hep-2 cells (bp1) and VC10488 on Hep-2 cells (bp1)] which were shown or suspected to show CPE were subject to a Direct Immunofluorescent Assay (DFA) test (Appendix A, 2.2). Only 3 out of 6 cultures (VC6536 on Hep-2 cells, VC5774 on A549 cells and VC5774 on Hep-2 cells) were positive for adenovirus by DFA. The cultures which did not show CPE were passaged once more and CPE was observed for 7 days. Only 1 (VC10488 on A549) out of 16 infected cultures shown suspected CPE after the second blind passage (Appendix B, Table B-5, B-6). However, it was demonstrated to be DFA negative (Table 3.1).

3.3.1.2 Molecular analysis

Of the 6 cultures that were suspected to show CPE, the three cultures (VC6536 on Hep-2 cells, VC5774 on A549 cells and VC5774 on Hep-2 cells) that were positive for adenovirus by CPE and DFA were tested by Taqman® PCR. Although one stool sample (VC5774) showed strong and obvious CPE on both Hep-2 and A549 cells, it was negative for Ad41 with real-time RT-PCR. It was previously reported that Hep-2 and A549 cell lines support the growth of several types of adenoviruses (Hashimoto et al. 1991; Perronhenry et al. 1988); DFA was not Ad41 selective but was applicable to general adenoviruses. The primers and probes for Taqman® RT-PCR were designed particularly to detect Ad41 thus the method was specific and accurate. Furthermore, both the Hep-2 and A549 cultured samples of VC5774 were demonstrated to be positive for Ad4 by Taqman® PCR with Ad4 specific primers and probes. Ad4 is a respiratory type of adenoviruses. The stool sample VC6536 infected onto Hep-2 cells was the only one that induced CPE, and was DFA positive for adenovirus, and was positive for Ad41 with Taqman® PCR (Table 3.2).

Table 3.2 Condition of stool samples cultured on Hep-2 and A549 cell lines

	Cell line	Hep-2	A549
Primary inoculation	CPE	1/11	2/11
	DFA	1/1	0/2
	Real-time RT-PCR	1/1	
First blind passage	CPE	2/10	1/9
	DFA	1/2	1/1
	Real-time RT-PCR	0/1	0/1
Second blind passage	CPE	0/8	1/8
	DFA		0/1
	Real-time RT-PCR		

3.3.2 Cell Culture (stool sample VC6536) and Virus Passage on Hep-2 Cells

Out of the 11 stool samples which were subject to initial and first blind passages, stool sample VC6536 infected Hep-2 cells was the only one that showed CPE and was demonstrated to be Ad41 positive by Taqman® PCR. To propagate more viruses and test the optimum inoculum level, stool sample VC6536 was infected on Hep-2 cells and passaged as shown in Figure 3.1. Filtered stool sample VC6536 10% PBS dilution was utilized to infect Hep-2 and A549 cells. Cells were infected when the cell monolayer achieved 80-90% confluence. Virus inoculums were removed from the flasks after contacted with the cells for 1 h without any medium; maintenance medium was added to the flasks then. Infected cells were kept at 37°C and under 5% CO_2 for observation of maximum CPE.

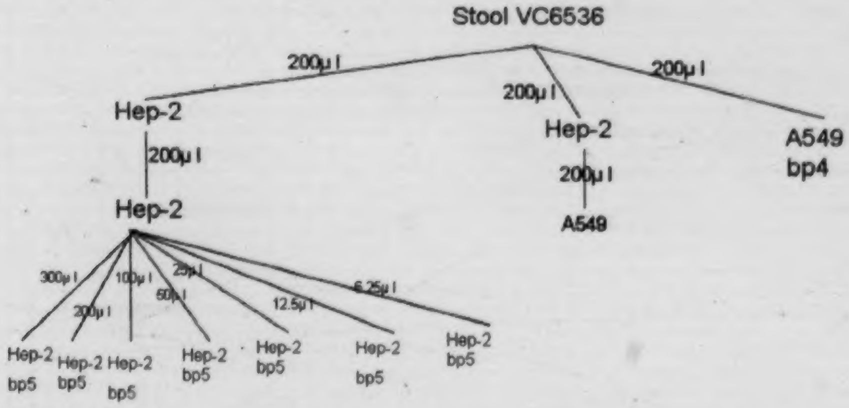

Figure 3.1 Flowchart of passage of stool sample VC6536 on Hep-2 and A549 Cells

Hep-2 and A549 cells were infected with 200 μL 10% PBS diluted stool sample VC6536 when 80-90% confluent growth was achieved in 25 cm^2 flasks. Experiments were carried out in duplicate. The original stool sample VC6536 was used to infect both Hep-2 and A549 cells. Different volumes of inoculum were applied to determine the optimum inoculum level on Hep-2 cells. Blind passages were applied if no signs of CPE had appeared after 7 days of observation.

3.3.2.1 Infectivity assay based on CPE

CPE was observed to appear on day 5 after viral stock infected on Hep-2 cells but was not observed up to day 7 on A549 cells. Hep-2 cells were suspended in the culture fluid and transferred to a 15 mL tube. The viruses were released by 3 freeze-thaw cycles; the suspension was harvested and the supernatant was kept as Ad41 viral stock. Fresh Hep-2 cells were then infected with Ad41 stock with different volumes which were 300 μL, 200 μL, 100 μL, 50 μL, 25 μL, 12.5 μL and 6.25 μL (Figure 3.1).

However, no signs of CPE were observed after 7 days for the primary inoculation in any of the cultures. Blind passages were processed up to 5 times, but still no CPE was observed. Fresh A549 cells were infected with 200 μL Ad41 stock and no CPE was observed after 7 days of culture. The A549 cells inoculated with 200 μL stool sample VC6536 without showing CPE were subject to blind passages up to 4 times, but still no CPE was observed.

3.3.2.2 Molecular analysis

Table 3.3 shows the Ct (threshold cycle) value of different cell cultures. Two hundred micro liters of stool VC6536 sample infected Hep-2 cells harvested culture supernatant was collected for nucleic acid extraction and Taqman® RT-PCR. Although none of these cultures showed signs of CPE, most were positive for Ad41 mRNA using Taqman® RT-PCR. Analyses were in duplicate.

Table 3.3 Ct (threshold cycle) value of cell cultures

cell culture	Ct (1)	Ct (2)
Stool VC6536 (200 μL)	24.59	24.57
VC6536 on Hep-2 bp5 (300 μL)	26.19	26.25
VC6536 on Hep-2 bp5 (200 μL)	26.00	25.94
VC6536 on Hep-2 bp5 (100 μL)	**23.09**	**23.12**
VC6536 on Hep-2 bp5 (50 μL)	27.78	27.50
VC6536 on Hep-2 bp5 (25 μL)	31.56	31.23
VC6536 on Hep-2 bp5 (12.5 μL)	37.59	37.95
VC6536 on Hep-2 bp5 (6.25 μL)	37.06	37.50
VC6536 on Hep-2 6536 (200 μL) - A549	28.73	29.17
Stool VC6536 (200 μL) - A549 bp4	>45	>45

It was concluded that 100 μL of stock Ad41 was the optimum volume of inoculum for 80-90% confluence of Hep-2 cells in 25 cm^2 flasks, because it resulted in the lowest Ct value at bp 5 (Table 3.2). The lower Ct indicated the higher concentration of viruses. Ct (23.09, 23.12) of stool sample VC6536 on Hep-2 cells at bp 5 with 100 μL inoculum was lower than Ct (24.59, 24.57) of original stool sample VC6536, which indicated that virus replication happened. For each passage, 100 μL viral stock was infected on Hep-2 cells in 5 mL medium and same amount of cell culture supernatant was withdrawn to detect. Therefore, as long as Ct remained same passage by passage, virus replication happened successfully. It was obvious that A549 cells were not as good as Hep-2 cells for supporting growth of Ad41 due to the high Ct values of Ad41 on A549 cells. The Ct of stool sample VC6536 on A549 cells at bp4 was larger than 45, which could be considered that the sample was negative for Ad41. Therefore, A549 cell line was not suitable to propagate Ad41 (stool sample originated from PLPH). Hep-2 cell line was able to propagate Ad41 (stool sample originated from PLPH) and could be successfully tested by Taqman® RT-PCR, however, the propagation of viruses did not reflected on traditional CPE based infectivity detection method. This also suggested that Taqman® RT-PCR was more sensitive. Another advantage of Taqman® RT-PCR is that it is quantitatively informative on trivial difference among viral mRNA concentrations (Table 3.2).

3.3.3 Comparison of mRNA and DNA in the Supernatant

Because only infectious viruses can enter cells and transcribe mRNA during replication, detection of viral mRNA during cultivation is reported to be a definitive indication of the presence of infectious viruses (Ko et al. 2003). The PCR assays with and without DNA digestion were performed on the same concentration of viral dilution. The RT-PCR assay with digestion was to quantify the mRNA level. The purpose of the PCR assay with digestion was to check for any residual contaminant DNA; the purpose of the PCR assay without digestion was to quantify the DNA level and to compare it to mRNA level. The Ct of supernatant of stool sample VC6536 passaged onto Hep-2 cells after harvesting is shown in Table 3.4. The DNA analysis by PCR was diluted the same fold as mRNA analysis by RT-PCR.

Table 3.4 Comparison of viral mRNA, viral DNA and residual DNA after digestion in supernatant

	mRNA (RT-PCR)	Total DNA (PCR)	Residual DNA after digestion (PCR)
Ct	26.77	21.87	>45

According to the standard curve (Appendix A, 2.8), the amount of total DNA in the supernatant was over 10 times more than the amount of mRNA. This also confirmed that the amount of DNA in Ad41 is much higher than mRNA since Ad41 is a DNA virus. A Ct of residual DNA was greater than 45 after digestion so that cannot be detected by Taqman® PCR (maximum cycle 45) in this study, which suggested that residual DNA had all been damaged by DNase I during digestion.

3.3.4 Consistency of Taqman® RT-PCR

To test the consistency of Taqman® RT-PCR, the supernatant of infected Hep-2 cells which showed complete CPE (all cell were rounding up and detached from flask walls) was collected and frozen at -70°C and thawed at 22°C for 3 times. The supernatant was withdrawn and processed 3 times on 3 different days, starting from extraction to obtain total nucleic acid, RT to transcriptase mRNA into cDNA thus able to be detected by PCR. Taqman® PCR was performed once with the three sets of cDNA collected on the 3 different days. A standard curve was generated when running PCR to quantify viral mRNA (Appendix A, 2.8). The results are shown in Table 3.5.

Table 3.5 RT-PCR results of three measurements

Day	1	2	3
Ct	27.02	26.91	26.66
Viral copies/mL	1.02×10^4	1.11×10^4	1.35×10^4

For the three viral copies, $\bar{x} = 1.16\times10^4$, $S = 1705.9$, according to t-distribution (n < 20), under 95% confidence, the accepted confidence interval is

$$\bar{x} \pm t_{\alpha/2,\gamma} \frac{S}{\sqrt{n}} = 1.16\times10^4 \pm 6116.24$$

The three viral copies results were within the confidence interval, thus it is reliable at 95% confidence.

The results indicated that the Taqman® RT-PCR is consistent at detection of the infectivity of Ad41 within a 95% confidence interval.

3.4 Conclusion

The results indicated that neither CPE nor DFA is specific in detection of Ad41, especially for stool sample origins which may contain several types of adenoviruses. Taqman® PCR and RT-PCR are more sensitive because primers and probes are specifically designed for the detection of Ad41. Taqman® RT-PCR was more sensitive for viral detection on cell culture than was observation of viral CPE on Hep-2 and A549 cells. For those infected cells that never showed CPE even after five blind passages, Ad41 could be detected by Taqman® RT-PCR. Hep-2 cells were believed to support the propagation of Ad41 better than A549 cells and this was confirmed by Taqman® RT-PCR. Because Ad41 is a DNA virus, Table 3.4 confirmed that the DNA viral copy number is much higher than the mRNA viral copy numbers. Table 3.5 indicated that the consistency of Taqman® RT-PCR is perfect. It is suggested that this method is reliable and can be applied in identification and quantification of Ad41 mRNA in the future.

However, because real-time quantitative RT-PCR is a newly emerged method which has not been used in many research studies yet, the traditional CPE based infectivity assays is still considered the benchmark. Although the stool sample VC6536 successfully infected Hep-2 cells for primary inoculation and confirmed with CPE, the viral stock failed to show CPE of continuous virus passage. To strengthen the persuasion and confirm the advantage of Taqman® RT-PCR, a comparison between traditional CPE based infectivity assay and Taqman® RT-PCR is essential.

HEK293 cells and Ad41 (Tak strain) were purchased from ATCC before commencement of cell culture with Hep-2 and A549 cells.

HEK293 cells were recommended in several studies to support the growth of Ad41 Tak strain (Dejong et al. 1983; Pieniazek 1989). Therefore, HEK293 cells and Ad41 Tak Strain were purchased from ATCC to verify the advantage of Taqman® RT-PCR indicated in this chapter and confirm the reliability by comparison with the CPE based cell culture infectivity assays.

Chapter 4 Comparison of Molecular Methods to the CPE Based Cell Culture Infectivity Assays for Determining UV Inactivation of Ad41

4.1 Introduction

Human adenoviruses are classified into six subgroups (A-F). Adenovirus 40 and 41 (subgroup F) are enteric adenoviruses which are important etiological agents of pediatric gastroenteritis (Ko et al. 2005a), and have been perceived to be the most prevalent adenovirus in water systems (Jothikumar et al. 2005). They are the second most commonly identified agent of pediatric gastroenteritis to rotavirus (Ko et al. 2005b). Enteric adenoviruses have been found in water and wastewater, and have been placed on the United States Environmental Protection Agency (USEPA) Contaminant Candidate List (CCL) (USEPA 1998).

UV disinfection has become more popular in recent years in drinking water treatment. In comparison to chemical disinfectants, UV does not inactivate microorganisms by chemical reaction; therefore, it does not result in the formation of disinfection by-products as other disinfectants (USEPA 1999). Germicidal UV is absorbed by nucleic acids of microorganisms, which causes photoproducts such as thymine dimers on the same nucleic acid strand (Ko et al. 2005b). It has been shown that adenoviral particles irradiated by UV are not capable of producing infectious progeny; however, repair occurs sometimes (Rainbow and Mak 1973). If damage is not repaired, DNA replication is blocked and the microorganism is inactivated (Ko et al. 2005b).

The HEK293 cell line, which is a Ad5 transformed 293 cell line, has been demonstrated to be particularly useful for Ad41 growth (Tiemessen and Kidd 1995). A standard approach for interpreting enteric adenoviruses inactivation after UV treatment has not been agreed upon. There is a lack of a standard method. Identification of enteric adenovirus methods can be achieved by cell culture infectivity assays based on observation of CPE, molecular techniques and methods that cell culture and molecular techniques. Infectivity methods involve inoculating the viral sample onto host cells and then allowing virus replication to progress to the point that visible signs of cell infection occur. Usually these visible signs are called cytopathic effects (CPE), which are observable changes that take place in the host cells as a result of virus replication. Such changes may be observed as changes in morphology, including rounding or formation of giant cells, or formation of a hole in the host cell monolayer due to localized lysis of virus-infected cells (Maier 2000). CPE is one of the most commonly used methods for detecting and quantifying viruses in cell culture. However, because adenovirus 40 and 41 grow slowly in cell culture, it usually takes up to 7-10 days to produce CPE. Sometimes, they do not produce clear and consistent CPE before cells become overgrown (Ko et al. 2005a). For Ad40 and Ad41 which do not plaque efficiently, the Most Probable Number (MPN) (Maier 2000) method may be used (Meng and Gerba 1996) to quantify infectious viruses.

Molecular methods such as PCR, RT-PCR, and probe hybridization have been used to detect adenoviruses because of their rapidity, sensitivity and specificity. PCR is capable of differentiating specific viruses. PCR is highly sensitive so that it is capable of detecting viruses in low numbers in cultures in which CPE was not observed or replication occurred without signs of CPE.

Real-time PCR is less time-consuming than conventional PCR, because a confirmation step such as gel electrophoresis and additional hybridization are generally not required. Taqman® is a PCR based assay with laser scanning technology to excite fluorescent dyes present in the specially designed Taqman® probes or SYBR green which emit a fluorescent signal upon binding to double strand DNA molecules. The results are plotted as a sigmoidal curve in which the numbers of cycles are plotted as against fluorescence. The x-intercept of the curve is proportional to the viral DNA copies. Viral mRNA copies can also be reflected in an RT-PCR, with a digestion and a RT step prior to PCR. However, there are a number of limitations of conventional nucleic acid amplification techniques. Detection by PCR indicates only the presence of nucleic acid which includes DNA and mRNA. It does not provide any information on infectivity, which is a primary interest for evaluating risks to public health (Ko et al. 2005a). Only infectious viruses can produce mRNA. It was shown that the ratio of Ad41 viral particles and the number of infectious units is high (~10^5) (Brown et al. 1992), thus it is difficult to estimate virus infectivity by PCR.

Integrated methods combine cell culture infectivity assays with molecular methods and are thus able to detect viruses that do not produce CPE, and can detect specific serotypes using post-assay genotyping of infectious viruses (Yates et al. 2006). It has been demonstrated that the combined methods integrate the reliability of infectivity detection of cell culture and the advantage of PCR based analysis. Integrated cell culture-PCR involves inoculating the sample onto suitable host cells. The viral DNA is extracted from the cells and analyzed using PCR (Chapron et al. 2000). To avoid false positive of Adenovirus 41, mRNA extracted from the infected cells can be detected by application of real-time quantitative RT-PCR following cell culture, which reflects viral infectivity (Ko et al. 2005a). Real-time Quantitative PCR and real-time quantitative RT-PCR can be used to quantify the number of adenovirus particles that are present following cell culture (Choi and Jiang 2005; He and Jiang 2005; Jiang et al. 2005; Jothikumar et al. 2005; Ko et al. 2005a).

It is not yet known how well cell culture infectivity assays based on observation of CPE correlates with integrated cell culture real-time PCR, real-time RT-PCR, direct PCR, and direct RT-PCR, when these assays are used to quantify infectious viruses following UV inactivation. Except direct RT-PCR, all of these methods have been applied in previous studies. However, no studies have made a direct comparison among these methods.

In this study, all real-time PCR and RT-PCR analysis was done using Taqman®. Taqman® sequence detector integrates a PCR-based assay and innovative hardware/software instrumentation to give a system for high-throughput quantification of nucleic acid sequences. Combining thermal cycling, fluorescence detection, and application of specific software, it enables the cycle-by-cycle detection of the increase in the amount of PCR product. In Taqman® PCR, the cycle number at which the increase in fluorescence is exponential is measured. This is shown by the horizontal line in the figure generated by the software. The point at which the fluorescence crosses the threshold is called the Ct. A standard curve is then computed from the Ct of the diluted adenovirus standards using the software, and absolute quantities for the unknown samples is then extrapolated based on their threshold cycle (Ct) values.

The objective of the experiments described in this Chapter was to determine the correlation CPE based cell culture infectivity assay with integrated cell culture real-time quantitative (Taqman®) PCR, integrated cell culture real-time quantitative (Taqman®) RT-PCR, direct real-time quantitative (Taqman®) PCR and direct real-time quantitative (Taqman®) RT-PCR for measuring infectivity of viruses following UV inactivation.

4.2 Materials and Methods

4.2.1 Cell Culture

Ad41 strain TAK 73-3544 (#VR 930) (1 mL) was obtained from American Type Culture Collection (ATCC). The HEK293 cells (CRL-1573) (1 mL) which were obtained from ATCC, originated from F.L. Graham at passage 35 and were used in this study between passage 35 and 60. HEK293 cells were subcultured once a week at a subcultivation ratio of 1:2 to 1:4. The cells were grown in growth medium (Appendix A, 1.1). For the primary passage of Ad41 from stock, HEK293 cells were seeded into a 75 cm^2 Biocoat flask (from ATCC) with growth medium and incubated for 24 to 48 h at 37° C, 5% CO_2. When the cells achieved 80-90% confluent growth, growth medium was removed. The monolayer was rinsed with 5 mL PBS and 1 mL Ad41 strain TAK 73-3544 (#VR 930) (ATCC) inoculum was added into the flask and spread out on the monolayer. The flask was incubated at 37°C and 5% CO_2 for 1 h. Maintenance medium (Appendix A, 1.1) was added to a 30 mL final volume without removing the inoculum because the HEK293 cells were easily detached from the flask walls, especially after 1 h incubation with viruses. The culture was examined under a microscope daily for CPE (cells rounded up and detached) until CPE development was observed or 7 days elapsed, whichever came first. Infected cells were disrupted by 3 cycles of freeze-thaw to release intracellular viruses. The flask was frozen at -70°C and thawed at 22°C. When the flask contents thawed to a "slush", the flask was shaken vigorously to dislodge any cells that still stuck to the walls. Gently shaking was continued until all large ice chunks were melted. The cell suspension was transferred to conical tubes and centrifuged at 1375 × g for 10 min. The suspension was collected and cell debris was removed after centrifugation. The suspension was dispensed into flat bottom screw cap tubes, parafilm sealed and frozen with liquid nitrogen for long term storage. Virus passages using the frozen Ad41 stock suspensions were carried out using the same procedure.

4.2.2 Virus Purification

AdEasy Virus Purification Kit (Strategene, #240244) was used to purify Ad41 for two UV exposure experiments. HEK293 cells were infected with Ad41 stock and cells were grown until most cells showed complete CPE. Infected cells and medium were pooled, and the cells were pelleted by centrifugation at 822 × g for 15 min. The supernatant was decanted into a sterile container and stored at 4°C. Cell pellets were re-suspended in 10 mL of the reserved supernatant. The cells were frozen using a -70°C freezer and thawed at 22°C three times to disrupt cells. Cell debris was concentrated by centrifugation at 822 × g for 15 min. The supernatant was decanted and reserved supernatant from the previous step was added to bring the final volume to 60 mL. Sixty micro liters of benzonase nuclease was added into the 60 mL of the sample. The sample was mixed and incubated at 37°C, 5% CO_2 for 30 min. The viral supernatant mixture was clarified by passing through a 0.45 μm filter, and 7 mL of 10 × loading buffer was added. Ad41 supernatant was purified using a Sartobind® filter. The Sartobind® filter unit was prepared by rinsing with PBS to remove air from the Sartobind® housing. Filtered supernatant was passed through the Sartobind® filter unit at 10 mL/min flow rate using a syringe. The Sartobind® filter unit was washed with 60 mL washing buffer at a flow rate of 10-20 mL/min and was then eluted with 1 mL elution buffer at a drop-by-drop flow rate. Viral eluate was collected in a sterile 15 mL tube. For long term storage and further concentration, viral eluate was transferred to a centrifuge concentrator and was centrifuged for 15 min at 604 × g at

22° C. The concentrate that remained in the upper chamber was further concentrated. Buffer was exchanged before use in the tissue cell culture. Filtrate was discarded when the sample volume reached 1 mL and 4 mL of maintenance medium was added to the concentrate to bring the volume to 5 mL. This brought the virus to normal physiological conditions. Purified virus was re-suspended by gently pipetting up and down a few times before recovery by pipette. Purified virus suspensions were dispensed into tubes and stored at -70°C.

4.2.3 UV Exposure

A collimated beam UV apparatus (Calgon Carbon Corporation, USA) containing a 10 W, low pressure mercury arc lamp (Ster-L-Ray Germicidal Lamp, model G12T6L, 15114, Atlantic Ultraviolet Corporation, Hawpange, NY) was used in this study. The lamp emitted monochromatic UV at nearly 254 nm and was suspended horizontally in the lamp chamber. The emitted UV light was delivered through a 24 cm long collimation tube with an aperture diameter of 7 cm to provide reasonably parallel and uniform radiation to the surface of the test suspension. The distance from the lamp to the surface of test suspension was 44 cm. The test suspension was placed on an adjusted platform mounted over a stirrer. For each UV exposure, a volume of 0.5 mL purified or unpurified Ad41 culture was suspended in a 5 mL 0.1M PBS in a sterile glass Petri dish (40 mm × 10 mm) containing a stir bar (10 mm × 2 mm), the stirring speed was 300 rpm. The virus suspension was vortexed for 30 s before pouring into the Petri dish. The Petri dish was fitted with a quartz lid to prevent potential exposure to biohazardous aerosols. Since UV is not believed to be affected by temperature or pH, only a single temperature and pH was investigated in the inactivation experiments. Four UV exposure experiments were performed at pH 7 and 22° C. The depth of the viral suspension in the Petri dish was 4 mm. Viral suspension were placed beneath the collimated beam and irradiated for predetermined times (methods in 4.2.4) (Figure 4.1).

Figure 4.1 Collimated beam apparatus

Samples were withdrawn for the viral assay. Control samples which were not subject to UV but treated in the same condition as those irradiated samples were collected at the same time to determine if viral inactivation occurred in the absence of UV irradiation.

4.2.4 Exposure Time and Fluence Rate Determination and Control

The UV dose is calculated as the product of fluence rate and exposure time (Bolton and Linden 2003). The UV exposure doses for Ad41 in this study were designed to be 40, 80, 160 and 320 mJ/cm^2. Exposure time was controlled with a shutter and measured using an automated stop watch in the UV apparatus. The fluence rate was measured by a calibrated UV radiometer. The reason to select high UV doses is that Ad41 was believed to be resistant to UV. Within the selected UV doses, it has been reported the inactivation of Ad41 between 1-log and 4-log in previous studies. The fluence rate at center of the Petri dish was measured and recorded with a calibrated UV 254 nm detector (Optometer P9710, P-9710-Z SN 3323M, Gigahertz optik). The UV detector was placed at the center of the collimated beam at the surface of the station with the quartz lid covered. Several corrections were required to obtain the average fluence rate which viruses were exposed in the water. Four factors were considered when using the low pressure UV lamp; they were *Reflection Factor*, *Petri Factor*, *Water Factor* and *Divergence Factor*.

According to one study (Bolton and Linden 2003), the *Reflection factor* for the air-water interface is 0.975.

The *Petri factor* was determined by drawing a 0.5 cm × 0.5 cm grid and placed the center of the grid at the center of the collimated beam. The fluence rate was measured with the radiometer every 0.5 cm in the x and y directions of the grid. The *Petri factor* was determined by dividing fluence rate at each point by the fluence rate at center, and taking the average these ratios (Bolton and Linden 2003).

The *Water Factor* was calculated by Eqn. 1 (Morowita 1950).

$$\textit{Water Factor} = \frac{1\text{-}10^{-al}}{al\ln(10)} \qquad \text{Eqn. (1)}$$

where a = decadic absorption coefficient (cm^{-1}) or absorbance for a 1 cm path length and l = vertical path length (cm) of the water in the Petri dish. The absorbance for a 1 cm path length of the samples at 254 nm was measured by a UV-Vis spectrophotometer (UV-2401 PC, Shimadzu Corp., Columbia, Maryland).

For distance from the lamp more than four times the aperture diameter, the *Divergence Factor* was calculated by Eqn 2.

$$\textit{Divergence Factor} = \frac{L^2}{(L+x)^2} \qquad \text{Eqn. (2)}$$

where L is the distance from lamp to the surface of the sample and x is the depth of the sample. The depth-average germicidal fluence rate E_{avg} (Wm^{-2}) was calculated as:

$$E_{avg} = E_0 \times \textit{Petri Factor} \times \textit{Reflection Factor} \times \textit{Water Factor} \times \textit{Divergence Factor} \qquad \text{Eqn. (3)}$$

where E_0 = UV radiometer reading at the center of the dish and at a vertical position, The UV dose was

$$H = E_{avg} \times t \qquad \text{Eqn. (4)}$$

where t is the exposure time (s).

The required exposure time t was determined by dividing the target UV dose by the product of correction factors and the UV fluence rate.

4.2.5 Set-up of UV Inactivation of Ad41 Experiments

Four sets of UV inactivation experiments were carried out with four passages of Ad41. The first one experiment was performed with unpurified Ad41 under UV exposure. This experiment was performed with only one sample. The second experiment was performed with unpurified Ad41 with three replicate samples under UV exposure. The third experiment was carried out with purified Ad41 with only one sample. The last experiment was carried out with purified Ad41 with three replicate samples under UV exposure. For those experiments with replicate samples, UV inactivation was finished in a single day to ensure consistent environmental and UV exposure conditions.

4.2.6 Assay of Ad41 after UV Inactivation

4.2.6.1 Cell culture CPE based $TCID_{50}$ infectivity assay

For the experiments that have only one sample exposed under UV, the only sample was withdrawn and analyzed by cell culture CPE based $TCID_{50}$. For those that have three UV exposure samples, one sample was randomly selected from the three samples for $TCID_{50}$ analysis. Because CPE based $TCID_{50}$ is labor intensive, thus only one out three samples was analyzed for each experiment.

Decimal dilutions (up to 10^{-6}) of UV-exposed suspensions of Ad41 and non-UV exposure negative controls were diluted. HEK293 cells were cultured in 25 cm^2 Biocoat flasks (from ATCC) until 60% confluence, and were inoculated with the decimal dilutions. The flasks were incubated at 37°C, 5% CO_2 for 1 h, and then 4 mL of maintenance medium were added without removing the inoculum. Culture flasks were prepared in quadruplicate for each dilution for the $TCID_{50}$ calculation. Flasks were incubated at 37°C, 5% CO_2 for 7 days and were examined CPE by microscope day by day until 7 days. The end point of the titration was the highest dilution showing evidence of viral infection in 50% of the four inoculated flasks. This $TCID_{50}$ end point can be calculated with the Karber equations. Details of the calculation method are provided in Appendix C. Some previous studies used infectious units (IU) as a unit of virus quantification instead $TCID_{50}$ infectious particles/mL in this study. It was suggested that 1 $TCID_{50}$ end point infectious particles was equal to 0.7 of a infectious unit (Vacquier and Cardiff 1979).

4.2.6.2 Direct and integrated cell culture real-time quantitative PCR and RT-PCR assay

For the experiments that have only one sample exposed under UV, the only sample was withdrawn and analyzed by direct real-time quantitative RT-PCR. For those that have three UV exposure samples, one sample was randomly selected from the three samples for direct real-time quantitative PCR and RT-PCR.

Integrated cell culture RT-PCR was reported to reflect the infectivity of viruses after inactivation thus gained great interest in this study. Each sample in each UV inactivation experiment was collected and analyzed with integrated cell vulture real-time quantitative PCR and RT-PCR.

Taqman® (real-time quantitative) PCR and RT-PCR were performed directly on dilutions of the UV-exposed and control suspensions, prior to inoculation on the HEK293 cells, as well as on the cell culture. Taqman® PCR tested the amount of nucleic acid which includes viral DNA and mRNA. Taqman® RT-PCR detects only viral mRNA under the condition that contaminant DNA has been completely damaged. Therefore, Taqman® RT-PCR with a DNA digestion step measured mRNA only. Because Ad41 is a DNA virus, there is a much higher copy number of DNA than mRNA. The accurate detection of mRNA depends on complete removal of the DNA in Ad41.

For direct Taqman® PCR and RT-PCR, samples were withdrawn after UV exposure. The difference between RT-PCR and PCR in this study was that RT-PCR had additional steps of digestion, which was aimed at removing contaminant DNA, and RT, which was transformed mRNA into cDNA. For direct real-time quantitative RT-PCR, total nucleic acid was extracted from the collected inactivation samples using MagaZorb RNA extraction kit (Cortex Biochem, CA, USA) (procedures in Appendix A, 2.3). Deoxyribonuclease I (DNase I) was added to the extracted products to remove contaminated DNA as a digestion (procedures in Appendix A, 2.4) for RT-PCR analysis. This step was not performed for PCR analysis. The RT reaction was performed using the GeneAmp® PCR System 2700 (Applied Biosystems). The RT reaction conditions were 42°C for 60 min followed by 70°C for 15 min (Appendix A, 2.5). The reaction mixture was then kept at 4°C (Appendix A, 1.2). PCR amplification was performed using an ABI PRISM 7000 Sequence

Detection System (Appendix A, 2.8). The PCR conditions were: amplification at 50°C for 2 min followed by 95°C for 10 min, 45 cycles of denaturation at 95°C for 15 s, annealing at 60°C for 1 min, and extension at 72°C for 1 min. Enteric adenovirus-specific primers (Hexon) were used to detect hexon gene sequences. These primers yielded an amplicon of 65 base pair DNA amplified by Ad41 specific primers (Table 3.1). The PCR analysis was following all the procedure of RT-PCR described above except digestion and RT.

For integrated cell culture Taqman® PCR and RT-PCR, Ad41 were harvested after incubation for 7 days using cell culture techniques described previously (4.2.1). The HEK293 cell pellet was discarded and the supernatant containing the viral particles was collected. All the other procedures in the following were exactly the same as their counterparts of direct PCR and RT-PCR.

4.3 Results

4.3.1 UV Inactivation Measured by cell culture CPE Based $TCID_{50}$

In total, four experiments of UV inactivation of Ad41 were performed. In experiment 1 and 2 purified Ad41 preparations were exposed to UV whereas in experiment 3 and 4 unpurified Ad41 preparations were exposed to UV. UV exposures in experiment 2 and 4 were done in triplicate. However, because of the complicated and laborious work of $TCID_{50}$ titration, only one UV inactivated virus sample was randomly selected for $TCID_{50}$ analysis in experiments 2 and 4. The calculation of the concentration of viruses was described in Appendix C. The results of UV inactivation measured by cell culture CPE based TCID$_{50}$ are shown in Table 4.1.

Table 4.1 UV inactivation of purified and unpurified Ad41 detected by cell culture CPE based TCID$_{50}$

UV dose (mJ/cm^2)	Log (N_0/N_t)*			
	Unpurified virus		Purified virus	
	Exp1	Exp2	Exp3	Exp4
0	0.00	0.00	0.00	0.00
40	0.77	0.54	1.00	1.21
80	1.01	1.00	2.32	1.44
160	2.16	1.77	3.32	2.21
320	3.19	2.71	4.00	3.21

*N_0 is the concentration of Ad41 before UV exposure; N_t is the concentration of Ad41 after UV exposure under certain UV doses (Raw data in Appendix B, table B-1 to B-26).

Table 4.1 shows the UV inactivation of both unpurified and purified Ad41 as determined by cell culture CPE based TCID$_{50}$. The inactivation of purified viruses was slightly higher than that of unpurified viruses. At the UV dose of 320 mJ/cm^2, the inactivation of purified Ad41 was as high as 4-log in experiment 3, whereas it was only 2.71-log for unpurified Ad41 in experiment 2. Figure 4.2 illustrates the UV inactivation of purified and unpurified Ad41 at different UV doses as determined by cell culture CPE based TCID$_{50}$.

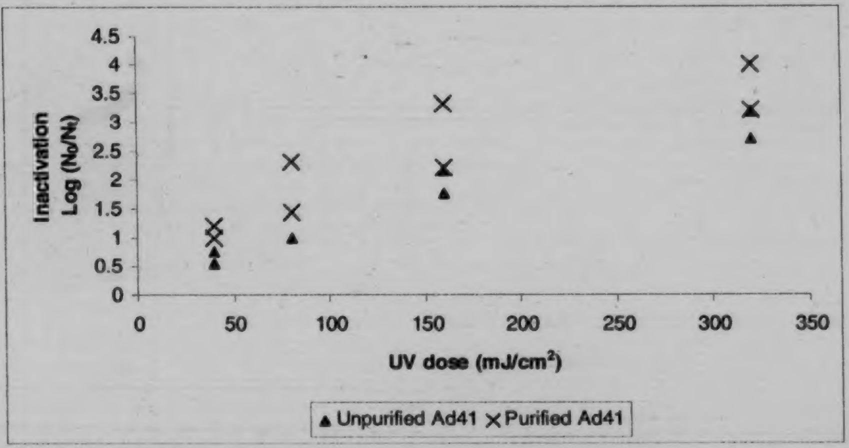

Figure 4.2 UV inactivation of Ad41 versus UV dose response curve tested by cell culture CPE based $TCID_{50}$. There are two replicates of purified and unpurified viruses with same UV dose inactivation (Raw data in Appendix B, table B-7 to B-32).

The titers of live Ad41 in the UV exposed suspensions before UV exposure in each experiment are shown in Table 4.2. The titers were determined by cell culture CPE based $TCID_{50}$.

Table 4.2 Ad41 initial titers before UV exposure in each experiment

	Unpurified virus		Purified virus	
	Exp1	Exp2	Exp3	Exp4
Viral Titer ($TCID_{50}$ infectious particles/mL)	$3.56*10^4$	$1.86*10^5$	$4.16*10^5$	$1.62*10^5$

The titer of experiment 2, 3 and 4 were all as high as 10^5 $TCID_{50}$ infectious particles/mL. The titer in experiment 1 was 3.56×10^4 $TCID_{50}$ infectious particles/mL (Table B-33 to B-36).

4.3.2 UV Inactivation Measured by Direct Taqman® PCR and RT-PCR

In previous research (Yates et al. 2006), direct molecular techniques such as PCR were applied to detect adenoviruses particles in environmental water samples. Although PCR could detect adenovirus particles, it was not known if PCR would provide an indication of infectivity of the virus particles that were detected. Both direct Taqman® PCR and RT-PCR were performed in this study to detect viral copy numbers after UV inactivation. A standard curve of the quantitative PCR response (Ct) versus the number of viral copies generated for quantified adenoviruses is shown in Figure 4.3. The adenovirus DNA copy number was quantified by spectrophotometer. The procedure to quantify virus concentration and generate standard curve is described in Appendix A, 2.6, 2.7 and 2.8. The quantification procedure was developed and verified with cytomegalovirus in other studies in PLPH. The protocol was adapted for quantification of Ad41 in this study and performed by the group members of Dr. Pang's group in PLPH.

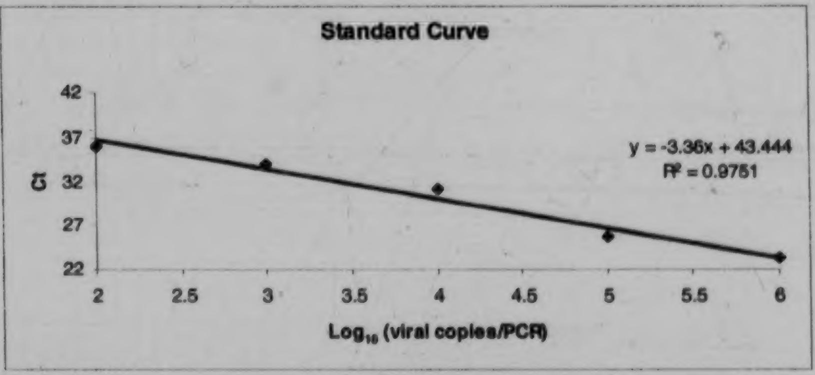

Figure 4.3 Standard curve of the viral copies/PCR versus Ct (threshold cycle) of adenovirus for Taqman® PCR. The Ad41 concentration in the following UV inactivation was determined by this standard curve. This is a first-order curve with $R^2 = 0.9751$.

The threshold cycle (Ct) is the cycle where there is the first detectable increase in fluorescence. It indicates the starting amount of DNA template which is correlated to the number or viral particles present in a sample. According to the model generated by the standard curve, the concentration of Ad41 in an unknown sample can be determined from the Ct value measured by Taqman® PCR.

Figure 4.4 shows the inactivation of viruses measured by direct Taqman® PCR and RT-PCR. One sample of exposure experiments 2 and 4 which have three replicates was randomly selected for direct mRNA and DNA detection. The only samples in experiments 1 and 3 were taken to analyze Ad41 by direct Taqman® RT-PCR. Due to some reason, sample of experiment 1 was not analyzed by Taqman® PCR, the sample of experiment 3 was analyzed by Taqman® PCR.

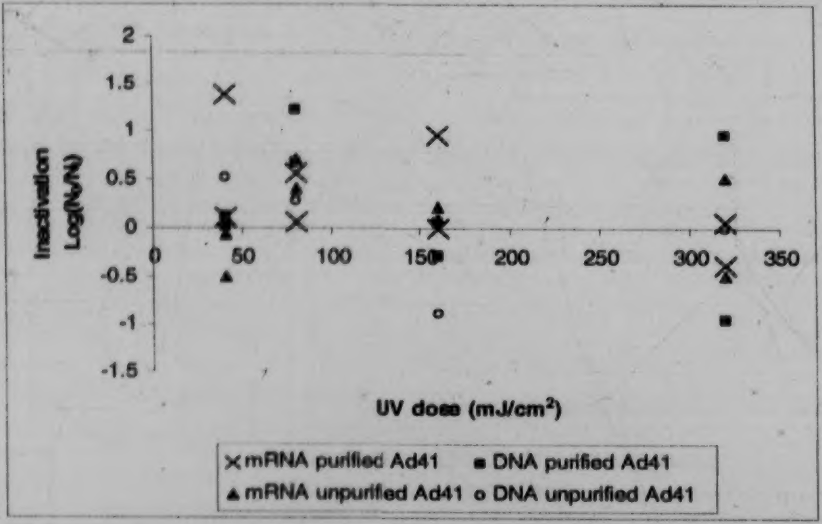

Figure 4.4 UV inactivation of Ad41 as measured by direct Taqman® PCR and RT-PCR. Two samples of purified and two samples of unpurified Ad41 were analyzed by Taqman® RT-PCR; two samples of purified and one sample of unpurified Ad41 were analyzed by Taqman® PCR (Raw data in Appendix B, table B-37 to B-39).

Figure 4.4 shows that the UV inactivation of Ad41 indicated by mRNA or DNA copies was randomly distributed. To calculate the inactivation of Ad41 by UV, the following Eqn (5) was used.

$$Log(Inactivation) = Log\frac{N_0}{N_t} \qquad \text{Eqn (5)}$$

where N_0 = viral titer of negative control, N_t = viral titer of inactivated Ad41. The titers for all molecular analysis in this study indicated the concentration of the diluted samples undertaken Taqman® PCR DNA amplification; those were not the absolute concentration of the inactivated virus samples. Non UV-exposure negative control samples were processed and analyzed by molecular methods followed the same procedure as for inactivated viruses; a logarithm inactivation was calculated following Eqn (5).

For example, to calculate the UV inactivation of Ad41 analyzed at 80 mJ/cm^2 by direct Taqman® RT-PCR of experiment 1, the required data was as follows in table 4.3 (reproduced from table B-37, B-38 and B-39 in Appendix B).

Table 4.3 Calculation of UV inactivation of Ad41 analyzed by direct Taqman® RT-PCR

UV dose of 80 mJ/cm^2	Threshold Ct	Viral titer (viral copies/PCR)	Log inactivation
Non UV-exposure negative control	28.12	$10^{4.56}$	0.699
Inactivated Ad41	30.47	$10^{3.86}$	

Based on Standard curve shown in figure 4.3, the viral titer for non UV-exposure sample was $10^{4.56}$ viral copies/PCR, the titer for inactivated Ad41 sample was $10^{3.86}$ viral copies/PCR. According to Eqn (5), the log inactivation is

$$Log\frac{N_0}{N_t} = Log\frac{10^{4.56}}{10^{3.86}} = 0.699$$

The calculation of inactivation analyzed by direct Taqman® PCR followed the same procedure of the inactivation analyzed by direct Taqman® RT-PCR described above.

It is hard to see any correlation between UV dose and the UV inactivation with this method. An ANOVA (Analysis of variance) of the data set was carried out based on a 95% confidence level, the assumption that the residuals were randomly distributed was confirmed by n-score plot (Figure C-1 and C-2 in Appendix C). However, neither UV dose nor purification had a significant effect on UV inactivation of Ad41 analyzed by direct Taqman® PCR and RT-PCR (ANOVA in Appendix C, table C-3, C-4). This result were definitely contradicted with cell culture CPE based TCID$_{50}$ analysis since inactivation was different under different UV doses. Further analysis was discussed in section 4.3.4. The negative results were probably due to variation and randomness. Therefore, direct Taqman® PCR or RT-PCR was not able to detect the infectivity changes that were measured by cell culture CPE based $TCID_{50}$ after UV exposure of Ad41.

4.3.3 UV Inactivation of Ad41 Measured by Integrated Cell Culture Taqman® PCR or RT-PCR

Figure 4.5 shows UV inactivation of both purified and unpurified Ad41 based on integrated cell culture Taqman® RT-PCR detection. To calculate the inactivation of Ad41 by UV analyzed by cell culture integrated Taqman® RT-PCR, Eqn (5) was used. For example, to calculate the UV inactivation of Ad41 analyzed at 80 mJ/cm^2 by integrated cell culture Taqman® RT-PCR of experiment 1, the required data was as follows in table 4.4 (reproduced from table B-40 in Appendix B).

Table 4.4 Calculation of UV inactivation of Ad41 at UV dose of 80 mJ/cm^2 analyzed by direct Taqman® RT-PCR

UV dose of 80 mJ/cm^2	Threshold Ct	Viral titer (viral copies/PCR)	Log inactivation
Non UV-exposure negative control	24.23	$10^{5.72}$	1.08
Inactivated Ad41	27.85	$10^{4.64}$	

Based on Standard curve shown in figure 4.3, the viral titer for non UV-exposure sample was $10^{5.72}$ viral copies/PCR, the titer for inactivated Ad41 sample was $10^{4.64}$ viral copies/PCR. According to Eqn (5), the log inactivation is

$$Log\frac{N_0}{N_t} = Log\frac{10^{5.72}}{10^{4.64}} = 1.08$$

The calculation of inactivation analyzed by integrated cell culture Taqman® PCR followed the same procedure of the inactivation analyzed by integrated cell culture Taqman® RT-PCR described above.

All samples after UV exposure in each experiment were withdrawn and collected for analyses. Samples were infected onto 60% confluent HEK293 cells. Inoculated HEK293 cells were incubated for 7 days at 37° C, 5% CO_2 before harvesting. Contaminant DNA was removed by digestion with DNase I (Procedures in Appendix A, 2.4) and the absence of residual DNA was confirmed by Taqman® PCR. In total, an ANOVA of the data was carried out based on 95% confidence level, residuals were randomly distributed by confirmation of n-score plot (Appendix C, figure C-3). There was a statistical significant difference between inactivation on purified and unpurified Ad41 (Appendix C, table C-7, C-8), which indicated that UV dose and purification have effects on UV inactivation of Ad41 analyzed by integrated cell culture Taqman® RT-PCR.

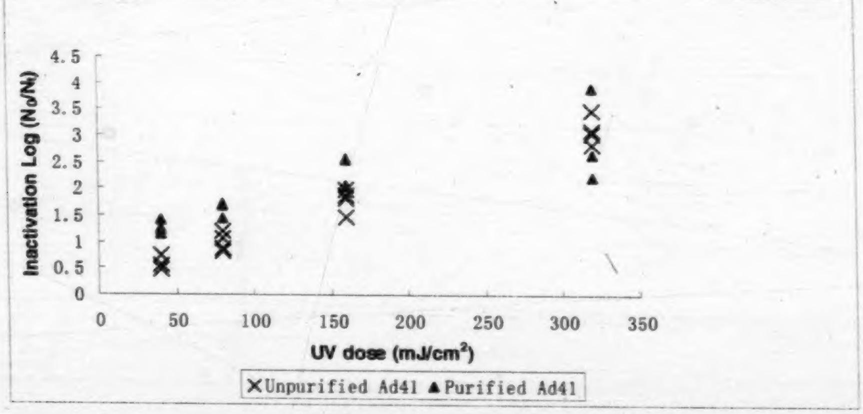

Figure 4.5 UV inactivation of Ad41 as function of UV dose as measured by HEK293 cell culture with Taqman® RT-PCR detection. Both purified and unpurified viral stocks were exposed to UV at doses of 40, 80, 160 and 320 mJ/cm^2. Samples were withdrawn after UV exposure and infected on HEK293 cells. After 7 days incubation, supernatant was withdrawn and analyzed by Taqman® RT-PCR (Raw data in Appendix B, table B-40 to B-43).

Figure 4.6 shows the UV inactivation of Ad41 detected by HEK293 cell culture integrated with Taqman® PCR for detection of viral infection on the cells. The highest measured inactivation was 2.15-log at a UV dose of 320 mJ/cm^2. This was much lower than that measured by integrated cell culture Taqman® RT-PCR or by cell culture CPE based TCID$_{50}$ determination, which was around or higher than 3.5-log in this study. The inactivation of unpurified viruses was higher than those of purified viruses at UV doses tested. An ANOVA was carried out based on a 95% confidence level, the residuals were randomly distributed by confirmation of n-score plot (Appendix C, figure C-4). The parameter of purification had a significant effect on UV inactivation of Ad41 (Appendix C, table C-9, C-10). However, based on 95% confidence level, there was a significant difference in analysis of UV inactivation of Ad41 between integrated cell culture Taqman® PCR and cell culture CPE based

TCID$_{50}$ (ANOVA in Appendix C, table C-11, C-12, figure C-5). Since cell culture based method is a traditional and well accepted method, integrated cell culture Taqman® PCR is not reliable in analysis infectivity of Ad41.

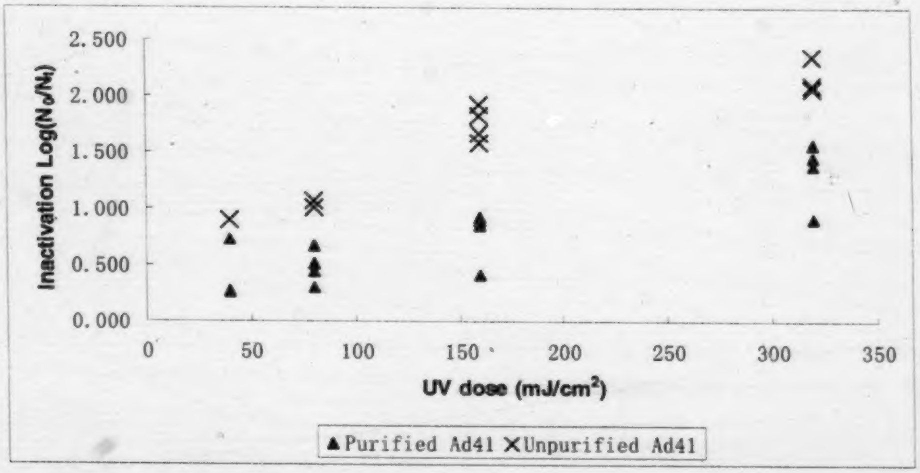

Figure 4.6 UV inactivation of Ad41 as a function of UV dose as measured by HEK293 cell culture with Taqman® PCR detection. Both purified and unpurified viral stocks were exposed to UV at doses of 40, 80, 160 and 320 mJ/cm^2. Samples were withdrawn after UV exposure and infected onto HEK293 cells. After 7 days incubation, supernatant was withdrawn and analyzed by Taqman® PCR (Raw data in Appendix B, table B-34 to B-37).

4.3.4 Comparison of Cell Culture CPE Based Infectivity Assay and Molecular Methods for Measuring Ad41 Inactivation by UV

UV dose - inactivation curves for Ad41 for all experiments as determined by HEK293 cell culture with detection by CPE and integrated with Taqman® RT-PCR are shown in figure 4.7 and 4.8 for unpurified and purified Ad41 virus preparations, respectively.

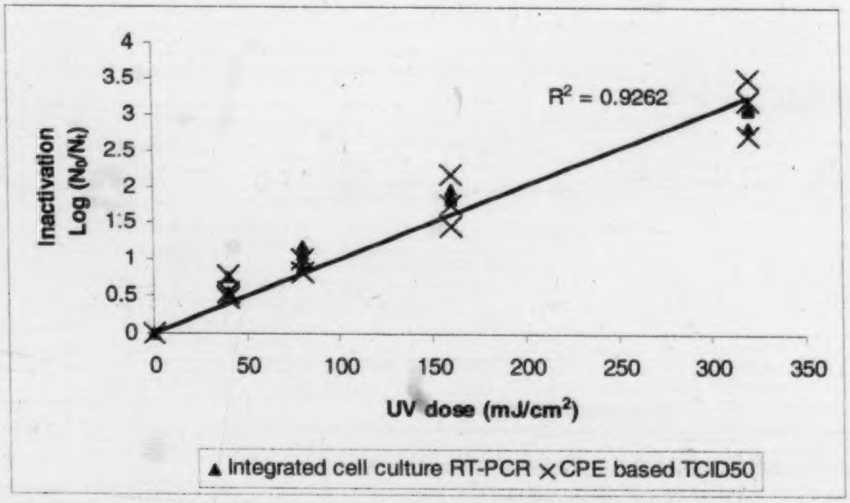

Figure 4.7 Comparison of cell culture with CPE and cell culture integrated with Taqman® RT-PCR for measuring UV inactivation of unpurified Ad41 (raw data in Appendix B, table B-40 to B-43).

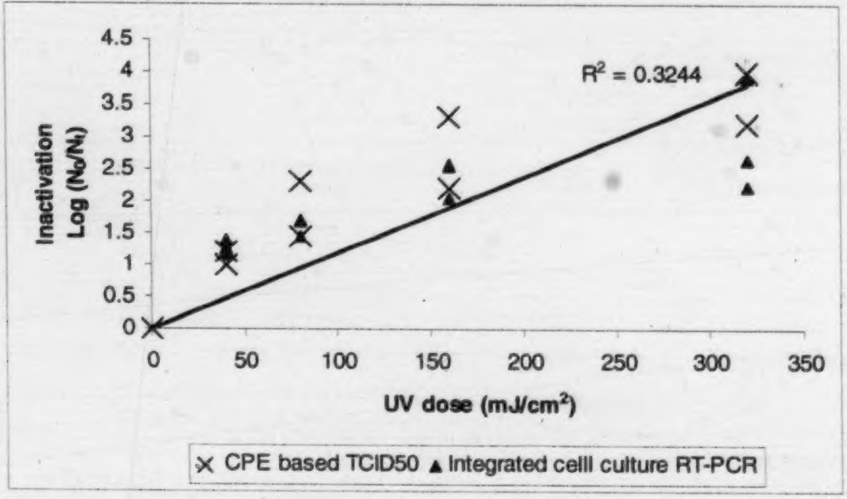

Figure 4.8 Comparison of cell culture with CPE and cell culture integrated with Taqman® RT-PCR for measuring UV inactivation of purified Ad41 raw data in Appendix B, table B-40 to B-43).

An ANOVA based on 95% confidence level of Ad41 inactivation measured by cell culture CPE based $TCID_{50}$ and cell culture integrated with RT-PCR was performed, there was no significant difference on UV inactivation as measured by traditional CPE based cell culture assay and integrated cell culture with RT-PCR analysis. The normal distribution of residuals was confirmed by n-score plot (Appendix C, figure C-5). Assuming that it was a first-order reaction, the UV inactivation of unpurified Ad41 as function of UV doses showed a good fit with an $R^2 = 0.9262$. However, the UV inactivation of purified Ad41 as function of UV doses showed a bad fit with an $R^2 = 0.3244$. This suggests that the inactivation of purified Ad41 in this study did not apply to a first-order model and that the tailing in the curve at higher dose was present.

Direct molecular analysis based on detection of either DNA by PCR or mRNA by RT-PCR as described in 4.3.2 was not able to reflect inactivation when compared to traditional cell culture with CPE detection. Integrated cell culture with detection of viral DNA on the HEK293 cells by Taqman® PCR was able to show the inactivation effect after inactivation and there was a trend of UV dose versus inactivation. However, the inactivation was lower than the one measured by cell culture CPE based $TCID_{50}$ at each UV dose. There was significance on UV inactivation of Ad41 between CPE method and integrated cell culture Taqman® PCR, which indicated the latter method is not reliable for analysis of UV inactivation of Ad41. Integrated cell culture Taqman® RT-PCR with detection of mRNA on HEK293 cell culture provided excellent agreement with the traditional CPE detection method.

4.4 Discussion

4.4.1 UV Inactivation of Ad41

Several researchers have compared the inactivation of Ad40 and Ad41 by UV at different UV doses. There is some variation between the UV dose inactivation-response of enteric adenovirus reported in these studies (Figure 4.9); however, there is general agreement between the studies.

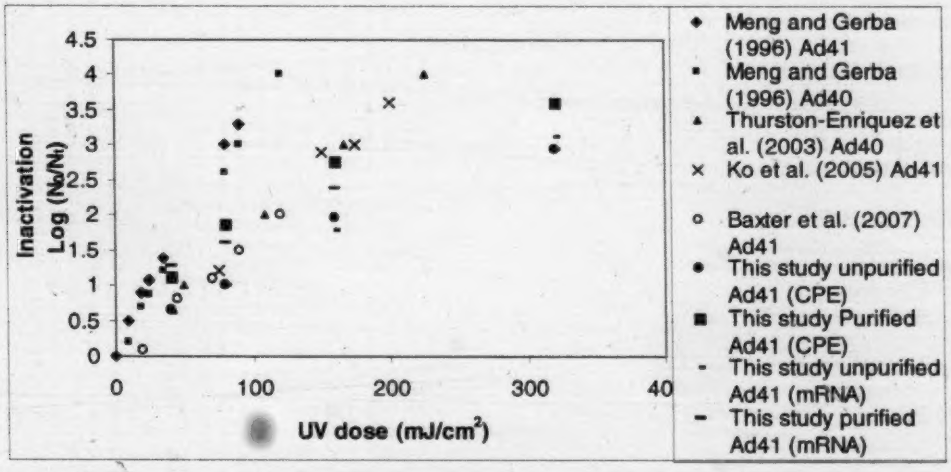

Figure 4.9 UV inactivation of enteric adenovirus reported in previous studies and this study. CPE represents cell culture CPE based $TCID_{50}$ method; mRNA represents integrated cell culture RT-PCR method.

According to the previous studies (Baxter et al. 2007; Ko et al. 2005b; Thurston-Enriquez et al. 2003a), Ad40 and Ad41 were very resistant to UV. A 4-log inactivation required more than UV dose of 200 mJ/cm^2. The inactivation of purified Ad41 exposed to UV doses up to 160 mJ/cm^2 in this study compared well to UV inactivation reported by Thurston-Enriquez et al. (2003), Ko et al. (2005), and Baxter et al. (2007) in their studies. The inactivation of unpurified Ad41 in this study was lower than purified Ad41 at the same UV doses. The results of Meng and Gerba (1996) for both Ad40 and Ad41 inactivation showed higher inactivation at the same UV doses. The UV inactivation of purified Ad41 at UV dose of 320 mJ/cm^2 was around 3.5-log in this study. This inactivation level was even lower than that reported in previous studies (Ko et al. 2005b; Thurston-Enriquez et al. 2003a) at UV doses of 200 and 225 mJ/cm^2. The lower inactivation at higher UV dose (320 mJ/cm^2) in this study could be related to the tailing in the inactivation curve (Figure 4.8) which could be related to virus aggregation. Virus aggregation may be related to purification procedures.

Because there is no standard method to analyze the UV inactivation of Ad41, there are some discrepancies between UV susceptibilities among previous studies. CPE based infectivity assays (Meng and Gerba 1996; Thurston-Enriquez et al. 2003a), CPE combined with fluorescence assays (Baxter et al. 2007), and cell culture integrated with real-time RT-PCR assays (Ko et al. 2005b) were used to detect UV inactivation of Ad41. Only 120 mJ/cm^2 UV dose was required to achieve a 4-log inactivation in one study (Meng and Gerba 1996), whereas higher doses were required in other studies (Figure 4.9). None of the previous studies tested UV dose as high as 320 mJ/cm^2. A dose of 300 mJ/cm^2 was applied in one study (Ko et al. 2005b), but reliable inactivation result was not obtained due to low initial Ad41 concentration. At UV doses lower than 200 mJ/cm^2, the UV inactivation of Ad41 was following a first-order reaction (Ko et al. 2005b; Meng and Gerba 1996; Thurston-Enriquez et al.

2003a). In previous studies (Ko et al. 2005b; Thurston-Enriquez et al. 2003a), the UV dose required for 4-log inactivation was extrapolated from a first-order extrapolation of the inactivation measured at lower UV doses, with the assumption that the equation is first order as followings:

$$\log_{10}(N_t / N_0) = -kEt \qquad \text{Eqn. (6)}$$

where N_0 is the concentration of infectious viruses at UV exposure time 0, N_t is the concentration of infectious viruses at UV exposure time t, k is the inactivation rate or slope of the inactivation curve, E is UV fluence rate (mW/cm^2), and t is the exposure time (s). In this study, however, we found that the UV inactivation reaction of purified Ad41 did not fit the first order but had a tailing at high UV dose (320 mJ/cm^2) (Figure 4.8).

In addition, there are many factors that may affect UV inactivation results on Ad41. There are variances on UV exposure procedure, the host cells to produce viruses, the measures of infection, procedures used for virus harvesting, purification and concentration. Table 4.4 summarizes the methods used in the different UV inactivation studies on enteric adenovirus.

Table 4.5 Experimental procedures and analysis methods in previous studies and this study on UV inactivation of enteric adenovirus

Reference	UV set-up	Host cells	Number of freeze-thaw cycles to release intracellular viruses	Purification and extraction product	Initial concentration of viruses	Analysis methods
Meng and Gerba (1996) (Ad40 and Ad41)	a low-pressue UV vapor, enclosed in a glass tube, intensity detection at 254 nm	PLC/PRF/5 (ATCC)	5	Freon treated cell pellet and medium mixture; cell lysate and cell pellet were collected and resuspended in PBS as viral stock	10^6 IU/ml	TCID$_{50}$, CPE observed up to 3 weeks
Thurston-Enriquez (2003) (Ad40)	an 8-W low pressure mercury vapor germicidal lamp, emitted UV light at 253.7 nm	PLC/PRF/5 (ATCC)	1	Polyethylene glycol treated the cell and medium mixture; cell pellet was clollected and resuspended in test water; virus suspension was purified by chloroform as viral stock	not indicate	Observation of CPE by MPN general purpose program on plating 5 or 10 fold dilution
Ko et al. (2005)	A collimated beam UV apparatus containing two 15-w low pressure mercury vapor germicidal lamps emitting nearly monochromatic UV radiation at 254 nm	HEK293 (ATCC)	3	Cell pellet was lysed by β-mercaptoethanol and guanidium isothiocynate (GITC), and purified by oligo-dT latex	2×10^3 IU/ml	cell culture mRNA-RT-PCR
Baxter et al. (2007)	A collimated beam apparatus containing two low pressure UV lamps, intensity mesured at 254 nm	HEK293 and PLC/PRF/5	5	cell lysate was treated with cesium chloride to purify	10^5 IU/ml	Observation of CPE integrated with detection of newly made viral protein by fluorescent antibody
This Study	A collimated beam apparatus containing a 10W low pressure UV lamp, intensity mesured at 254 nm	HEK293 (ATCC)	3	cell lysate was either purified with AdEasy purification kit (Strategene) or without purification	Around 7×10^4 IU/ml	TCID$_{50}$, CPE observed up to 7 days; Intergrated cell culture RT-PCR

Although there were differences in UV exposure procedures, the number of freeze-thaw cycles, purification procedures and analysis methods, there was no statistically significant difference among inactivation enteric viruses in Thurston-Enriques (2003), Ko et al. (2005) and Baxter et al. (2007). The reason that Ad41 in one study (Meng and Gerba 1996) was less resistant to UV than Ad41 in other studies, including this study, is not clear. Previous speculated reasons such as the greater number of freeze-thaw cycles increased viral susceptibility (Thurston-Enriquez et al. 2003a) were ruled out by a later study (Ko et al. 2005b). This was confirmed by this study, since repeated freeze-thaw cycles were used.

The quality of the cells used in the infectivity assay could be a factor that determined the difference in reported inactivation of Ad41 between studies. It was suspected that the passage of viruses and infection conditions may have influence on the infectivity of viruses (Brown et al. 1992). It was reported that Ad41 (strain TAK) lost its infectivity selectively in HEK293 cells. The reason was unclear (Pieniazek 1989). The reason that a lower number of passages of HEK293 cells were used was to ensure that the cells were fresh and healthy enough to support the growth of viruses although results did vary sometimes. HEK293 cells did not attach well on regular culture flasks, thus Biocoat flasks were used in this study. However, inconsistent qualities of cells were observed during the experiments. It is recommended that flasks from the same batch be used in each experiment.

4.4.2 Correlation between CPE based Cell Culture Infectivity Assay and Direct Taqman® PCR/RT-PCR

Direct real-time PCR was used in detection of human adenovirus in environmental water in one study (Choi and Jiang 2005). This method was mainly used for qualification of Ad41 but not for quantification. Direct RT-PCR is generally used for detection of norovirus in environmental water after inactivation because tissue culture methods are not available for norovirus (Barker and Vipond 2004; Shin and Sobsey 1998). The limitation of direct RT-PCR as suggested in one study (Barker and Vipond 2004) is that it does not give any indication as to the viability and infectivity of residual viral RNA. This may lead to false positive indication of infectivity as inactivated norovirus could potentially release the viral RNA genome which could then be detected by RT-PCR. In this study, this was also observed with Ad41. DNA and mRNA from UV exposed viruses that were not able to replicate and produce CPE in HEK293 cells were still detected by direct PCR and RT-PCR. This study demonstrated that there is no statistical relation between traditional cell culture infectivity assays based on cell culture CPE observation $TCID_{50}$ and direct molecular assays for Ad41 detection after UV inactivation.

The advantage of real-time quantitative PCR/RT-PCR is apparent. First, it shows the increase of DNA copies as it amplifies, thus is called real-time. Second, no confirmation step such as gel electrophoresis which is involved in conventional PCR is required. Third, it is able to quantify the DNA copies of a virus as soon as a PCR run was done based on a standard curve. Although direct real-time quantitative PCR and RT-PCR is not reliable to analyze the infectivity of Ad41, real-time quantitative RT-PCR is powerful and efficient when integrated with cell culture.

4.4.3 Correlation between CPE based Cell Culture Infectivity Assay and Integrated Cell Culture Real-time Quantitative RT-PCR

Both CPE based tissue cell culture infectivity assays and integrated cell culture real-time RT-PCR have been used in previous UV inactivation studies for determining Ad41 inactivation. However, no studies did a direct comparison between the two methods. And no study utilized real-time quantitative RT-PCR. This study tested the cell culture CPE based $TCID_{50}$ and integrated cell culture real-time quantitative RT-PCR side-by-side for measuring the UV inactivation of Ad41. Within 95% confidence level, there was no significant difference between these two methods based on an ANOVA (section 4.3.3). This suggested that the laborious cell culture with CPE method may be substituted by the integrated cell culture real-time quantitative RT-PCR method for future studies.

Cell culture integrated with real-time RT-PCR has been used to analyze UV inactivation of Ad41 in one study (Ko et al. 2005b), viral titers were estimated by MPN method based on positive and negative mRNA RT-PCR results from replicate cell culture flasks per dilution for serially diluted samples. The quantification step needed a lot of work. The Taqman® PCR used in this study combined PCR and quantification together. According to the standard curve, quantitative results were available directly after PCR without additional purification or analysis steps. The results of UV inactivation of Ad41 by the integrated cell culture Taqman® RT-PCR and traditional cell culture CPE based $TCID_{50}$ were consistent, based on a 95% confidence level (section 4.3.3). Moreover, this method is rapid and easily quantifying a large number of virus samples.

4.4.4 Comparison of UV Inactivation of Purified and Unpurified Ad41

It was reported that there was no statistically significance in inactivation of Ad5 in clarified cell lysate compared with that of Ad5 fully purified by cesium chloride, based on a t-test at 95% confidence level (Baxter et al. 2007). In this study, purification was a significant factor on UV inactivation for most analysis methods. The inactivation of purified Ad41 was about 0.5-log higher than inactivation of unpurified Ad41 at same UV dose (Figure 4.2). Appropriate purification is able to remove those substances that may inhibit or affect inactivation effects. However, it might also increase the degree of virus aggregation.

In previously studies (Baxter et al. 2007; Ko et al. 2005b; Meng and Gerba 1996; Thurston-Enriquez et al. 2003a), the inactivation was characterized by first-order reaction kinetics. The dose required for 4-log inactivation was extrapolated based on this assumption for some of previous studies (Ko et al. 2005b; Thurston-Enriquez et al. 2003a). In our study, however, it was found out that the inactivation did not follow first-order reaction kinetics, especially for purified Ad41 (Figure 4.8); there was a tailing in the UV dose-inactivation curve (Figure 4.8).

Tailings have been observed in UV dose-inactivation curves of *Cryptosporidium parvum* oocysts using medium and low pressure UV (Craik et al. 2001). *Cryptosporidium parvum* is 4-6 μm in diameter, which is about 50 times larger than Ad41. Shielding of organisms due to high oocyst densities, poor mixing or the presence of small sub-population that was resistant to UV were proposed as possible explanations for the tailing (Craik et al. 2001). It is known that Ad41 is very resistant to UV, a UV dose as high as 320 mJ/cm^2 was tested in our study. The tailing was appeared at UV dose of 320 mJ/cm^2, and was apparent for purified Ad41. The appearance of tailings is often associated with aggregation, or clumping of microorganisms. It could be also induced by the presence of more UV resistant sub-population. Because Ad41 is one of the most UV-resistant viruses, there are fewer possibilities that more resistant sub-population existed. Therefore, virus aggregation may be the reason of tailing in the UV dose-inactivation curves. Furthermore, the tailing was more significant on purified Ad41 than on unpurified Ad41. Since the purification procedure removed inhibitors of UV exposure such as extraneous cell debris, proteins etc, viral particles might be easily contacting with each other. The degree of the remaining virus aggregation was increased. This might explain why the tailing was more pronounced with purified Ad41. The tailing in the UV dose-inactivation curve (figure 4.8) may indicate that a high level of inactivation of Ad41 may be difficult to achieve with UV.

4.5 Conclusion

Around 3.5-log inactivation of purified and 3-log inactivation of unpurified Ad41 were demonstrated at a germicidal UV dose at 320 mJ/cm^2 for a low-pressure UV lamp. A higher UV dose may be needed to meet the 4-log inactivation removal requirement of USEPA. It is possible that the infected cells' quality and origin, incubation condition may have affected the inactivation results. The purification procedure may also have effect on inactivation results. Direct molecular analyses by PCR or RT-PCR without cell culture were not reliable for measuring the inactivation of Ad41 by UV. Viruses which lost their infectivity could still be detected by these methods. UV inactivation measured by integrated cell culture real-time quantitative RT-PCR and inactivation measured by the traditional analysis of cell culture with CPE detection were highly correlated at the UV doses tested in this study. At the 95% confidence level, there was no significant difference between these two methods. Inactivation measured using integrated cell culture PCR assay was lower than the inactivation measured using cell culture with CPE at same UV dose. The unique advantage of Taqman® PCR/RT-PCR is that it generated quantitative PCR results after PCR reaction without additional analysis step such as gel electrophoresis. This saved plenty of work and time. The UV dose-inactivation curve did not follow first-order reaction kinetics for purified Ad41, and was characterized by tailing at higher UV doses. This indicates that a very high level of inactivation of Ad41 maybe difficult to achieve by UV in practice. Inactivation of purified Ad41 was around 0.5-log greater than unpurified Ad41 at UV doses of 40, 80, 160 and 320 mJ/cm^2 applied in this study. Purification procedure removed extraneous cell debris and other impurities that might interfere with UV inactivation. Purification procedure might also increase the degree of virus aggregation which was more obvious at high UV doses.

The objective of this study was to determine how the direct molecular analysis and the integrated cell culture molecular analysis compared to cell culture with CPE detection for measuring UV inactivation of Ad41. Among those tested methods, integrated cell culture real-time quantitative RT-PCR was found to be highly correlated with the CPE method. Because Ad41 is fastidious and does not plaque efficiently and produce consistent CPE, a most probable number procedure (MPN) is always used for quantifying virus infectivity in a sample. For the MPN method, at least 4 replicate samples are required for each dilution. If the initial concentration of Ad41 is about 10^5 infectious particle/mL; 5 levels of dilution are required for quantification at least. The experimental procedure is laborious and very time-consuming. Examination of each culture flask or well under the microscope for CPE for 7 days is necessary. Examination of over 100 flasks or wells may be required in each inactivation experiment when non-UV exposure negative control samples and samples exposed to different UV doses are considered. HEK293 is a semi-attachable cell line. HEK293 cells do not attach well on regular, uncoated flasks. Flasks coated with collagen on the bottom surfaces inside are available from ATCC and support growth of HEK293 cells. But those are twenty times more expensive than regular flasks. Although integrated cell culture real-time quantitative RT-PCR requires culturing, it does not essentially need to be replicated, because the results were shown quantitatively. In that case, flasks are much saved and a large amount of microscopy work can be omitted. Integrated cell culture with real-time quantitative RT-PCR was able to quantify the number of infectious virus in the inoculum accurately and rapidly without resorting to additional analysis.

Chapter 5 Detection of UV Inactivation of Ad41 with RT-CES^{TM} System

5.1 Introduction

RT-CES^{TM} System is a cell-based assay system to monitor cellular events by measuring the electronic impedance of sensor electrodes integrated on the bottom of microtiter E-Plates. Based on measured impedance a dimensionless parameter, Cell Index (CI), is derived and reported to provide quantitative information about the biological status of the cells, including cell number, viability, morphology, and cytoskeletal dynamics. A wide range of cell-based assays can be performed on the RT-CES^{TM} system. The objective of using RT-CES^{TM} in this study is to determine if RT-CES^{TM} could be used as an infectivity assay for enteric adenovirus. The advantage of RT-CES^{TM} is that it can automatically and quantitatively reflect cell morphological changes.

5.2 Materials and Methods

5.2.1 RT-CES^{TM} System

The RT-CES^{TM} system (ACEA Biosciences, San Diego, CA, USA) has three components. They are an electronic sensor analyzer, a device station, and a 16 × sensor device with 16 plastic wells with 9 mm well to well spacing, which is called E-Plate

(Figure 5.1). Six E-Plates can be received by the device station at most at one time for impedance measurement.

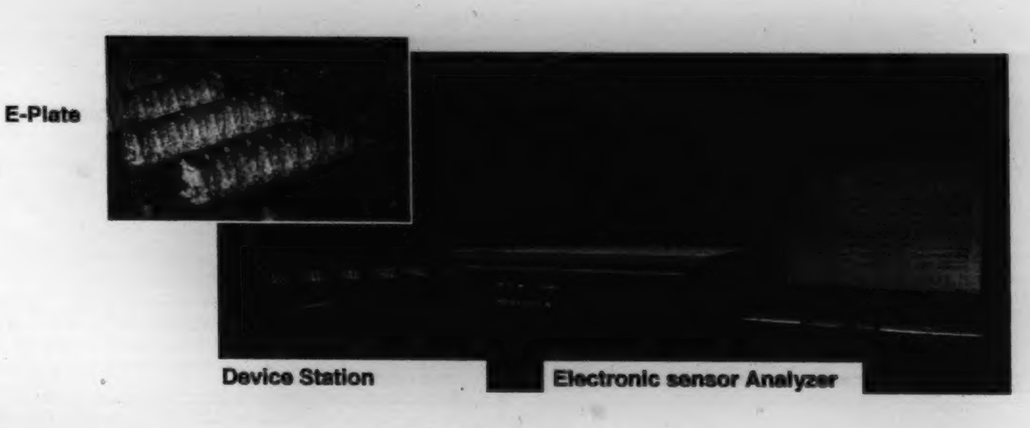

Figure 5.1 RT-CES™ System work station

In operation, the E-Plates with cultured cells were mounted onto the device station that was placed in a CO_2 incubator at 37°C, 5% CO_2. The device station was connected with the electronic sensor analyzer by an electronic cable. Under control of RT-CES™ software, wells were continuously measured. The electronic impedance was transferred to a computer and plotted.

The wells in an E-Plate were connected with an electrode impedance sensor array which is called the circle-on-line electrode sensors. They were specifically designed to cover approximately 80% of the bottom surface area of a well, and are fabricated on glass slides with lithographical microfabrication methods; and the electrode containing slides are assembled onto plastic trays to form electrode-containing wells (Figure 5.2).

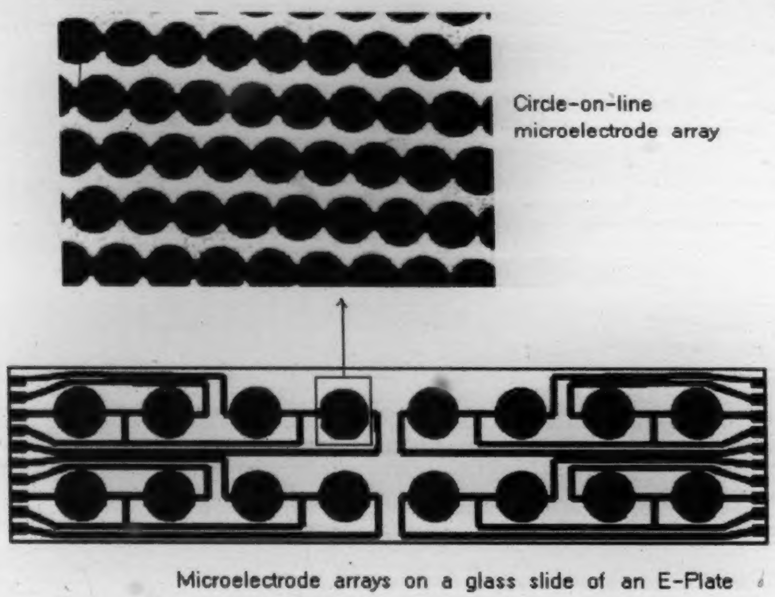
Circle-on-line microelectrode array
Microelectrode arrays on a glass slide of an E-Plate

(A) (Adapted from (Xing et al. 2005))

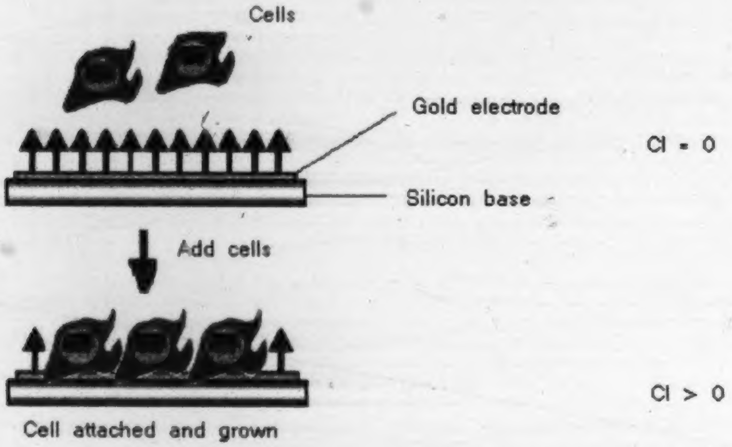

(B) (reproduced from (Xing et al. 2005))

Figure 5.2 E-Plates and cell electronic sensing system (A) 16 × sensor devices with 16 circle-on-line electrode array units are fabricated on glass slides with lithographic microfabrication methods. An enlarged unit of the circle-on-line electrode array is shown in the top panel. (B) A schematic illustration of the principle of cell detection on the RT-CES™ system. The presence of cells affects the local ionic environment at the electrode/solution interface, leading to an increase in the electrode impedance. More cells attaching to the electrodes leads to an increase in electrode impedance, which results in a larger cell index.

5.2.2 Cell Index (CI)

A parameter termed cell index (CI) represents cell status based on the measured electrical impedance. The CI is calculated by Eqn. (6):

$$\mathrm{CI} = \max_{i=1,\ldots,N}\left[\frac{R_{\mathrm{cell}}(f_i)}{R_{\mathrm{b}}(f_i)} - 1\right] \qquad \text{Eqn. (6)}$$

where N is the total number of the frequency points in each well of an E-Plate at which the impedance is measured, $R_{\mathrm{b}}(f_i)$ is the frequency dependent electrode impedance without cells present for point i, $R_{\mathrm{cell}}(f_i)$ is the frequency dependent electrode impedance with cells present for point i. i is the number of frequency points (Figure 5.2 (A)). Under the same physiological conditions, a larger CI is detected when more cells are attached onto the E-Plates, which means larger electrode impedance. A larger $R_{\mathrm{cell}}(f)$ induces a larger CI. In this way, CI functions as a quantitative parameter to reflect the number of cells attached. When no cells are attached to the E-Plates, the electrode cannot detect impedance, and $R_{\mathrm{cell}}(f)$ is equal to $R_{\mathrm{b}}(f)$, leading to CI = 0. When the number of cells which are attached onto the E-Plates is identical, the CI may change with changes in the cell condition. For example, an increase in cell adhesion which leads to an increase of cell/electrode contact area will lead to an increase in $R_{\mathrm{cell}}(f)$ and a larger CI.

5.2.3 Cell Culture and Cell Count

HEK293 and Hep-2 cells were grown in 75 cm^2 tissue culture flasks as described in sections 4.2.1 and 3.2.2. Once the cell monolayer achieved 80-90% confluence, growth medium was removed. The monolayer was rinsed with PBS and shaken or trypsinized and pipetted off the flasks. Cells were re-suspended in fresh growth medium and pipetted to distribute evenly in the medium. A small sample (0.1 mL) of cell suspension was removed from the culture aseptically and placed into a separate test tube. A hemocytometer and cover slip were set up. A drop of the culture combination was placed on the hemocytometer immediately. Cells were observed under a low power microscopy.

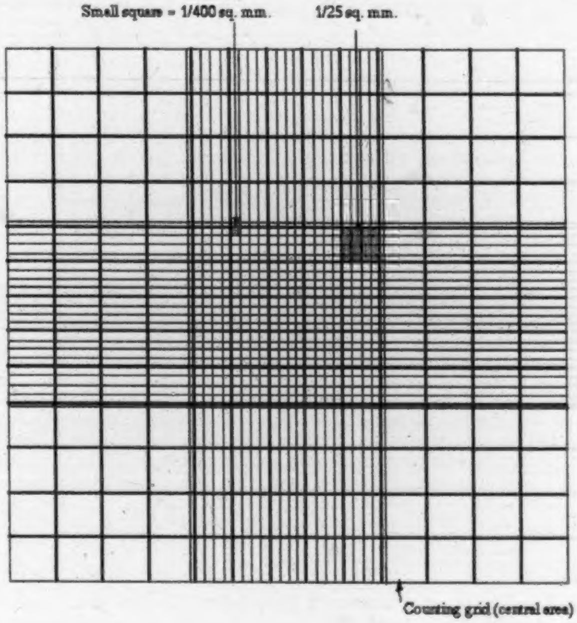

Figure 5.3 Hemocytomer counting grid

One entire grid on a standard hemacytometer with Neubauer rulings could be seen at 40 × magnifications (using the 4 × objective with 10 × ocular). The main divisions separated the grid into 9 large squares. Each square had a surface area of one mm^2, and the depth of the chamber was 0.1 mm. Suspensions were diluted enough so that the cells did not overlap each other on the grid, and were uniformly distributed. The total number of cells in the four large corner squares was counted. Each square had a surface area of 1 mm^2 and a depth of 0.1 mm, giving it a volume of 0.1 mm^3. The total number counted, X, was the cell number per 0.4 mm^3; X/4 multiplied by 10,000 determined the cell count per mL.

5.2.4 Cell Quantification

To test cell quantification on the RT-CES™ system, a cell calibration experiment was performed. The objective of the procedure was to determine which cell number of a certain cell line best facilitates the observation of viral infection. The "Scan Plate" function on the RT-CES™ software was performed to ensure every well was of good quality. If the message showed that there were problems with a certain well, that well was not used for experiments. For real time calculation of CI, based on impedance values as described above, the background impedance of each sensor well was measured in the absence of the cells. To do so, 50 µL of growth medium was added into each well, and the well was left at 25°C for 30 min for the baseline measurement. After the background impedance was measured, a message from the software indicated every well was ready to use. Then, 100 µL of the HEK293 cell suspensions, containing 5000, 10,000, 15,000, 20,000, 40,000 cells, respectively, were added into each of the 16 wells of an E-Plate. Or 100 µL of Hep-2 cell suspension, containing 4000 cells, were added into each well of an E-Plate. The sensor devices were placed into the CO_2 incubator at 37°C, 5% CO_2, and CI values were determined every 1 h automatically by the RT-CES™ system for up to several hundred hours depending on how fast the cells grew.

5.2.5 Sample loading

Ad41 was prepared as described in section 4.2.1. The viruses used in this chapter were not undergone purification. HEK293 cells were first mixed with serially diluted Ad41, and the mixture was added to the wells of an E-Plate. Hep-2 cells were added to the wells of an E-Plate and the E-Plate was inoculated with Ad41 after 25 h incubation under 37°C, 5% CO_2. The accommodated E-plates were located inside a tissue culture incubator at 37°C, 5% CO_2. The station was capable of switching any one of the wells on the E-Plates to the RT-CES^{TM} analyzer for impedance measurement. Under the control of RT-CES^{TM} Software, the electrode impedance was continuously monitored in real time over 200 h on the RT-CES^{TM} System and the measured impedance data was transferred to the computer. Cell index values, derived from the measured impedances, were continuously displayed on the integrated software user-interface.

5.3 Results and Discussion

5.3.1 Propagation of Ad41 on HEK293 Cells

To determine the optimum HEK293 cell E-Plate inoculum size, 40,000, 30,000, 20,000 and 15,000 cells were inoculated into different wells and the cell index was monitored over several days. Figure 5.4 shows the cell index of HEK293 cells from 76 h to 172 h after inoculation. HEK293 cells do not attach to flask surfaces readily, and they attached to the bottom surface of the E-Plates only after about 76 h of incubation following inoculation.

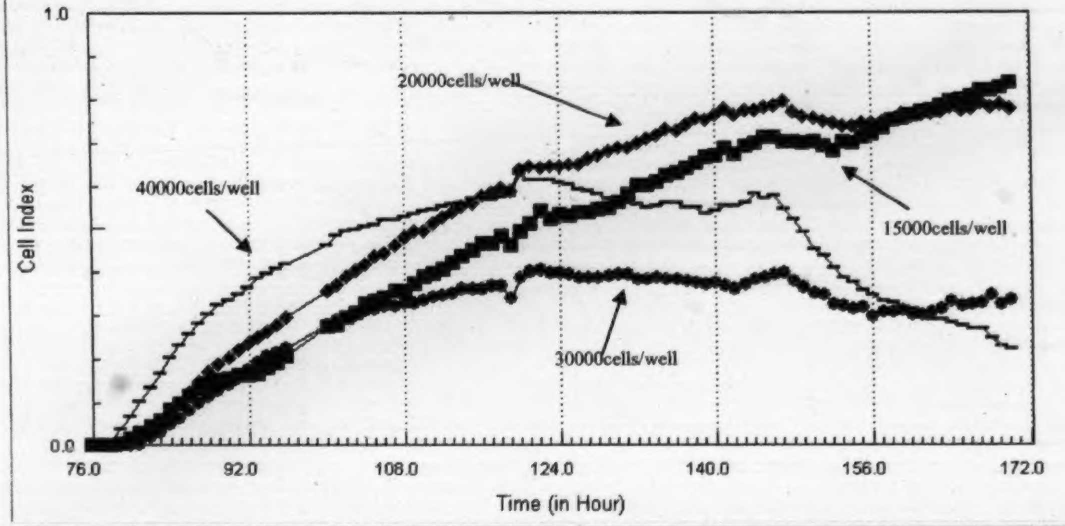

Figure 5.4 Cell Index versus time curve for different sizes of HEK293 cells inoculated into the E-plates. Cells were mixed with Ad41 in each well of E-Plates before which were accommodated onto the device station. Monitoring was lasted for 172 h.

CI started decreasing at around 150 h for inoculum sizes of 40,000 and 30,000 cells/well due to overgrowth of the cells. Cells stopped growing and maintained cell index was constant after 170 h for the inoculum of 20,000 cells/well. In contrast, cells continued to grow of the 15,000 cells/well inoculum even after 172 h. HEK293 cells are very easily detached from surfaces, thus growth medium was not taken out after inoculation. In terms of this, it was better to keep cells growing at a comparatively slow but constant pace. Therefore, an inoculum size of 15,000 cells/well was chosen as the optimum because it resulted in a continuous increase in the cell index. Thus, it should be easy to observe the effect of viruses on the cell growth without confusion with cell overgrowth.

Ad41 was inactivated by UV doses of 40, 160 and 320 mJ/cm^2. The UV exposed virus samples and non-UV exposed negative control samples were collected to monitor the infectivity on RT-CES™. HEK293 cells (15,000 cells/well, passage 38) were mixed with 10 μL of UV exposed or non-UV exposed negative control Ad41 suspensions in each well of E-Plates. The mixture of non-UV exposure Ad41 sample was at around 10^5 $TCID_{50}$ infectious viral particles/well. UV exposure experiments were carried out in duplicates and the results are shown in Figure 5.5.

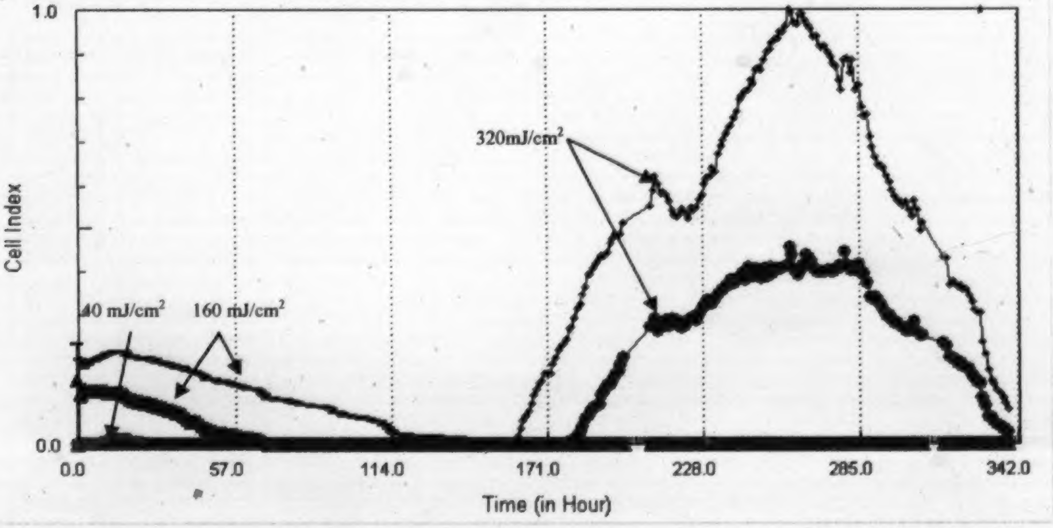

Figure 5.5 Growth of HEK293 cells inoculated with UV exposed Ad41 as monitored by RT-CES™. Cells were mixed with 10 μL of UV inactivated Ad41 and non-UV exposure negative controls. UV doses were 40, 160, 320 mJ/cm². Analyses were in duplicates.

There was significant variation in the cell index curve from duplicate UV exposure experiments. This variation was due to the poor adherence characteristics of HEK293 cells. For non UV-exposed negative control viruses and viruses exposed to UV doses of 40 and 160 mJ/cm², there was no obvious measurable appearance of CI curve after incubation for more than 100 h and thus, no cell growth. Cells were detected at time 0, however, they were gradually disappeared with time for samples including Ad41 inactivated by UV at dose of 40 and 160 mJ/cm^2. These results suggested that Ad41 did have a negative and measurable impact on HEK293 cell proliferation as the effect was somewhat proportional to the number of live virus in the inoculum. At high UV dose of 320 mJ/cm^2, the number of surviving Ad41 was low and the effect on cell proliferation was less.

Figure 5.6 shows the results of 10 times diluted UV inactivated Ad41 described in previous paragraph inoculated onto HEK293 cells in the wells of E-Plates. The mixture of non-UV exposure Ad41 sample was at around 10^4 TCID$_{50}$ infectious viral particles/well.

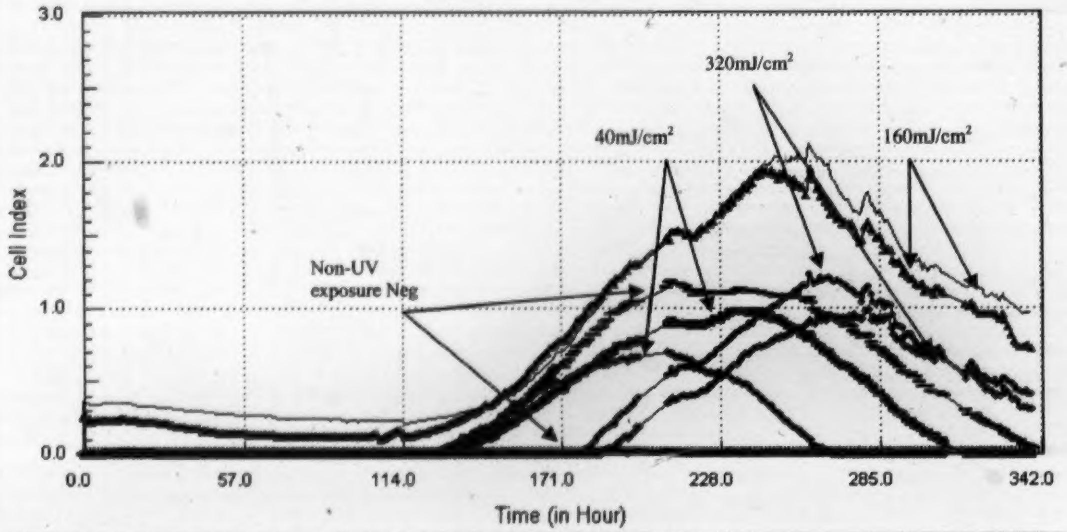

Figure 5.6 Growth of HEK293 cells inoculated with 10 times diluted UV exposed Ad41 as monitored by RT-CES^{TM}. Cells were mixed with 10 μL of 10 times diluted UV inactivated Ad41 and non-UV exposure negative controls. UV doses were 40, 160, 320 mJ/cm^2. Analyses were in duplicates.

Of the duplicate non-UV exposed negative control samples, one showed an obvious propagation of viruses with maximum CI around 1. However, the other duplicate did not show any growth during the 342 h observation period. This variation in response could have been due to differences in cell attachment between the two wells. It was not clear why the appearance of cell growth on wells infected with Ad41 exposed to a UV dose of 320 mJ/cm^2 was delayed. It was interesting that the cells with Ad41 exposed to UV at UV dose of 160 mJ/cm^2 appeared to grow better than those exposed to a UV dose of 320 mJ/cm^2. A similar phenomenon was observed in other experiments in this study (the curve not shown here, in Appendix B). The results indicated that HEK293 cells mixed with low concentrations of Ad41 grew better than those without mixing with any Ad41 and those mixed with high concentrations of Ad41. This is suggestive of a cell growth stimulation mechanism.

When 10^{-2} dilutions of UV exposed virus was mixed with HEK293 cells and inoculated in the wells of E-Plates, there was little difference between in CI curves for UV exposed and non-UV exposed negative control samples (the curve not shown, in Appendix B). They all grew the same as non-infected cells.

With passages increasing, HEK293 cells attached less readily to the wells. Coating buffers were considered to help the cells attach. Two adhesion reagents were used by previous researchers (Huang and Xing 2006). These were extracellular matrix (ECM) proteins and Poly-L-Lysine (PPL). In this study, PPL was selected and demonstrated to strengthen the adhesion of HEK293 cells onto the surface of the E-Plate. With PPL, HEK293 cells could be attached onto E-Plates with less time with fewer passages (less than 50). Two concentrations of PPL (50 μL/mL and 100 μL/mL) were coated on E-Plates. There was no significant difference on the cells growth effect (Figure 5.7).

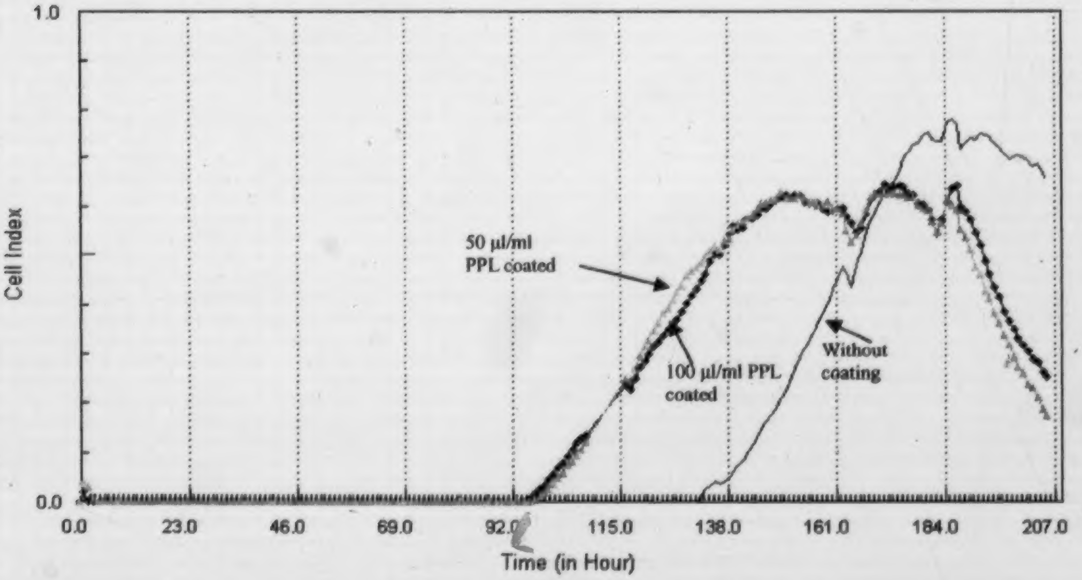

Figure 5.7 Growth of Ad41 infected HEK293 cells with and without PPL adhesion coating on RT-CES™. 50 μL/ml and 100 μL/ml PPL were coated onto the wells of E-Plates and stayed for 30 min. PPL was then removed with pipettes, fresh HEK293 cells of 15,000 cells/well were added into wells and monitored by RT-CES™.

HEK293 cells did not propagate consistently in the wells of E-Plates, especially after a higher number of passages (curves not shown, passage 45 and above in this study). Even if PPL was coated on the surface, growth was still not promising. The reason could be: a) HEK293 cells inherently do not attach readily; b) the surface of RT-CES™ wells was too small to support growth. In addition, RT-CES™ is not as sensitive as traditional cell culture for detecting slight morphological changes of cells. The size of the non-UV exposed negative control Ad41 inoculum was around 10^5 $TCID_{50}$ infectious particles/mL when applied to the RT-CES wells. As indicated above, when non-UV exposure negative control Ad41 was diluted to 100 fold (up to 10^3 infectious particles), the virus does not have effect on cell growth in detection of RT-CES™. The ratio of infectious viral particles of Ad41 to host cell number applied on RT-CES™ was similar to that applied in traditional cell culture. In traditional viral culture, Ad41 infection could be detected as low as around 10^2 $TCID_{50}$ infectious viral particles/mL. The reason for the lower RT-CES™ sensitivity could be:

a) The concentration of HBS in growth medium was greater than that in maintenance medium. Adenovirus virus type 4 was demonstrated to have a lower infectivity titer with 10% horse serum than with the same concentration of chicken, calf and rabbit serum in detection of cell culture CPE based $TCID_{50}$ (Gold and Ginsberg 1962). There is no published study on the influence of inhibitors in the growth medium on Ad41 propagation. However, this suggests that inhibitors of Ad41 propagation might be present in HBS. Therefore, the higher concentration of HBS in Ad41 growth medium (10%) when applied on RT-CES™ than that in maintenance medium (2%) when applied in traditional cell culture may account for the low infectivity monitored on RT-CES™.

b) The addition of poly-L-lysine (PPL). HEK293 cells which subject to more than 50 passages in this study did not attach to the small surfaces of the RT-CES™ E-Plates very well, however, when the E-plates were coated with PPL, the cells were able to attach. The PPL coating may have had an effect on how Ad41 impacted the growth of the HEK293 cells in the RT-CES™ system.

5.3.2 Propagation of Ad41 on Hep-2 Cells

Hep-2 cells attached very well to the RT-CES™ E-Plate wells. Serially diluted Ad41 (~10^5 $TCID_{50}$ infectious viral particles/mL) was inoculated onto seeded Hep-2 cells after cell incubation for 25 h. Figure 5.8 shows the CI curve of diluted Hep-2 cells inoculated with different dilutions of Ad41. Experiments were carried out in duplicates.

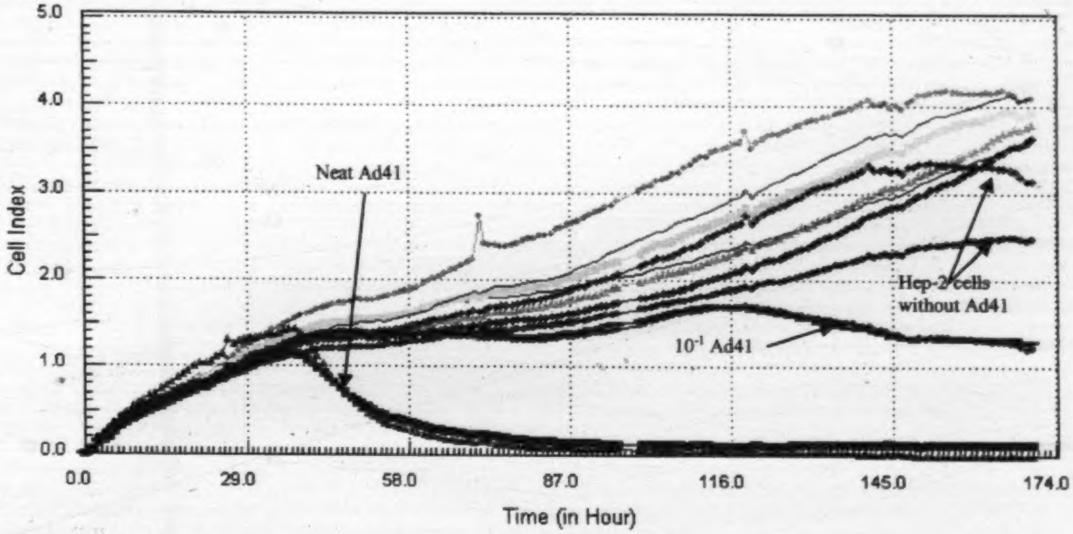

Figure 5.8 Growth of Hep-2 cells inoculated with different dilutions of Ad41 in RT-CES™. Around 10^5 $TCID_{50}$ infectious viral particles/mL Ad41 was diluted to 10^4 to 10^1 $TCID_{50}$ infectious viral particles/mL. Non-diluted Ad41 and HEK293 cells without infected with Ad41 control samples were detected along with dilution samples too. The neat (without dilution) Ad41, 10^{-1} diluted Ad41, and HEK293 cells controls were marked in this curve.

The detection of growth of Hep-2 cells by RT-CES™ was better than that of HEK293 cells, in terms of good agreement of the curves of duplicate experiments (Figure 5.8). This confirmed that Hep-2 cells attached more readily to the wells of E-Plates than HEK293 cells. It is apparent that RT-CES™ was able to detect neat (~10^5 $TCID_{50}$

infectious viral particles/mL) and 10-fold diluted (~10^4 $TCID_{50}$ infectious viral particles/mL) Ad41 which was inoculated onto Hep-2 cells. However, it was unable to detect Ad41 at 100 fold or greater dilutions. The curves in Figure 5.8 without marking included 100-fold to 10^4-fold diluted Ad41 infected Hep-2 cells. It is difficult to tell the difference between the different CI curves among these dilutions and the Hep-2 negative control sample curve. If Ad41 samples were diluted between 10^5 and 10^4 $TCID_{50}$ infectious viral particles/mL, a relationship between the CI curve and inoculum might be obtained. However, this does not help with quantification of inactivated viruses. It is also suggested that Hep-2 is not a perfect cell line to support the growth of Ad41 (ATCC Tak Strain). Therefore, UV inactivated Ad41 samples were not applied on Hep-2 cells for RT-CES™ detection.

5.4 Conclusions and Recommendations

Although RT-CES™ has previously been used successfully in quantitative cytotoxicity assays, it is not a perfect method for detection of Ad41 infection based on current materials and methods in this study. Because of the small surface area of the wells of E-plates and HEK293 cells's lack of adherence, the cell growth and CI curves were not very consistent. With the help of the coating buffer poly-L-lysine, the attachment was improved for lower passages of HEK293 cells. However, as the number of cell passages increased, poly-L-lysine did not help in cell attachment. At a comparatively low number or cell passages (35-45), RT-CES™ was able to detect the effect of different UV doses on Ad41. Furthermore, the detection level of virus concentration on RT-CES™ was very high. It could only successfully detect live viruses roughly between 10^5 and 10^4 $TCID_{50}$ infectious viral particles/mL. Hep-2 cells grew consistently and attached well onto wells of E-Plates, however, Ad41 inoculums lower than 10^4 $TCID_{50}$ infectious viral particles/mL were not detected on RT-CES™.

Although difficult to quantify the Ad41, RT-CES™ is able to qualify for Ad41 automatically with less work as long as Ad41 is more than 10^4 $TCID_{50}$ infectious viral particles/mL infected on HEK293 cells. To strengthen the consistency, future work on increasing the adherence of HEK293 cells to E-Plates may be performed. To apply the virus quantification of Ad41 on RT-CES™, a cell line with good attachment ability and also supporting the propagation of Ad41 need to be investigated.

Chapter 6 Conclusions and Recommendations

6.1 Conclusions

The objective of this study was to propagate highly infectious particles of Ad41 and determine the correlation between traditional cell culture infectivity assays and direct real-time quantitative PCR, direct real-time quantitative RT-PCR, cell culture integrated with real-time quantitative PCR and RT-PCR for measuring UV inactivation of Ad41. In real-time quantitative PCR/RT-PCR the progress of the PCR reaction is monitoring continuously in a real-time thermocyler using a Taqman fluorescent probe. A second objective was to determine if a RT-CES System is efficient and effective for monitoring dynamic cellular response before and after viral inoculation and can, therefore, be used as an indicator of viral infectivity in UV inactivation experiments. The conclusions that were drawn from the results of this study are as followings.

- Hep-2 cells were able to support the growth of adenovirus 41 detected by real-time quantitative RT-PCR. However, viral propagation was not detectable with CPE. Therefore, the real-time quantitative RT-PCR method is sensitive for detection of viruses on cell culture which do not produce observable CPE.
- Around 3.5-log inactivation of purified and 3-log inactivation of unpurified Ad41 were achieved with a germicidal UV dose of 320 mJ/cm^2 produced by a low-pressure UV lamp in this study. The UV inactivation of Ad41 in this

study was lower than that reported in previous studies, especially for purified viruses. Possible reasons for the difference include differences in the cell quality and origin, incubation conditions and procedures of purification used between the studies.

- Based on ANOVA at the 95% confidence level, there was no significant difference between cell culture with CPE detection and cell culture integrated with real-time quantitative RT-PCR detection for determining UV inactivation of Ad 41. However, direct PCR/RT-PCR correlated poorly to cell culture with CPE for determining UV inactivation of Ad41. Cell culture integrated with real-time quantitative PCR also correlated poorly to cell culture with CPE for determining UV inactivation of Ad41.
- Based on ANOVA at the 95% confidence level, there was a significant difference between UV inactivation of purified Ad41 and unpurified Ad41 as determined by both cell culture integrated with real-time quantitative RT-PCR and cell culture with CPE. The inactivation of purified Ad41 was about 0.5-log higher than that of unpurified Ad41 at each UV dose. The reason could be that the purification procedure increased the possibility of virus aggregation.
- The unique advantage of real-time quantitative PCR/RT-PCR is that it generated quantitative PCR results after the PCR reaction without an additional analysis step such as gel electrophoresis. This saved work and time.
- RT-CES was not promising in detection of Ad41 infection on HEK293 cells.

HEK293 did not attach well to the wells of the E-Plates. RT-CES could not detect Ad41 fewer than 10^4 $TCID_{50}$ infectious viral particles/mL infected on HEK293 cells.

6.2 Recommendations

The recommendations of this study are as following.

- A549 cells were not able to propagate clinical stool isolates of Ad41, thus are not recommended in later studies. Hep-2 cells were able to support the growth of Ad41 but lacked production of observable CPE. HEK293 cells were able to propagate Ad41 with observable CPE. However, HEK293 cells did not adhere to the walls of flasks. Biocoat flaks are recommended for future work.
- Cell culture integrated with real-time quantitative RT-PCR for detection of infection correlated well with traditional cell culture with CPE for detection of infection. The cell culture integrated real-time quantitative RT-PCR method thus can potentially be substituted for CPE based cell culture infectivity assay for disinfection studies. Taqman® RT-PCR is real-time quantitative PCR. It generates quantitative results without resorting to additional analysis steps such as gel electrophoresis. The Taqman® PCR instrument and reagent kits are expensive. However, the method saves much labor and time compared to cell culture with CPE detection.
- RT-CES was not suitable for detecting Ad41 infection on HEK293 cells

quantitatively due to its lack of sensitivity and HEK293 cells' lack of adherence to the RT-CES wells. Further investigation of suitable cell lines is recommended to test.

References

Barker, J., and Vipond, I. B. (2004). "Effects of cleaning and disinfection in reducing the spread of Norovirus contamination via environmental surfaces." In: Journal of Hospital Infection, 42-49.

Baxter, C. S., Hofmann, R., Templeton, M. R., Brown, M., and Andrews, R. C. (2007). "Inactivation of adenovirus types 2, 5, and 41 in drinking water by UV light, free chlorine, and mlonochloramine." Journal of Environmental Engineering-Asce, 133(1), 95-103.

Bolton, J. R. (2001). Ultraviolet Applications Handbook, Bolton Photosciences Inc.

Bolton, J. R. (2006). "Lecture note Civ E 729." University of Alberta, Edmonton.

Bolton, J. R., and Linden, K. G. (2003). "Standardization of methods for fluence (UV dose) determination in bench-scale UV experiments." Journal of Environmental Engineering-Asce, 129(3), 209-215.

Brandt, C. D., Kim, H. W., Rodriguez, W. J., Arrobio, J. O., Jeffries, B. C., Stallings, E. P., Lewis, C., Miles, A. J., Gardner, M. K., and Parrott, R. H. (1985). "Adenoviruses and Pediatric Gastroenteritis." Journal of Infectious Diseases, 151(3), 437-443.

Brown, M. (1985). "Selection of Nonfastidious Adenovirus Species in 293 Cells Inoculated with Stool Specimens Containing Adenovirus-40." Journal of Clinical Microbiology, 22(2), 205-209.

Brown, M., Petric, M., and Middleton, P. J. (1984). "Diagnosis of Fastidious Enteric Adenovirus-40 and Adenovirus-41 in Stool Specimens." Journal of Clinical Microbiology, 20(3), 334-338.

Brown, M., Wilsonfriesen, H. L., and Doane, F. (1992). "A Block in Release of Progeny Virus and a High Particle-to-Infectious Unit Ratio Contribute to Poor Growth of Enteric Adenovirus Type-40 and Type-41 in Cell-Culture." Journal of Virology, 66(5), 3198-3205.

Carter, M. J. (2005). "Enterically infecting viruses: pathogenicity, transmission and significance for food and waterborne infection." Journal of Applied Microbiology, 98(6), 1354-1380.

Chapron, C. D., Ballester, N. A., Fontaine, J. H., Frades, C. N., and Margolin, A. B. (2000). "Detection of astroviruses, enteroviruses, and adenovirus types 40 and 41 in surface waters collected and evaluated by the information collection rule and an integrated cell culture-nested PCR procedure." Applied and Environmental Microbiology, 66(6), 2520-2525.

Choi, S., and Jiang, S. C. (2005). "Real-time PCR quantification of human adenoviruses in urban rivers indicates genome prevalence but low infectivity." Applied and Environmental Microbiology, 71(11), 7426-7433.

Craik, S. A., Weldon, D., Finch, G. R., Bolton, J. R., and Belosevic, M. (2001). "Inactivation of Cryptosporidium parvum oocysts using medium- and low-pressure ultraviolet radiation." Water Research, 35(6), 1387-1398.

Dejong, J. C., Wigand, R., Kidd, A. H., Wadell, G., Kapsenberg, J. G., Muzerie, C. J., Wermenbol, A. G., and Firtzlaff, R. G. (1983). "Candidate Adenovirus-40 and Adenovirus-41 - Fastidious Adenoviruses from Human Infant Stool." Journal of Medical Virology, 11(3), 215-231.

Fong, T. T., and Lipp, E. K. (2005). "Enteric viruses of humans and animals in aquatic environments: Health risks, detection, and potential water quality assessment tools." Microbiology and Molecular Biology Reviews, 69(2), 357-+.

Fout, G. S., Martinson, B.C., Moyer, N.W., Dahling, D.R. . (2003). "A multiplex reverse transcription-PCR method for detection of human enteric viruses in groundwater." Applied and Environmental Microbiology, 69, 3158-3164.

Gallagher, E. M., and Margolin, A. B. (2007). "Development of an integrated cell culture - Real-time RT-PCR assay for detection of reovirus in biosolids." Journal of Virological Methods, 139(2), 195-202.

Gold, E., and Ginsberg, H. S. (1962). "An Inhibitor of Adenoviruses in Ox Serum." Journal of Immunology, 88(4), 513-&.

Haramoto, E., Katayama, H., Oguma, K., and Ohgaki, S. (2005). "Application of cation-coated filter method to detection of noroviruses, enteroviruses, adenoviruses, and torque teno viruses in the Tamagawa River in Japan." Applied and Environmental Microbiology, 71(5), 2403-2411.

Hashimoto, S., Sakakibara, N., Kumai, H., Nakai, M., Sakuma, S., Chiba, S., and Fujinaga, K. (1991). "Fastidious human adenovirus type 40 can propagate efficiently and produce plaque on a human cell line, A549, derived from lung carcinoma." Journal of Virology, 65, 2429-2435.

He, J. W., and Jiang, S. (2005). "Quantification of enterococci and human adenoviruses in environmental samples by real-time PCR." Applied and Environmental Microbiology, 71(5), 2250-2255.

Heim, A., Ebnet, C., Harste, G., and Pring-Akerblom, P. (2003). "Rapid and quantitative detection of human adenovirus DNA by real-time PCR." Journal of Medical Virology, 70(2), 228-239.

Hijnen, W. A. M., Beerendonk, E. F., and Medema, G. J. (2006). "Inactivation credit of UV radiation for viruses, bacteria and protozoan (oo)cysts in water: A review." Water Research, 40(1), 3-22.

Huang, B., and Xing, J. Z. (2006). "Dynamic modelling and prediction of cytotoxicity on microelectronic cell sensor array." Canadian Journal of Chemical Engineering, 84(4), 393-405.

Jagger, J. (1966). "Koller,Lr - Ultraviolet Radiation." Quarterly Review of Biology, 41(3), 340-&.

Jiang, S., Dezfulian, H., and Chu, W. P. (2005). "Real-time quantitative PCR for enteric adenovirus serotype 40 in environmental waters." Canadian Journal of Microbiology, 51(5), 393-398.

Jothikumar, N., Cromeans, T. L., Hill, V. R., Lu, X. Y., Sobsey, M. D., and Erdman, D. D. (2005). "Quantitative real-time PCR assays for detection of human adenoviruses and identification of serotypes 40 and 41." In: Applied and Environmental Microbiology, 3131-3136.

Kidd, A. H., and Madeley, C. R. (1981). "In vitro growth of some fastidious adenoviruses from stool specimens." Journal of Clinical Pathology, 34, 213-216.

Ko, G., Cromeans, T. L., and Sobsey, M. D. (2003). "Detection of infectious adenovirus in cell culture by mRNA reverse transcription-PCR." Applied and Environmental Microbiology, 69(12), 7377-7384.

Ko, G., Jothikumar, N., Hill, V. R., and Sobsey, M. D. (2005a). "Rapid detection of infectious adenoviruses by mRNA real-time RT-PCR." Journal of Virological Methods, 127(2), 148-153.

Ko, G. P., Cromeans, T. L., and Sobsey, M. D. (2005b). "UV inactivation of adenovirus type 41 measured by cell culture mRNA RT-PCR." Water Research, 39(15), 3643-3649.

Lee, C., Lee, S. H., Han, E., and Kim, S. J. (2004). "Use of cell culture-PCR assay based on combination of A549 and BGMK cell lines and molecular identification as a tool to monitor infectious andenoviruses and enteroviruses in river water."

Leland, D. S., and French, M. L. V. (1988). Virus isolation and identification, New York.

Linden, K. G., Johnson, S., Moore, A., Malley, J.P. (Year). "Importance of wavelength for UV inactivation of adenovirus in water." Proc. 3rd International congress on ultraviolet technologies (IUVA), Whistler, B.C.

Maier, R. M., Pepper, I.L., Gerba, C.P. (2000). Enivironment Microbiology, Academic Press, Orlando.

Meng, Q. S., and Gerba, C. P. (1996). "Comparative inactivation of enteric adenoviruses, poliovirus and coliphages by ultraviolet irradiation." Water Research, 30(11), 2665-2668.

Meyer-Arendt, J. R. (1984). Introduction to classical and modern optics, 2nd Ed., Prentice-Hall, Englewood cliffs, N.J.

Noble, R. T., Allen, S. M., Blackwood, A. D., Chu, W., Jiang, S. C., Sobsey, M. D., Stewart, J. R., and Wait, D. A. (2003). "Use of viral pathogens and indicators to differentiate between human and non-human fecal contamination in a microbial source tracking comparison study." Journal of Water and Health, 1(4), 195-207.

Pang, X. L. L., Preiksaitis, J. K., and Lee, B. (2005). "Multiplex real time RT-PCR for the detection and quantitation of norovirus genogroups I and II in patients with acute gastroenteritis." Journal of Clinical Virology, 33(2), 168-171.

Perron-Henry, D. e. a. (1988). "Isolation and propagation of enteric adenoviruses in Hep-2 cells." Journal of clinical microbiology, 1445-1447.

Perronhenry, D. M., Herrmann, J. E., and Blacklow, N. R. (1988). "Isolation and Propagation of Enteric Adenoviruses in Hep-2 Cells." Journal of Clinical Microbiology, 26(8), 1445-1447.

Pieniazek, D. e. a. (1989). "Differential growth of human enteric adenovirus 41 (TAK) in continuous cell lines " Virology, 174, 239-249.

Pieniazek, N. J., Slemenda, S. B., Pieniazek, D., Velarde, J., and Luftig, R. B. (1989). "Sequence of Human Enteric Adenovirus Type-41 Tak Fiber Protein Gene." Nucleic Acids Research, 17(22), 9474-9474.

Rainbow, A. J., and Mak, S. (1973). "DNA Damage and Biological Function of Human Adenovirus after Uv-Irradiation." International Journal of Radiation Biology, 24(1), 59-72.

Seiradake, E., and Cusack, S. (2005). "Crystal structure of enteric adenovirus serotype 41 short fiber head." Journal of Virology, 79(22), 14088-14094.

Shin, G. A., and Sobsey, M. D. (1998). "Reduction of norwalk virus, poliovirus 1 and coliphage MS2 by monochloramine disinfection of water." Water Science and Technology, 38(12), 151-154.

Solly, K., Wang, X. B., Xu, X., Strulovici, B., and Zheng, W. (2004). "Application of real-time cell electronic sensing (RT-CES) technology to cell-based assays." Assay and Drug Development Technologies, 2(4), 363-372.

Thurston-Enriquez, J. A., Haas, C., Jacangelo, J., Riley, K., and Gerba, C. P. (2003a). "Inactiavation of feline calicivirus and adenovirus type 40 by UV radiation." Applied and Environmental Microbiology, 69(1), 577-582.

Thurston-Enriquez, J. A., Haas, C. N., Jacangelo, J., and Gerba, C. P. (2003b). "Chlorine inactivation of adenovirus type 40 and feline calicivirus." Applied and Environmental Microbiology, 69(7), 3979-3985.

Tiemessen, C. T., and Kidd, A. H. (1990). "Adenovirus-41 Growth in Semipermissive Cells Shows Multiple-Hit Kinetics." Archives of Virology, 110(3-4), 239-245.

Tiemessen, C. T., and Kidd, A. H. (1995). "The Subgroup-F Adenoviruses." Journal of General Virology, 76, 481-497.

Uhnoo, I., Wadell, G., Svensson, L., and Johansson, M. E. (1984). "Importance of enteric adenoviruses 40 and 41 in acute gastroenteritis in infants and young children." Journal of Clinical Microbiology, 20, 365-372.

USEPA. (1998). "Announcement of the Drinking Water Contaminant Candidate List; Notice." Fed. Reg., 63:40:10274.

USEPA. (1999). "Alternative disinfectants and oxidants Guidance Manual." Office of water (4607).

Vacquier, J. P., and Cardiff, R. D. (1979). "In vitro infectivity assay for mouse mammary tumor virus." Proc. Natl. Acad. Sci. USA, 76, 4117-4121.

Wassermann, F. E. (1962). "The inactivation of adenoviruses by ultraviolet irradiation and nitrous acid " Virology, 17, 335-341.

Watanabe, M., Kohdera, U., Kino, M., Haruta, T., Nukuzuma, S., Suga, T., Akiyoshi, K., Ito, M., Suga, S., and Komada, Y. (2005). "Detection of adenovirus DNA in clinical samples by SYBR Green real-time polymerase chain reaction assay." Pediatrics International, 47(3), 286-291.

Xing, J. Z., Zhu, L. J., Jackson, J. A., Gabos, S., Sun, X. J., Wang, X. B., and Xu, X. (2005). "Dynamic monitoring of cytotoxicity on microelectronic sensors." Chemical Research in Toxicology, 18(2), 154-161.

Yates, M., Malley, J., Rochelle, P., and Hoffman, R. (2006). "Effect of adenovirus resistance on UV disinfection requirements: A report on the state of adenovirus science." AWWA, 93-106.

Appendix A

1. Reagent used in the study

1.1 Composition of the medium used in cell culture

Hep-2, A549 cell culture

Growth medium: Minimum essential medium with 2mM L-glutamine, 20 µg/mL gentamicin, 150 µg/mL sodium bicarbonate, 0.02 M HEPES, suspended in 10% feline bovine serum (FBS).

Maintenance medium: Minimum essential medium with 2mM L-glutamine, 20 µg/mL gentamicin, 150 µg/mL sodium bicarbonate, 0.02 M HEPES, suspended in 2% feline bovine serum (FBS).

HEK293 cell culture

Growth medium: Minimum essential medium with 2mM L-glutamine, 1.0 mM sodium pyruvate, 20 µg/mL gentamicin, 150 µg/mL sodium bicarbonate, 0.02 M HEPES, suspended in 10% horse bovine serum (HBS).

Maintenance medium: Minimum essential medium with 2mM L-glutamine, 1.0 mM sodium pyruvate, 20 µg/mL gentamicin, 150 µg/mL sodium bicarbonate, 0.02 M HEPES, suspended in 2% horse bovine serum (HBS).

1.2 Composition of Master Mix

RT: 4.0 µL 5 × First Strand Buffer (250 mM Tris- HCl, pH 8.3 at room temperature; 375 mM KCl; 15 mM $MgCl_2$), 1.0 µL 0.1 mM DTT, 3.0 µL 2.5 mM dNTP, 2.0 µL 300 ng/µL Random Primer oligonucleotides [mostly hexamers in 0.009 OD_{260} units/µL in 0.3 mM Tris-HCl (pH 7.0) and 0.02 mM EDTA], 0.5 µL 40U/µL Recombinant Ribonuclease Inhibitor (RNaseOut^{TM}), 0.5 µL 200 U/µL SuperScript^{TM} II Reverse Transcriptase, and 4.0 µL PCR grade water.

Taqman® PCR: 12.5 μL 2 × Taqman® Universal PCR Master Mix (Applied Biosystems) and 1.0 μL 10 μM eADV-TaqF, 1.0 μL 10μM eADV-TaqR, 1.0 μL 5 μM eADV-TaqP, and 4.5 μL PCR grade water.

2. Techinical Methods

2.1 Cell passage

Both of the Hep-2 and A549 cells were maintained in minimal essential medium (MEM) with 2mM L-glutamine, 202.5 μg/mL sodium bicarbonate, 0.02 M HEPES, plus 10% fetal bovine serum (FBS) and passaged twice a week at a subsulture ratio of 1:50. When the cells in the flask reached 90-100% confluence, culture medium was removed and discarded. Cell monolayer was rinsed with 0.1 M PBS (pH 7.3) to remove dead cells. Five ml of 0.25% trypsin-0.53mM EDTA solution was added to the flask and the flask was rocked for 1 minute before 4 mL of typsin was removed. The flask was then incubated at 37°C for 5-10 minutes until cells are all detached. Fourteen milliliters or 49 mL complete MEM was added depending on the size of the flasks ($25cm^2$ or $75cm^2$) and cells were aspirated by pipetting until all cell clumps were broken. Depending on the time to utilize the cells, different amount of suspended cells was transferred into new flasks with MEM medium added. Cells were incubated in 37°C, 0.5% CO_2 until ready to use or need to passage again.

2.2 Direct Immunofluorescent Assay (DFA)

Infected cells were tested by Light Diagnostics Adenovirus Direct Immunofluorescent Assay (DFA) Kit (Millipore, Chemicon, #3130) to confirm the presence of CPE. The DFA Kit utilizes a direct immunofluorescent antibody technique for identifying virus in infected tissue cultures and direct respiratory specimen cell preparations. The antibody is labeled with FITC (Fluorescein isothiocyanate) which produces an apple green fluorescence when illuminated with ultraviolet light. The labeled antibody bind to antigen present in the specimen. The FITC label on the antibody allows the antigen/antibody complex to be visualized by fluorescence microscopy. Positive specimens exhibit apple green cell fluorescence while non-infected cells are stained a dull red due to the presence of Evans Blue in the conjugate diluents.

When CPE was observed, infected cells were washed off the flasks with the media and 1 mL was transfered into an Eppendorf tube. The cells and medium mixture was centrifuged at 500 rpm for 10 minutes. Most supernatant was discarded; the cell pellet was vortexed for 3 s and then was spot onto an acetone cleaned slide and allowed to dry. The slide was fixed in chilled acetone (4°C) for 10 minutes and air dried completely. One drop of adenovirus/FITC was placed on the appropriate wells of the sample slide after allowing the slides to equilibrate to room temperature. The slides on a humid chamber were incubated at 37°C for 15 minutes. Slides were then gently rinsed with a stream of PBS wash solution to remove the access antibody. Slides were socked in a staining dish and covered with wash solution, rinsed for 5 minutes with a magnetic stirring bar gently agitated. The slides were dried after socking and mounted with coverslips using mounting fluid provided in the kit. The access fluid was wiped off from the edges of coverslip. Slides were examined with a fluorescent microscope (Olympus, BX51) at 100-200 × magnification for cells exhibiting the apple-green flurescence of FITC. The pictures of infected HEK293 cells with DFA stained are shown in Fig A-1.

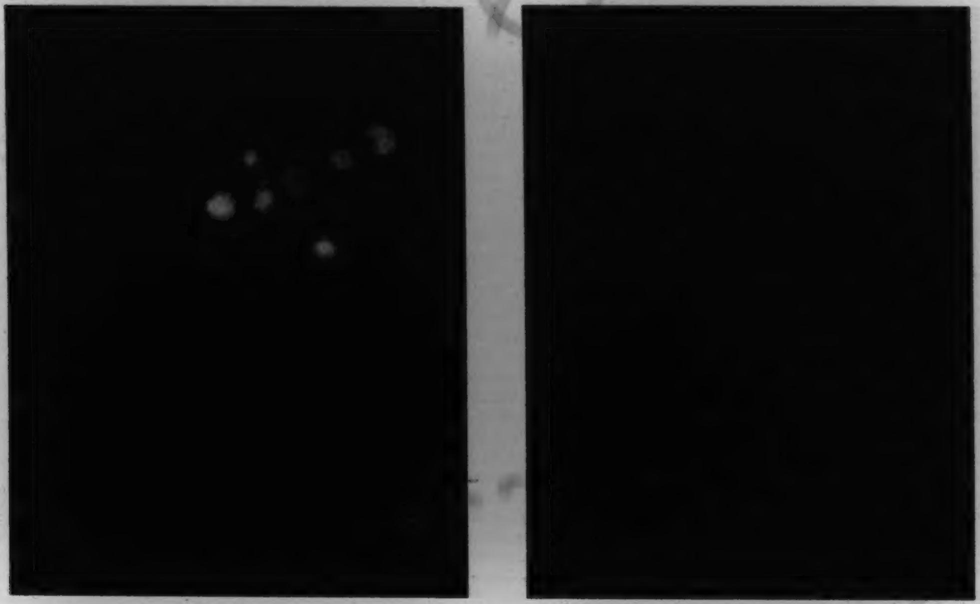

a) b)

Figure A-1 DFA stained Ad41 infected HEK293 cells. a) neat Ad41 infected HEK293 cells after incubation for 7 days, viral titer around 10^6 infectious particles/mL. b) diluted Ad41 infected HEK293 cells after incubation for 7 days, viral titer around 10^3 infectious viral particles/mL.

2.3 Extraction

Two hundred microliters of supernatant was transferred into a 1.5 mL microcentrifuge tube. Twenty micro litres of PK solution was pipetted into the bottom of the tube followed by 200 µL of lysis buffer to liberate RNA. The mixture was incubated at 56°C for 10 minutes followed by addition of 500 µL of binding buffer and 20 µL of well-mixed MagaZorb Reagent so that the released RNA was bounded exclusively and specifically to the MagaZorb particles. The tube was gently mixed and incubated for 10 minutes at room temperature. A magnetic rack was used to settle the MagaZorb RNA bound particles and the supernatant was aspirated. One milliliter of wash buffer was added to the tubes after they were removed from the rack and the tubes were mixed well by inverting tubes several times to ensure the particles were completely dispersed. Tubes were then settled back to the rack followed by supernatant aspirating. Washing was repeated once to ensure all contaminants were removed. One hundred microliters of

RNAse-free water were added and the tube contents were mixed for 10 minutes. Particles were settled on the rack, supernatant was transferred to RNAse/DNAse free tubes and freezed at -70°C until analysis.

2.4 Digestion

Fifty-microliter extraction products were diluted to 500 μL with sterilized water and treated with 5 μL 122.5 U/μL Deoxyribonuclease I (DNase I) and 50 μL 10 × DNase buffer to damage contaminant DNA. DNase I digests single- and double- stranded DNA to oligodeoxyribonucleotides containing a 5' phosphate. Ribonuclease was reduced to non-detectable levels. DNase I removes DNA from RNA and protein preparations. It is purified from bovine pancreas.

2.5 RT

The RT reaction was performed in 20 μL volumes using 4.0 μL 5 × First Strand Buffer (250 mM Tris- HCl, pH 8.3 at room temperature; 375 mM KCl; 15 mM $MgCl_2$), 1.0 μl 0.1 mM DTT, 3.0 μl 2.5 mM dNTP, 2.0μL 300 ng/μL Random Primer oligonucleotides [mostly hexamers in 0.009 OD_{260} units/μL in 0.3 mM Tris-HCl (pH 7.0) and 0.02 mM EDTA], 0.5 μL 40U/μL Recombinant Ribonuclease Inhibitor (RNaseOut™), 0.5 μL 200 U/μL SuperScript™ II Reverse Transcriptase, and 4.0 μL PCR grade water. Five microliter digestion product described above was added into the mixture. A total 20 μL mix was incubated at 42°C for 60 minutes, 70°C for 15 minutes and kept at 4°C with GeneAmp® PCR System 2700 (Applied Biosystems).

2.6 Quantification of standard adenovirus and generation of standard curve

Adenovirus DNA was extracted from known adenovirus containing cultured cells. A PCR product was obtained using a forward primer and a reverse primer from the same region of the adenovirus. The product was analyzed by electrophoresis on a 2% agarose gel and further purified using a Qiagen PCR purification kit. The purified product was quantified by spectrophotometry, dispensed in aliquots containing 10^6 genome copies per tube, and stored at -70°C. These aliquots were used to prepare a fresh series of log dilutions (10^6 to 10^1 genome copies) in order to establish a positive standard curve for the

Taqman® PCR. The procedure was adapted from a standard protocol for quantification of cytomegalovirus in PLPH.

2.7 Taqman® PCR

Five microliters of RT product, digestion product or RNA extraction product was added to a final volume of 25 µL containing 12.5 µL 2 × Taqman® Universal PCR Master Mix (Applied Biosystems) and 1.0 µL 10 µM eADV-TaqF, 1.0 µL 10µM eADV-TaqR, 1.0 µL 5 µM eADV-TaqP described in Table 3.1 and 4.5 µL PCR grade water. PCR amplification was performed using an ABI PRISM 7000 Sequence Detection System (Figure A-2). Amplification was performed with 50°C for 2 minutes, 95°C for 10 minutes, 45 cycles of denaturation at 95°C for 15 seconds, annealing at 60°C for 1 minute, and extension at 72°C for 1 minute. During thermal cycling, emission from each sample was recorded and ABI Prism 7000 SDS Software v. 1.1 processed the raw fluorescence data to produce the threshold cycle (Ct) values for each sample. A standard curve was then computed from the Ct values of the diluted adenovirus standards using SDS software, and absolute quantities for the unknown samples were then extrapolated based on their shreshold cycle (Ct) values. Standard curves were generated for quantification of assay sensitivities using stocks of adenoviruses for which viral concentration had been determined and using GEC from cloned sequences of the hexon gene region. A PCR product (320 base pairs) was obtained using a forward primer and a reverse primer described in Table 3.1. The product was analyzed by electrophoresis on a 2% agarose gel and further purified using a Qiagen PCR purified kit. The purified product was quantified by spectrophotometry, dispensed into aliquots containing 10^6 genome copies per tube, and stored at -70°C. These aliquots were used to prepare a fresh series of log dilutions (10^6 to 10^1 genome copies) in order to establish a standard curve for Taqman® PCR.

Figure A-2 ABI PRISM 7000 Sequence Detection System (Applied Biosystems)

All standard precautions were followed to prevent any PCR contamination by adhering to strict laboratory practices. PCR set-up master mix was performed in a dead box which was designed specifically and separated from PCR replication area. The pre-PCR manipulation (DNA isolation and PCR set-up master mix) was performed isolated from the real-time PCR machine. Dedicated pipettes and reagents were used for each location. Negative controls were run with all assays. The plasmid used for generate standard curves were prepared in a separate room. Every step and area was designated for specific purpose to strictly avoid contamination.

2.8 Taqman® PCR Standard Curve

The amplification plot reflects the generations of the reporter dye during amplification and is related directly to the formation of PCR products. The intersection between the amplification plot and the threshold is defined as the cycle threshold, or Ct value which is related directly to the amount of RT-PCR product, and therefore, related to the original amount of target present in the RT-PCR reaction. Figure A-3 shows the standard curve for quantification of Ad41 using real time Taqman® RT-PCR.

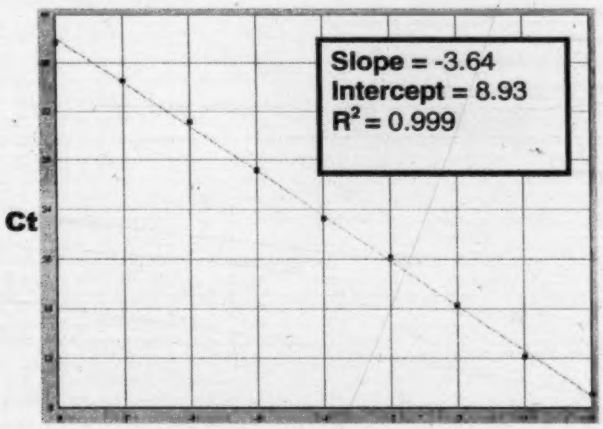

Figure A-3 Standard curve

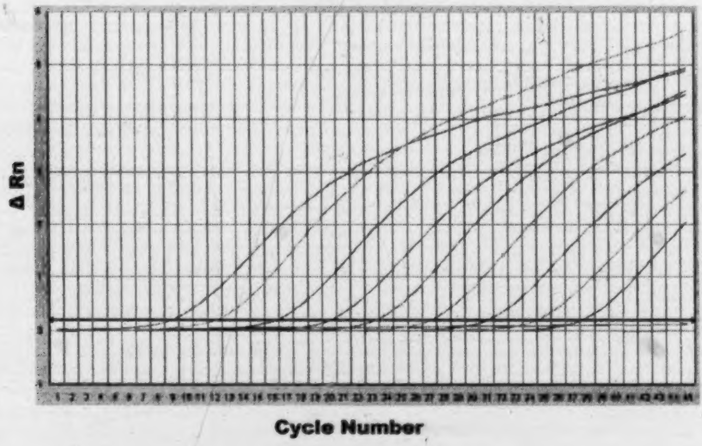

Figure A-4 Cycle number versus ΔRn curve

The standard DNA fragment amplified from adenovirus type 4, in serial dilutions ranging from 10^8 to 10^0 copies, was amplified. Fluorescence density was plotted against cycle numbers. From this curve, the slope is -3.64, intercept is 8.93; R^2 is 0.999. Figure A-4 is the cycle number versus ΔRn curve.

$$\Delta Rn = (R_n^+) - (R_n^-) \qquad \text{Eqn. (A1)}$$

where R_n^+ = (emission intensity of reporter dye)/(emission intensity of passive reference dye) in PCR with template and R_n^- = (emission intensity of reporter dye)/(emission intensity of passive reference dye) in PCR without template or early cycles of a real time reaction.

Two hundred micro liter of harvested cell culture supernatant was taken for extraction and real time RT-PCR. Although all of those did not show CPE, most were detected by real time Taqman® RT-PCR which is supposed to be more rapid than traditional cell culture infectivity assays.

2.9 UV apparatus set-up

A collimated beam UV apparatus (Calgon Carbon Corporation, USA) containing a 10W, low pressure mercury arc lamp (Ster-L-Ray Germicidal Lamp, model G12T6L, 15114, Atlantic Ultraviolet Corporation, Hawpauge, NY) was used in this study. The lamp emitted monochromatic UV radiation at nearly 254 nm and was suspended horizontally in the lamp chamber. The unit included a timer controlled pneumatically driven shutter which can be opened and closed automatically for UV exposure. The shutter is an assembly that blocks the ultraviolet light during the lamp startup stage allowing the experiment to begin at the maximum output of the lamp. The emitted UV light was delivered through a collimation tube of 24 cm long with an aperture diameter of 7 cm to provide reasonably parallel and uniform radiation to the surface of the test suspension. The distance from the lamp to the surface of test suspension was 44 cm. The test suspension was placed on an adjusted platform mounted over a stirrer (Figure A-2).

Appendix B

Table B-1 CPE track of 11 clinical stool samples cultured on Hep-2 cell line. Daily entries indicate if CPE was observed or not.

Day Sample number	1	2	3	4	5	6	7
VC 1436	No	No	No	No	No	No	No
VC5774	No	No	No	No	No	No	No
VC6536	No	No	No	No	No	Yes	Yes
VC4378	No	No	No	No	No	No	No
VC7941	No	No	No	No	No	No	No
VC8775	No	No	No	No	No	No	No
VC10488	No	No	No	No	No	No	No
VC11678	No	No	No	No	No	No	No
VC16513	No	No	No	No	No	No	No
VC2361	No	No	No	No	No	No	No
VC6612	No	No	No	No	No	No	No

Table B-2 CPE track of 11 clinical stool samples cultured on A549 cell line. Daily entries indicate if CPE was observed or not.

Day Sample number	1	2	3	4	5	6	7
VC 1436	No	No	No	No	No	No	No
VC5774	No	No	No	No	No	No	No
VC6536	No	No	No	No	No	No	No
VC4378	No	No	No	No	No	No	No
VC7941	No	No	No	No	No	No	Yes
VC8775	No	No	No	No	No	No	Yes
VC10488	No	No	No	No	No	No	No
VC11678	No	No	No	No	No	No	No
VC16513	No	No	No	No	No	No	No
VC2361	No	No	No	No	No	No	No
VC6612	No	No	No	No	No	No	No

Table B-3 CPE track of 10 stool samples blind passage on Hep-2 cell line. Daily entries indicate if CPE was observed or not.

Day / Sample number	1	2	3	4	5	6
VC5774	No	No	No	No	Yes	Yes
VC1436	No	No	No	No	No	No
VC4378	No	No	No	No	No	No
VC7941	No	No	No	No	No	No
VC8778	No	No	No	No	No	No
VC10488	No	No	No	No	No	No
VC11678	No	No	No	No	Yes	Yes
VC16513	No	No	No	No	No	No
VC2361	No	No	No	No	No	No
VC6612	No	No	No	No	No	No

Table B-4 CPE track of 9 stool samples blind passage on A549 cell line. Daily entries indicate if CPE was observed or not.

Day / Sample number	1	2	3	4	5	6
VC1436	No	No	No	No	No	No
VC5774	No	No	No	No	Yes	Yes
VC6536	No	No	No	No	No	No
VC4378	No	No	No	No	No	No
VC10488	No	No	No	No	No	No
VC11678	No	No	No	No	No	No
VC16513	No	No	No	No	No	No
VC2361	No	No	No	No	No	No
VC6612	No	No	No	No	No	No

Table B-5 CPE track of 8 stool samples 2nd blind passage on Hep-2 cells. Daily entries indicate if CPE was observed or not.

Day / Sample number	1	2	3	4	5	6
VC4378	No	No	No	No	No	No
VC7941	No	No	No	No	No	No
VC8778	No	No	No	No	No	No
VC1436	No	No	No	No	No	No
VC11678	No	No	No	No	No	No
VC16513	No	No	No	No	No	No
VC2361	No	No	No	No	No	No
VC6612	No	No	No	No	No	No

Table B-6 CPE track of 8 stool samples 2nd blind passage on A549 cells. Daily entries indicate if CPE was observed or not.

Day / Sample number	1	2	3	4	5	6
VC1436	No	No	No	No	No	No
VC6536	No	No	No	No	No	No
VC4378	No	No	No	No	No	No
VC10488	No	No	No	No	No	Yes
VC11678	No	No	No	No	No	No
VC16513	No	No	No	No	No	No
VC2361	No	No	No	No	No	No
VC6612	No	No	No	No	No	No

The followings are Raw data and calculations of Table 4.2 in the text.

Table B-7 to Table B-13 show unpurified Ad41 titer under difference UV dose exposure in experiment 1 analyzed by $TCID_{50}$. 1 mL Ad41 was infected onto HEK293 cells and incubated with 4 mL maintenance medium. The calculation procedure is described in Appendix C, 1.1.

Table B-7 The titer of Ad41 of non-UV exposure negative control under 40 mJ/cm^2

A	B	C	D	E	F	G
virus dilution	No. affected	No. Unaffected	Affected ratio (100%)	Cumulative no. affected	Cumulative no. unaffected	Affected ratio (%)
10^-1	4	0	4/4 (100)	19	0	100
10^-2	4	0	4/4 (100)	15	0	100
10^-3	4	0	4/4 (100)	11	0	100
10^-4	4	0	4/4 (100)	7	0	100
10^-5	2	2	4/4 (100)	3	2	60
10^-6	1	3	2/4 (50)	1	5	17
10^-7	0	4	1/4 (25)	0	9	0

Karber equation:
-1-[((100+100+100+100+100+60+16.67)/100-0.5)*(log of dilution)] =
-5.266666667
Therefore, the $TCID_{50}$ end point is $10^{-5.27}$

Infectious particles=1.86*10^5 infectious particles/5mL = 3.72*10^4 infectious particles/mL

Table B-8 The titer of Ad41 of non-UV exposure negative control under 320 mJ/cm^2

A	B	C	D	E	F	G
virus dilution	No. affected	No. Unaffected	Affected ratio (100%)	Cumulative no. affected	Cumulative no. unaffected	Affected ratio (%)
10^-1	4	0	4/4 (100)	19	0	100
10^-2	4	0	4/4 (100)	15	0	100
10^-3	4	0	4/4 (100)	11	0	100
10^-4	3	1	4/4 (100)	7	1	87.5
10^-5	2	2	4/4 (100)	4	3	57
10^-6	2	2	2/4 (50)	2	5	29
10^-7	0	4	1/4 (25)	0	9	0

Karber equation:
-1-[((100+100+100+100+100+60+16.67)/100-0.5)*(log of dilution)] =
-5.232142857
Therefore, the $TCID_{50}$ end point is $10^{-5.23}$

Infectious particles=1.70*10^5 infectious particles/5mL = 3.40*10^4 infectious particles/mL

Table B-9 The titer of Ad41 under exposure of UV dose of 40 mJ/cm^2

A	B	C	D	E	F	G
virus dilution	No. affected	No. Unaffected	Affected ratio (100%)	Cumulative no. affected	Cumulative no. unaffected	Affected ratio (%)
10^-1	4	0	4/4 (100)	16	0	100
10^-2	4	0	4/4 (100)	12	0	100
10^-3	4	0	4/4 (100)	8	0	100
10^-4	0	4	4/4 (100)	4	4	50
10^-5	4	0	4/4 (100)	4	4	50
10^-6	0	4	2/4 (50)	0	8	0
10^-7	0	4	1/4 (25)	0	12	0

Karber equation:
-1-[((100+100+100+100+100+60+16.67)/100-0.5)*(log of dilution)] =
-4.5
Therefore, the $TCID_{50}$ end point is $10^{-4.5}$

Infectious particles=3.16*10^4 infectious particles/5mL = 6.32*10^3 infectious particles/mL

Table B-10 The titer of Ad41 under exposure of UV dose of 80 mJ/cm^2

A	B	C	D	E	F	G
virus dilution	No. affected	No. Unaffected	Affected ratio (100%)	Cumulative no. affected	Cumulative no. unaffected	Affected ratio (%)
10^-1	2	2	4/4 (100)	16	2	89
10^-2	4	0	4/4 (100)	14	2	88
10^-3	2	2	4/4 (100)	10	4	71
10^-4	2	2	4/4 (100)	8	6	57
10^-5	4	0	4/4 (100)	6	6	50
10^-6	2	2	2/4 (50)	2	8	20
10^-7	0	4	1/4 (25)	0	12	0

Karber equation:
-1-[((100+100+100+100+100+60+16.67)/100-0.5)*(log of dilution)]
-4.249603175
Therefore, the $TCID_{50}$ end point is $10^{-4.24}$

Infectious particles=$1.74*10^4$ infectious particles/5mL = $3.48*10^3$ infectious particles/mL

Table B-11 The titer of Ad41 under exposure of UV dose of 160 mJ/cm^2

A	B	C	D	E	F	G
virus dilution	No. affected	No. Unaffected	Affected ratio (100%)	Cumulative no. affected	Cumulative no. unaffected	Affected ratio (%)
10^-1	4	0	4/4 (100)	10	0	100
10^-2	3	1	4/4 (100)	6	1	86
10^-3	1	3	4/4 (100)	3	4	43
10^-4	1	3	4/4 (100)	2	7	22
10^-5	1	3	4/4 (100)	1	10	9
10^-6	0	4	2/4 (50)	0	14	0
10^-7	0	4	1/4 (25)	0	18	0

Karber equation:
-1-[((100+100+100+100+100+60+16.67)/100-0.5)*(log of dilution)]
-3.098845599
Therefore, the $TCID_{50}$ end point is $10^{-3.09}$

Infectious particles=$1.23*10^3$ infectious particles/5mL = $2.46*10^2$ infectious particles/mL

Table B-12 The titer of Ad41 under exposure of UV dose of 320 mJ/cm^2

A	B	C	D	E	F	G
virus dilution	No. affected	No. Unaffected	Affected ratio (100%)	Cumulative no. affected	Cumulative no. unaffected	Affected ratio (%)
10^-1	4	0	4/4 (100)	6	0	100
10^-2	1	3	4/4 (100)	2	3	40
10^-3	1	3	4/4 (100)	1	6	14
10^-4	0	4	4/4 (100)	0	10	0
10^-5	0	4	4/4 (100)	0	14	0
10^-6	0	4	2/4 (50)	0	18	0
10^-7	0	4	1/4 (25)	0	22	0

Karber equation:
-1-[((100+100+100+100+100+60+16.67)/100-0.5)*(log of dilution)] =
-2.042857143
Therefore, the $TCID_{50}$ end point is $10^{-2.04}$

Infectious particles=$1.09*10^2$ infectious particles/5mL = $2.19*10^1$ infectious particles/mL

Inactivation was analyzed by cell culture CPE based $TCID_{50}$, UV dose of 80 and 160 mJ/cm^2 non-UV exposure negative control samples were not analyzed, thus and average of those of UV dose of 40 and 320 mJ/cm^2 were derived. The inactivation of Ad41 was calculated with Eqn. (B1).

$$Inactivation = Log \frac{N_0}{N_t} \qquad \text{Eqn (6)}$$

Where N_0 = viral titer of negative control, N_t = viral titer of inactivated Ad41

Table B-13 Inactivation of Ad41 under UV dose of 40, 80, 160 and 320 mJ/cm^2

UV dose (mJ/cm^2)	TCID$_{50}$ infectious particles/mL
40 mJ/cm^2 non UV-exposure negative control	37200
80 mJ/cm^2 non UV-exposure negative control	35600
160 mJ/cm^2 non UV-exposure negative control	35600
320 mJ/cm^2 non UV-exposure negative control	34000
40 mJ/cm^2	6320
80 mJ/cm^2	3480
160 mJ/cm^2	246
320 mJ/cm^2	21.9
Inactivation	
UV dose (mJ/cm^2)	Log (N_0/N_t)
40	0.770
80	1.010
160	2.161
320	3.191

Table B-14 to Table B-19 show unpurified Ad41 titer under difference UV dose exposure in experiment 2 analyzed by cell culture CPE based TCID$_{50}$. Only 1 sample of three replicate UV exposure samples was randomly selected for each UV exposure. 1 mL Ad41 was infected onto HEK293 cells and incubated with 4 mL maintenance medium. The calculation procedure is described in Appendix C, 1.1. Only one non-UV exposure negative control was analyzed in this experiment.

Table B-14 The titer of Ad41 of non-UV exposure negative control

A	B	C	D	E	F	G
virus dilution	No. affected	No. Unaffected	Affected ratio (100%)	Cumulative no. affected	Cumulative no. unaffected	Affected ratio (%)
10^-1	4	0	4/4 (100)	23	0	100
10^-2	4	0	4/4 (100)	19	0	100
10^-3	4	0	4/4 (100)	15	0	100
10^-4	4	0	4/4 (100)	11	0	100
10^-5	4	0	4/4 (100)	7	0	100
10^-6	2	2	2/4 (50)	3	2	60
10^-7	1	3	1/4 (25)	1	5	17

Karber equation:
-1-[((100+100+100+100+100+60+16.67)/100-0.5)*(log of dilution)] =
-6.266666667
Therefore, the TCID$_{50}$ end point is $10^{-6.27}$

Infectious particles=1.86*10^6 infectious particles/5mL = 3.7*10^5 infectious particles/mL

Table B-15 The titer of Ad41 under exposure of UV dose of 40 mJ/cm^2

A	B	C	D	E	F	G
virus dilution	No. affected	No. Unaffected	Affected ratio (100%)	Cumulative no. affected	Cumulative no. unaffected	Affected ratio (%)
10^-1	4	0	4/4 (100)	21	0	100
10^-2	4	0	4/4 (100)	17	0	100
10^-3	4	0	4/4 (100)	13	0	100
10^-4	4	0	4/4 (100)	9	0	100
10^-5	3	1	4/4 (100)	5	1	83
10^-6	2	2	2/4 (50)	2	3	40
10^-7	0	4	1/4 (25)	0	7	0

Karber equation:
-1-[((100+100+100+100+100+60+16.67)/100-0.5)*(log of dilution)] =
-5.733333333
Therefore, the TCID$_{50}$ end point is $10^{-5.73}$

Infectious particles=$5.37*10^5$ infectious particles/5mL = $1.07*10^5$ infectious particles/mL

Table B-16 The titer of Ad41 under exposure of UV dose of 80 mJ/cm^2

A	B	C	D	E	F	G
virus dilution	No. affected	No. Unaffected	Affected ratio (100%)	Cumulative no. affected	Cumulative no. unaffected	Affected ratio (%)
10^-1	4	0	4/4 (100)	19	0	100
10^-2	4	0	4/4 (100)	15	0	100
10^-3	4	0	4/4 (100)	11	0	100
10^-4	4	0	4/4 (100)	7	0	100
10^-5	2	2	4/4 (100)	3	2	60
10^-6	1	3	2/4 (50)	1	5	17
10^-7	0	4	1/4 (25)	0	9	0

Karber equation:
-1-[((100+100+100+100+100+60+16.67)/100-0.5)*(log of dilution)] =
-5.266666667
Therefore, the TCID$_{50}$ end point is $10^{-5.27}$

Infectious particles=$1.86*10^5$ infectious particles/5mL = $3.7*10^4$ infectious particles/mL

Table B-17 The titer of Ad41 under exposure of UV dose of 160 mJ/cm^2

A	B	C	D	E	F	G
virus dilution	No. affected	No. Unaffected	Affected ratio (100%)	Cumulative no. affected	Cumulative no. unaffected	Affected ratio (%)
10^-1	4	0	4/4 (100)	16	0	100
10^-2	4	0	4/4 (100)	12	0	100
10^-3	3	1	4/4 (100)	8	1	89
10^-4	3	1	4/4 (100)	5	2	71
10^-5	1	3	4/4 (100)	2	5	29
10^-6	1	3	2/4 (50)	1	8	11
10^-7	0	4	1/4 (25)	0	12	0

Karber equation:
-1-[((100+100+100+100+100+60+16.67)/100-0.5)*(log of dilution)] =
-4.5
Therefore, the TCID$_{50}$ end point is $10^{-4.5}$

Infectious particles=$3.16*10^4$ infectious particles/5mL = $6.3*10^3$ infectious particles/mL

Table B-18 The titer of Ad41 under exposure of UV dose of 320 mJ/cm^2

A	B	C	D	E	F	G
virus dilution	No. affected	No. Unaffected	Affected ratio (100%)	Cumulative no. affected	Cumulative no. unaffected	Affected ratio (%)
10^-1	4	0	4/4 (100)	12	0	100
10^-2	4	0	4/4 (100)	8	0	100
10^-3	2	2	4/4 (100)	4	2	67
10^-4	1	3	4/4 (100)	2	5	29
10^-5	1	3	4/4 (100)	1	8	11
10^-6	0	4	2/4 (50)	0	12	0
10^-7	0	4	1/4 (25)	0	16	0

Karber equation:
-1-[((100+100+100+100+100+60+16.67)/100-0.5)*(log of dilution)] =
-3.563492063
Therefore, the TCID$_{50}$ end point is $10^{-3.56}$

Infectious particles=$3.16*10^3$ infectious particles/5mL = $7.3*10^2$ infectious particles/mL

Inactivation analyzed by cell culture CPE based TCID$_{50}$ of experiment 2 was calculated according to Eqn (B1).

Table B-19 Inactivation of Ad41 under UV dose of 40, 80, 160 and 320 mJ/cm^2

UV dose	TCID$_{50}$ Infectious particles/mL
40 mJ/cm^2 non UV-exposure negative control	370000
80 mJ/cm^2 non UV-exposure negative control	370000
160 mJ/cm^2 non UV-exposure negative control	370000
320 mJ/cm^2 non UV-exposure negative control	370000
40 mJ/cm^2	107000
80 mJ/cm^2	37000
160 mJ/cm^2	6300
320 mJ/cm^2	730
Inactivation	
UV dose (mJ/cm^2)	Log (N_0/N_t)
40	0.539
80	1.000
160	1.769
320	2.705

Table B-20 to Table B-26 show purified Ad41 titer under difference UV dose exposure in experiment 3 analyzed by cell culture CPE based TCID$_{50}$. 1 mL Ad41 was infected onto HEK293 cells and incubated with 4 mL maintenance medium. The calculation procedure is described in Appendix C, 1.1.

Table B-20 The titer of Ad41 of non-UV exposure negative control under 40 mJ/cm^2

A	B	C	D	E	F	G
virus dilution	No. affected	No. Unaffected	Affected ratio (100%)	Cumulative no. affected	Cumulative no. unaffected	Affected ratio (%)
10^-1	4	0	4/4 (100)	24	0	100
10^-2	4	0	4/4 (100)	20	0	100
10^-3	4	0	4/4 (100)	16	0	100
10^-4	4	0	4/4 (100)	12	0	100
10^-5	4	0	4/4 (100)	8	0	100
10^-6	3	1	2/4 (50)	4	1	80
10^-7	1	3	1/4 (25)	1	4	20

Karber equation:
-1-[((100+100+100+100+100+60+16.67)/100-0.5)*(log of dilution)] =
-6.5
Therefore, the $TCID_{50}$ end point is $10^{-6.5}$

Infectious particles=$3.16*10^6$ infectious particles/5mL = $6.32*10^5$ infectious particles/mL

Table B-21 The titer of Ad41 of non-UV exposure negative control under 320 mJ/cm^2

A	B	C	D	E	F	G
virus dilution	No. affected	No. Unaffected	Affected ratio (100%)	Cumulative no. affected	Cumulative no. unaffected	Affected ratio (%)
10^-1	4	0	4/4 (100)	22	0	100
10^-2	4	0	4/4 (100)	18	0	100
10^-3	4	0	4/4 (100)	14	0	100
10^-4	4	0	4/4 (100)	10	0	100
10^-5	4	0	4/4 (100)	6	0	100
10^-6	2	2	2/4 (50)	2	2	50
10^-7	0	4	1/4 (25)	0	6	0

Karber equation:
-1-[((100+100+100+100+100+60+16.67)/100-0.5)*(log of dilution)] =
-6
Therefore, the $TCID_{50}$ end point is 10^{-6}

Infectious particles=$1*10^6$ infectious particles/5mL = $2*10^5$ infectious particles/mL

Table B-22 The titer of Ad41 under exposure of UV dose of 40 mJ/cm^2

A	B	C	D	E	F	G
virus dilution	No. affected	No. Unaffected	Affected ratio (100%)	Cumulative no. affected	Cumulative no. unaffected	Affected ratio (%)
10^-1	4	0	4/4 (100)	20	0	100
10^-2	4	0	4/4 (100)	16	0	100
10^-3	4	0	4/4 (100)	12	0	100
10^-4	4	0	4/4 (100)	8	0	100
10^-5	4	0	4/4 (100)	4	0	100
10^-6	0	4	2/4 (50)	0	4	0
10^-7	0	4	1/4 (25)	0	8	0

Karber equation:
-1-[((100+100+100+100+100+60+16.67)/100-0.5)*(log of dilution)] =
-5.5
Therefore, the $TCID_{50}$ end point is $10^{-5.5}$

Infectious particles=$3.16*10^5$ infectious particles/5mL = $6.32*10^4$ infectious particles/mL

Table B-23 The titer of Ad41 under exposure of UV dose of 80 mJ/cm^2

A	B	C	D	E	F	G
virus dilution	No. affected	No. Unaffected	Affected ratio (100%)	Cumulative no. affected	Cumulative no. unaffected	Affected ratio (%)
10^-1	4	0	4/4 (100)	14	0	100
10^-2	4	0	4/4 (100)	10	0	100
10^-3	4	0	4/4 (100)	6	0	100
10^-4	2	2	4/4 (100)	2	2	50
10^-5	0	4	4/4 (100)	0	6	0
10^-6	0	4	2/4 (50)	0	10	0
10^-7	0	4	1/4 (25)	0	14	0

Karber equation:

-1-[((100+100+100+100+100+60+16.67)/100-0.5)*(log of dilution)] =

-4

Therefore, the $TCID_{50}$ end point is 10^{-4}

Infectious particles=$1*10^4$ infectious particles/5mL = $2*10^3$ infectious particles/mL

Table B-24 The titer of Ad41 under exposure of UV dose of 160 mJ/cm^2

A	B	C	D	E	F	G
virus dilution	No. affected	No. Unaffected	Affected ratio (100%)	Cumulative no. affected	Cumulative no. unaffected	Affected ratio (%)
10^-1	4	0	4/4 (100)	10	0	100
10^-2	4	0	4/4 (100)	6	0	100
10^-3	2	2	4/4 (100)	2	2	50
10^-4	0	4	4/4 (100)	0	6	0
10^-5	0	4	4/4 (100)	0	10	0
10^-6	0	4	2/4 (50)	0	14	0
10^-7	0	4	1/4 (25)	0	18	0

Karber equation:

-1-[((100+100+100+100+100+60+16.67)/100-0.5)*(log of dilution)] =

-3

Therefore, the 50% end point is 10^{-3}

Infectious particles=$1*10^3$ infectious particles/5mL = $2*10^2$ infectious particles/mL

Table B-25 The titer of Ad41 under exposure of UV dose of 320 mJ/cm^2

A	B	C	D	E	F	G
virus dilution	No. affected	No. Unaffected	Affected ratio (100%)	Cumulative no. affected	Cumulative no. unaffected	Affected ratio (%)
10^-1	2	2	4/4 (100)	6	2	75
10^-2	2	2	4/4 (100)	4	4	50
10^-3	2	2	4/4 (100)	2	6	25
10^-4	0	4	4/4 (100)	0	10	0
10^-5	0	4	4/4 (100)	0	14	0
10^-6	0	4	2/4 (50)	0	18	0
10^-7	0	4	1/4 (25)	0	22	0

Karber equation:

-1-[((100+100+100+100+100+60+16.67)/100-0.5)*(log of dilution)] =

-2

Therefore, the 50% end point is 10^{-2}

Infectious particles=$1*10^2$ infectious particles/5mL = $2*10^1$ infectious particles/mL

Inactivation was analyzed by cell culture CPE based TCID$_{50}$, UV dose of 80 and 160 mJ/cm^2 non-UV exposure negative control samples were not analyzed, thus and average of those of UV dose of 40 and 320 mJ/cm^2 were derived. The inactivation of Ad41 was calculated with Eqn. (B1).

Table B-26 Inactivation of Ad41 under UV dose of 40, 80, 160 and 320 mJ/cm^2

UV dose	TCID$_{50}$ Infectious particles/mL	
40 mJ/cm^2 non UV-exposure negative control	6320000	
80 mJ/cm^2 non UV-exposure negative control		4160000
160 mJ/cm^2 non UV-exposure negative control		4160000
320 mJ/cm^2 non UV-exposure negative control	2000000	
40 mJ/cm^2	632000	
80 mJ/cm^2	20000	
160 mJ/cm^2	2000	
320 mJ/cm^2	200	
Inactivation		
UV dose (mJ/cm^2)	Log (N_0/N_t)	
40	1.00	
80	2.318	
160	3.318	
320	4.00	

Table B-27 to Table B-32 show purified Ad41 titer under difference UV dose exposure in experiment 4 analyzed by cell culture CPE based TCID$_{50}$. Only 1 sample of three replicate UV exposure samples was randomly selected for each UV exposure. 1 mL Ad41 was infected onto HEK293 cells and incubated with 4 mL maintenance medium. The calculation procedure is described in Appendix C, 1.1. Only one non-UV exposure negative control was analyzed in this experiment.

Table B-27 The titer of Ad41 of non-UV exposure negative control

A	B	C	D	E	F	G
virus dilution	No. affected	No. Unaffected	Affected ratio (100%)	Cumulative no. affected	Cumulative no. unaffected	Affected ratio (%)
10^-1	4	0	4/4 (100)	23	0	100
10^-2	4	0	4/4 (100)	19	0	100
10^-3	4	0	4/4 (100)	15	0	100
10^-4	4	0	4/4 (100)	11	0	100
10^-5	3	1	4/4 (100)	7	1	88
10^-6	3	1	2/4 (50)	4	2	67
10^-7	1	3	1/4 (25)	1	5	17

Karber equation:

-1-[((100+100+100+100+100+60+16.67)/100-0.5)*(log of dilution)] =
-6.208333333

Therefore, the $TCID_{50}$ end point is $10^{-6.21}$

Infectious particles=$1.62*10^{6}$ infectious particles/5mL = $3.24*10^{5}$ infectious particles/mL

Table B-28 The titer of Ad41 under exposure of UV dose of 40 mJ/cm^2

A	B	C	D	E	F	G
virus dilution	No. affected	No. Unaffected	Affected ratio (100%)	Cumulative no. affected	Cumulative no. unaffected	Affected ratio (%)
10^-1	4	0	4/4 (100)	18	0	100
10^-2	4	0	4/4 (100)	14	0	100
10^-3	4	0	4/4 (100)	10	0	100
10^-4	3	1	4/4 (100)	6	1	86
10^-5	2	2	4/4 (100)	3	3	50
10^-6	1	3	2/4 (50)	1	6	14
10^-7	0	4	1/4 (25)	0	10	0

Karber equation:

-1-[((100+100+100+100+100+60+16.67)/100-0.5)*(log of dilution)] =
-5

Therefore, the $TCID_{50}$ end point is 10^{-5}

Infectious particles=$1.00*10^{5}$ infectious particles/5mL = $2.00*10^{4}$ infectious particles/mL

Table B-29 The titer of Ad41 under exposure of UV dose of 80 mJ/cm^2

A	B	C	D	E	F	G
virus dilution	No. affected	No. Unaffected	Affected ratio (100%)	Cumulative no. affected	Cumulative no. unaffected	Affected ratio (%)
10^-1	4	0	4/4 (100)	17	0	100
10^-2	4	0	4/4 (100)	13	0	100
10^-3	4	0	4/4 (100)	9	0	100
10^-4	2	2	4/4 (100)	5	2	71
10^-5	2	2	4/4 (100)	3	4	43
10^-6	1	3	2/4 (50)	1	7	13
10^-7	0	4	1/4 (25)	0	11	0

Karber equation:

-1-[((100+100+100+100+100+60+16.67)/100-0.5)*(log of dilution)] =
-4.767857143

Therefore, the 50% end point is $10^{-4.77}$

Infectious particles=$5.89*10^{4}$ infectious particles/5mL = $1.18*10^{4}$ infectious particles/mL

Table B-30 The titer of Ad41 under exposure of UV dose of 160 mJ/cm^2

A	B	C	D	E	F	G
virus dilution	No. affected	No. Unaffected	Affected ratio (100%)	Cumulative no. affected	Cunulative no. unaffected	Affected ratio (%)
10^-1	4	0	4/4 (100)	14	0	100
10^-2	4	0	4/4 (100)	10	0	100
10^-3	3	1	4/4 (100)	6	1	86
10^-4	2	2	4/4 (100)	3	3	50
10^-5	1	3	4/4 (100)	1	6	14
10^-6	0	4	2/4 (50)	0	10	0
10^-7	0	4	1/4 (25)	0	14	0

Karber equation:

-1-[((100+100+100+100+100+60+16.67)/100-0.5)*(log of dilution)] =

-4

Therefore, the $TCID_{50}$ end point is 10^{-4}

Infectious particles=$1.00*10^4$ infectious particles/5mL = $2.00*10^3$ infectious particles/mL

Table B-31 The titer of Ad41 under exposure of UV dose of 320 mJ/cm^2

A	B	C	D	E	F	G
virus dilution	No. affected	No. Unaffected	Affected ratio (100%)	Cumulative no. affected	Cunulative no. unaffected	Affected ratio (%)
10^-1	4	0	4/4 (100)	10	0	100
10^-2	4	0	4/4 (100)	6	0	100
10^-3	2	2	4/4 (100)	2	2	50
10^-4	0	4	4/4 (100)	0	6	0
10^-5	0	4	4/4 (100)	0	10	0
10^-6	0	4	2/4 (50)	0	14	0
10^-7	0	4	1/4 (25)	0	18	0

Karber equation:

-1-[((100+100+100+100+100+60+16.67)/100-0.5)*(log of dilution)] =

-3

Therefore, the 50% end point is 10^{-3}

Infectious particles=$1.00*10^3$ infectious particles/5mL = $2.00*10^2$ infectious particles/mL

Inactivation analyzed by cell culture CPE based $TCID_{50}$ of experiment 4 was calculated according to Eqn. (B1).

Table B-32 Inactivation of Ad41 under UV dose of 40, 80, 160 and 320 mJ/cm^2

UV dose	TCID$_{50}$ Infectious particles/mL
40 mJ/cm^2 non UV-exposure negative control	324000
80 mJ/cm^2 non UV-exposure negative control	324000
160 mJ/cm^2 non UV-exposure negative control	324000
320 mJ/cm^2 non UV-exposure negative control	324000
40 mJ/cm^2	20000
80 mJ/cm^2	11800
160 mJ/cm^2	2000
320 mJ/cm^2	200
Inactivation	
UV dose (mJ/cm^2)	Log (N_0/N_t)
40	1.21
80	1.44
160	2.21
320	3.21

Table B-33 to B-36 show the raw data of table 4.3 in the text.

Table B-33 Titration for the titer of Ad41 used in experiment 1

A	B	C	D	E	F	G
virus dilution	No. affected	No. Unaffected	Affected ratio (100%)	Cumulative no. affected	Cumulative no. unaffected	Affected ratio (%)
10^-1	4	0	4/4 (100)	19	0	100
10^-2	4	0	4/4 (100)	15	0	100
10^-3	4	0	4/4 (100)	11	0	100
10^-4	4	0	4/4 (100)	7	0	100
10^-5	2	2	4/4 (100)	3	2	60
10^-6	1	3	2/4 (50)	1	5	17
10^-7	0	4	1/4 (25)	0	9	0

Karber equation:
-1-[(((100+100+100+100+100+60+16.67)/100-0.5)*(log of dilution)] =
-5.266666667
Therefore, the TCID$_{50}$ end point is $10^{-5.27}$

Infectious particles=1.78*10^5 infectious particles/5mL = 3.56*10^4 infectious particles/mL

Table B-34 Titration for the titer of Ad41 used in experiment 2

A	B	C	D	E	F	G
Virus dilution	No. affected	No. Unaffected	Affected ratio (100%)	Cumulative no. affected	Cumulative no. unaffected	Affected ratio (%)
10^-1	4	0	4/4 (100)	19	0	100
10^-2	4	0	4/4 (100)	15	0	100
10^-3	4	0	4/4 (100)	11	0	100
10^-4	4	0	4/4 (100)	7	0	100
10^-5	2	2	4/4 (100)	3	2	60
10^-6	1	3	2/4 (50)	1	5	17
10^-7	0	4	1/4 (25)	0	9	0

Karber equation:
-1-[((100+100+100+100+100+60+16.67)/100-0.5)*(log of dilution)] =
-5.266666667
Therefore, the $TCID_{50}$ end point is $10^{-5.27}$

Infectious particles=9.30*10^5 infectious particles/5mL = 1.86*10^5 infectious particles/mL

Table B-35 Titration for the titer of Ad41 used in experiment 3

A	B	C	D	E	F	G
virus dilution	No. affected	No. Unaffected	Affected ratio (100%)	Cumulative no. affected	Cunulative no. unaffected	Affected ratio (%)
10^-1	4	0	4/4 (100)	24	0	100
10^-2	4	0	4/4 (100)	20	0	100
10^-3	4	0	4/4 (100)	16	0	100
10^-4	3	1	4/4 (100)	12	1	92
10^-5	3	1	4/4 (100)	9	2	82
10^-6	3	1	2/4 (50)	6	3	67
10^-7	3	1	1/4 (25)	3	4	43

Karber equation:
-1-[((100+100+100+100+100+60+16.67)/100-0.5)*(log of dilution)] =
-6.336496836
Therefore, the $TCID_{50}$ end point is $10^{-6.34}$

Infectious particles=2.10*10^6 infectious particles/5mL = 4.16*10^5 infectious particles/mL

Table B-36 Titration for the titer of Ad41 used in experiment 4

A	B	C	D	E	F	G
Virus dilution	No. affected	No. Unaffected	Affected ratio (100%)	Cumulative no. affected	Cumulative no. unaffected	Affected ratio (%)
10^-1	4	0	4/4 (100)	22	0	100
10^-2	4	0	4/4 (100)	18	0	100
10^-3	4	0	4/4 (100)	14	0	100
10^-4	3	1	4/4 (100)	10	1	91
10^-5	3	1	4/4 (100)	7	2	78
10^-6	3	1	2/4 (50)	4	3	57
10^-7	1	3	1/4 (25)	1	6	14

Karber equation:
-1-[((100+100+100+100+100+60+16.67)/100-0.5)*(log of dilution)] =
-5.901154401
Therefore, the $TCID_{50}$ end point is $10^{-5.9}$

Infectious particles=9.08*10^5 infectious particles/5mL = 1.62*10^5 infectious particles/mL

Table B-37 to table B-39 includes raw data for figure 4.4 in the text.

Table B-37 Threshold Ct results for UV inactivated unpurified and purified Ad41 analyzed by direct Taqman® RT-PCR and PCR

		Unpurified Ad41		Purified Ad41	
		Exp1	Exp2	Exp3	Exp4
40 mJ/cm^2 non-UV exposure negative control	RT-PCR (mRNA)	28.73	27.50	34.16	38.28
	PCR (DNA)		25.50	29.40	32.97
80 mJ/cm^2 non-UV exposure negative control	RT-PCR (mRNA)	28.12	27.14	33.81	36.14
	PCR (DNA)		26.15	29.19	29.12
160 mJ/cm^2 non-UV exposure negative control	RT-PCR (mRNA)	28.16	30.96	35.97	35.12
	PCR (DNA)		30.40	33.59	32.56
320 mJ/cm^2 non-UV exposure negative control	RT-PCR (mRNA)	29.27	29.13	35.13	36.40
	PCR (DNA)		27.42	29.85	34.17
40 mJ/cm^2	RT-PCR (mRNA)	27.01	27.29	34.50	42.95
	PCR (DNA)		27.23	29.42	33.36
80 mJ/cm^2	RT-PCR (mRNA)	30.47	28.52	35.72	36.36
	PCR (DNA)		27.10	33.32	31.39
160 mJ/cm^2	RT-PCR (mRNA)	28.91	31.25	35.94	38.35
	PCR (DNA)		27.44	32.64	32.75
320 mJ/cm^2	RT-PCR (mRNA)	31.02	27.46	35.32	35.14
	PCR (DNA)		27.41	33.05	31.00

The logarithm of viral copies were obtained by the standard curve (Figure 4.3). The titers were not converted to viral titer per mL. To obtain an inactivation, the unit of the viral titer was offset.

Table B-38 The logarithm of viral titer results for UV inactivated unpurified and purified Ad41 by direct Taqman® RT-PCR and PCR

		Unpurified Ad41		Purified Ad41	
		Exp1	Exp2	Exp3	Exp4
40 mJ/cm^2 non-UV exposure negative control	RT-PCR (mRNA)	4.38	4.75	2.76	1.54
	PCR (DNA)		5.34	4.18	3.12
80 mJ/cm^2 non-UV exposure negative control	RT-PCR (mRNA)	4.56	4.85	2.87	2.17
	PCR (DNA)		5.15	4.24	4.26
160 mJ/cm^2 non-UV exposure negative control	RT-PCR (mRNA)	4.55	3.72	2.22	2.48
	PCR (DNA)		3.88	2.93	3.24
320 mJ/cm^2 non-UV exposure negative control	RT-PCR (mRNA)	4.22	4.26	2.47	2.10
	PCR (DNA)		4.77	4.05	2.76
40 mJ/cm^2	RT-PCR (mRNA)	4.89	4.81	2.66	0.15
	PCR (DNA)		4.83	4.17	3.00
80 mJ/cm^2	RT-PCR (mRNA)	3.86	4.44	2.30	2.11
	PCR (DNA)		4.86	3.01	3.59
160 mJ/cm^2	RT-PCR (mRNA)	4.33	3.63	2.23	1.52
	PCR (DNA)		4.76	3.22	3.18
320 mJ/cm^2	RT-PCR (mRNA)	3.70	4.76	2.42	2.47
	PCR (DNA)		4.77	3.09	3.70

The inactivation was calculated with Eqn (B1). Because the viral titer was shown in logarithm format in table B-32, to calculate inactivation, the real titer should be converted.

Table B-39 Inactivation of unpurified and purified Ad41 analyzed by direct Taqman® RT-PCR and PCR

Exp	UV dose (mJ/cm^2)	Inactivation detected by RT-PCR	Inactivation detected by PCR
Exp1	40	-0.512	
	80	0.699	
	160	0.223	
	320	0.521	
Exp2	40	-0.063	0.515
	80	0.411	0.283
	160	0.086	-0.881
	320	-0.497	-0.003
Exp3	40	0.101	0.006
	80	0.568	1.229
	160	-0.009	-0.283
	320	0.057	0.952
Exp4	40	1.390	0.116
	80	0.065	0.676
	160	0.961	0.057
	320	-0.375	-0.943

Table B-40 to B-43 show the raw data of integrated cell culture Taqman® RT-PCR and PCR results. Table B-40 shows the Ct of non UV-exposure negative control samples. Based on the standard curve in figure 4.3 in the text, the logarithm of viral titer was calculated. This titer did not equal to the concentration of original cultured viral samples since it was been diluted before molecular test. However, because non UV-exposure negative control samples and UV inactivated samples were diluted with same fold, the absence of converting units would not affect inactivation. All UV exposure samples were analyzed by integrated cell culture Taqman® RT-PCR and PCR.

Table B-40 to table B-43 include the raw data of figure 4.5 and figure 4.6 in the text.

Table B-40 Threshold Ct results for UV inactivated unpurified and purified Ad41 analyzed by integrated cell culture Taqman® RT-PCR and PCR of experiment 1

	RT-PCR		PCR	
	log (viral copies/PCR)	Ct	log (viral copies/PCR)	Ct
40 mJ/cm^2 non UV-exposure negative control	5.47	25.06	5.61	24.60
80 mJ/cm^2 non UV-exposure negative control	5.72	24.23	4.90	26.98
160 mJ/cm^2 non UV-exposure negative control	5.78	24.02	5.13	26.21
320 mJ/cm^2 non UV-exposure negative control	5.94	23.47	5.34	25.50
40 mJ/cm^2	4.72	27.60	4.71	27.61
80 mJ/cm^2	4.64	27.85	3.83	30.57
160 mJ/cm^2	3.90	30.33	3.46	31.82
320 mJ/cm^2	2.83	33.93	3.27	32.45

Inactivation (Log N_0/N_t)

UV dose	RT-PCR	PCR
40 mJ/cm^2	0.76	0.90
80 mJ/cm^2	1.08	1.07
160 mJ/cm^2	1.88	1.67
320 mJ/cm^2	3.11	2.07

Table B-41 Threshold Ct results for UV inactivated unpurified and purified Ad41 analyzed by integrated cell culture Taqman® RT-PCR and PCR of experiment 2

	RT-PCR		PCR	
	log (viral copies/PCR)	Ct	log (viral copies/PCR)	Ct
40 mJ/cm^2 non UV-exposure negative control	5.08	26.38	5.25	21.80
	5.15	26.14	5.41	25.26
	5.32	25.56	5.41	25.25
80 mJ/cm^2 non UV-exposure negative control	5.25	25.80	6.57	21.37
	5.41	25.26	6.63	21.16
	5.42	25.25	6.58	21.33
160 mJ/cm^2 non UV-exposure negative control	5.28	25.69	6.63	21.17
	5.17	26.08	6.53	21.51
	5.38	25.36	6.73	20.82
320 mJ/cm^2 non UV-exposure negative control	5.35	25.46	6.95	20.10
	5.17	26.08	6.53	21.51
	4.89	27.02	6.66	21.07
40 mJ/cm^2	4.60	27.98	5.55	24.78
	4.59	28.01	5.82	23.88
	n/a	n/a	n/a	n/a
80 mJ/cm^2	4.42	28.58	5.56	24.76
	4.52	28.26	5.56	24.75
	4.22	29.28	5.51	24.93
160 mJ/cm^2	3.81	30.63	4.80	27.30
	3.35	32.20	4.94	26.83
	3.41	31.98	4.80	27.31
320 mJ/cm^2	1.86	37.19	4.59	28.01
	2.27	35.82	4.54	28.19
	2.05	36.54	4.56	28.12

Inactivation Log (N_0/N_t)	RT-PCR	PCR
40 mJ/cm^2	0.48	-0.30
	0.56	-0.41
80 mJ/cm^2	0.83	1.01
	0.89	1.07
	1.20	1.07
160 mJ/cm^2	1.47	1.82
	1.82	1.58
	1.97	1.93
320 mJ/cm^2	3.49	2.35
	2.90	1.99
	2.83	2.10

Table B-42 Threshold Ct results for UV inactivated unpurified and purified Ad41 analyzed by integrated cell culture Taqman® RT-PCR and PCR of experiment 3

	RT-PCR		PCR	
	log (viral copies/PCR)	Ct	log (viral copies/PCR)	Ct
40 mJ/cm^2 non UV-exposure negative control	6.91	20.21	7.53	18.14
80 mJ/cm^2 non UV-exposure negative control	6.89	20.30	7.51	18.20
160 mJ/cm^2 non UV-exposure negative control	6.82	20.53	7.57	18.01
320 mJ/cm^2 non-UV exposure negative control	7.12	19.51	7.59	17.93
40 mJ/cm^2	5.51	24.94	6.80	20.60
80 mJ/cm^2	5.45	25.13	7.21	19.21
160 mJ/cm^2	4.75	27.47	7.16	19.39
320 mJ/cm^2	4.89	27.00	6.68	21.01

Inactivation Log (N_0/N_t)		
UV dose	RT-PCR	PCR
40 mJ/cm^2	1.41	0.73
80 mJ/cm^2	1.44	0.30
160 mJ/cm^2	2.07	0.41
320 mJ/cm^2	2.23	0.92

Table B-43 Threshold Ct results for UV inactivated unpurified and purified Ad41 analyzed by integrated cell culture Taqman® RT-PCR and PCR of experiment 4

	RT-PCR		PCR	
	log (viral copies/PCR)	Ct	log (viral copies/PCR)	Ct
40 mJ/cm^2 non UV-exposure negative control	5.30	25.63	6.84	20.46
	5.36	25.42	7.19	19.28
	5.43	25.20	7.27	19.02
80 mJ/cm^2 non UV-exposure negative control	5.48	25.03	7.28	18.97
	5.45	25.12	7.32	18.86
	5.46	25.10	7.32	18.85
160 mJ/cm^2 non UV-exposure negative control	5.49	25.01	7.27	19.01
			7.27	19.02
	5.47	25.07	7.32	18.84
320 mJ/cm^2 non UV-exposure negative control	5.47	25.06	7.32	18.84
	5.52	24.91	7.27	19.02
	5.45	25.14	7.25	19.07
40 mJ/cm^2	4.03	29.90	7.02	19.85
	4.21	29.3	6.92	20.18
	4.19	29.38	7.01	19.89
80 mJ/cm^2	1.46	38.55	6.84	20.45
	3.77	30.78	6.80	20.6
	3.74	30.87	6.65	21.1
160 mJ/cm^2	2.94	33.55	6.34	22.13
	2.97	33.47	6.42	21.88
	2.90	33.71	6.42	21.88
320 mJ/cm^2	2.81	34	5.86	23.75
	1.59	38.09	5.88	23.68
			5.69	24.34

Inactivation Log (N_0/N_t)

UV dose	RT-PCR	PCR
40 mJ/cm^2	1.27	-0.18
	1.15	0.27
	1.24	0.26
80 mJ/cm^2	4.02	0.44
	1.68	0.52
	1.72	0.67
160 mJ/cm^2	2.54	0.93
		0.85
	2.57	0.90
300 mJ/cm^2	2.66	1.46
	3.92	1.39
		1.57

Appendix C

1.1 CPE based cell culture infectivity assay

Twenty one sterile 1.5 ml conical tubes were labeled with dilutions 10^{-1}, 10^{-2}, 10^{-3}, 10^{-4}, 10^{-5}, 10^{-6}, 10^{-7} (3 tubes of each dilution) and 0.9 ml of PBS was added into each tube. 0.1 mL of Ad41 suspension was pipetted into the first dilution tube and the tube contents were mixed well. With a fresh pipette, 0.1 ml of dilution 10^{-1} was transferred to tube of dilution 10^{-2} and mixed well. Serial dilution was continued through tube 7 with a fresh pipette for each transfer. It is important to discard pipettes between dilutions in order to avoid carrying viral particles on the pipettes to the next dilution. Thirty 25 cm^2 biocoat flasks were cultured with HEK293 cells until 60% confluence was achieved. Flasks were labeled with dilutions 10^{-1} through 10^{-7}. Quadruplicate flasks were prepared for each dilution. Growth medium was removed from each flask and 0.5 mL of each dilution of Ad41 suspension was added into the corresponding flask with clean pipettes. Two flasks of HEK293 cells were not inoculated with Ad41 suspension but were inoculated with PBS instead as negative control. The flasks were incubated at 37°C, 5% CO_2 for 1 hour and then 4 mL of maintenance medium were added without removing virus suspension. Flasks were incubated at 37°C, 5% CO_2 for 7 days to observe CPE. Maintenance medium was added up during intervals if necessary. The end point of the titration was the highest dilution showing evidence of viral infection in 50% of the cell cultures. This end point can be calculated with Karber equations.

Table C-1 $TCID_{50}$ endpoints determination factors

Column	Data
A	Virus dilution tested
B	Number of hosts affected (killed, paralyzed, showing CPE) by virus at each dilution
C	Number of hosts not affected by virus at each dilution
D	Ratio of affected hosts (%): Column B divided by the total of Column B + C (%)
E	Cumulative number of hosts affected. Calculated by adding numbers starting at the bottom of Column B and adding up
F	Cumulative number of hosts unaffected. Calculated by adding numbers

	starting at the top of Column C and adding down.
G	Cumulative ratio of affected hosts (%): number from Column E divided by the total of Column E + F. Calculate percentage.

For example:

Table C-2 Data for 50% infectivity end point determination

A	B	C	D	E	F	G
virus dilution	No. affected	No. Unaffected	Affected ratio (100%)	Cumulative no. affected	Cunulative no. unaffected	Affected ratio (%)
10^-1	4	0	4/4 (100)	19	0	100
10^-2	4	0	4/4 (100)	15	0	100
10^-3	4	0	4/4 (100)	11	0	100
10^-4	3	1	4/4 (100)	7	1	87.5
10^-5	2	2	4/4 (100)	4	3	57.14285714
10^-6	2	2	2/4 (50)	2	5	28.57142857
10^-7	0	4	1/4 (25)	0	9	0

Karber equation:

Negative logarithm of the 50% end point =

Negative logarithm of the highest virus concentration –

$$[(\frac{\text{Sum of \% affected at each dilution}}{100} - 0.5)\times(\text{log of dilution})] \qquad \text{Eqn. (C1)}$$

Using the data [illegible]om Table B-2, the 50% end point is calculated as follows using the

Karber equation:

$$-1-[(\frac{100+100+100+100+100+60+16.67}{100}-0.5)\times 1] = -5.23$$

Therefore the 50% end point is $10^{-5.23}$

The volume of the total medium is 5 mL, the viral concentration is $10^{5.23}/5 = 3.4\times10^{4}$ $TCID_{50}$ infectious particles/mL.

Raw data of ANOVA

Direct Taqman® RT-PCR

Table C-3 Data for ANOVA of direct Taqman® PCR to analyze UV inactivation of Ad41

A	B	C	D	E	F	G	H	I
UV dose (mJ/cm^2)	pu/un	real inactivation	estimate inactivation	Residuals	Residuals	I	P	n-score
40	1	0.101	0.518	-0.417	-0.794	1	0.03125	-1.86273
80	1	0.568	0.478	0.090	-0.613	2	0.09375	-1.31801
160	1	-0.009	0.398	-0.407	-0.499	3	0.15625	-1.00999
320	1	0.057	0.238	-0.181	-0.417	4	0.21875	-0.77642
40	-1	-0.512	0.282	-0.794	-0.413	5	0.28125	-0.57913
80	-1	0.699	0.242	0.457	-0.407	6	0.34375	-0.40225
160	-1	0.223	0.162	0.061	-0.345	7	0.40625	-0.2372
320	-1	0.521	0.002	0.519	-0.181	8	0.46875	-0.07841
40	1	1.390	0.518	0.872	-0.076	9	0.53125	0.078412
80	1	0.065	0.478	-0.413	0.061	10	0.59375	0.237202
160	1	0.961	0.398	0.563	0.090	11	0.65625	0.40225
320	1	-0.375	0.238	-0.613	0.169	12	0.71875	0.579132
40	-1	-0.063	0.282	-0.345	0.457	13	0.78125	0.776422
80	-1	0.411	0.242	0.169	0.519	14	0.84375	1.00999
160	-1	0.086	0.162	-0.076	0.563	15	0.90625	1.318011
320	-1	-0.497	0.002	-0.499	0.872	16	0.96875	1.862732

In Table C-3, column A represents UV dose; column B represents purification, -1 means unpurified, 1 means purified; column C shows real inactivation; column D shows estimated inactivation based on parameters generated in ANOVA shown in table C-4. $Y^{\wedge} = 0.439 - 0.0014 X_1 + 0.118X_2$, where X_1 is UV dose (number is column A), X_2 is purification (number in column B); column E represents residuals; column F is the increasing order of residuals; column I is the counting number in an increasing number; column H equals the number in column G subtracting 0.5 then divided by 16 which is the total number of samples; column I is the n-score, which is calculated using NORMSINV function in EXCEL.

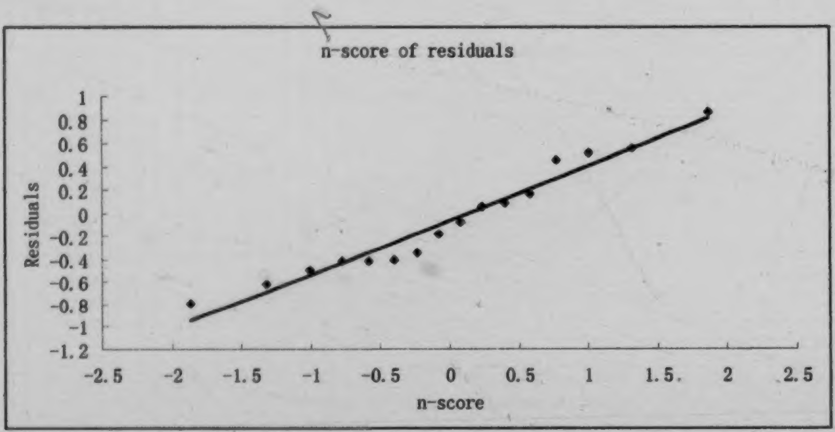

Figure C-1 n-score of residuals plot of ANOVA of Direct Taqman® RT-PCR

The curve in figure C-1 is linear, which indicated that the data was normally distributed. ANOVA can be used to analyze.

Table C-4 ANOVA of direct Taqman® RT-PCR to analyze UV inactivation of unpurified and purified Ad41

ANOVA

	df	SS	MS	F	Significance F
Regression	2	0.59171367	0.295856835	1.123787	0.354672007
Residual	13	3.422480256	0.263267712		
Total	15	4.014193926			

	Coefficients	Standard Error	t Stat	P-value	Lower 95%	Upper 95%	Lower 95.0%	Upper 95.0%	
Intercept	0.4390204	0.220561317	1.990468913	0.0679901	-0.03747331	0.9155142	-0.03747331	0.9155142	
UV dose	-0.0014151	0.001196162	-1.18307289	0.2579651	-0.0039993	0.001169	-0.0039993	0.001169	nsig
Purification	0.1181176	0.12827405	0.920821937	0.3739157	-0.15900168	0.3952368	-0.15900168	0.3952368	nsig

The upper 95% and lower 95% of UV dose fell between zero, p-value of UV dose which was 0.26 was lager than 0.05, which indicated that the parameter of UV dose did not have significant effect on direct Taqman® RT-PCR method in analysis of UV inactivation of Ad41. Similarly, the upper 95% and lower 95% of purification fell between zero, p-value of purification which was 0.37 was larger than 0.05, which indicated that the parameter of purification did not have significant effect on direct Taqman® RT-PCR method in analysis of UV inactivation of Ad41.

Direct Taqman® PCR

Table C-5 ANOVA of direct Taqman® PCR to analyze UV inactivation of unpurified and purified Ad41

A	B	C	D	E	F	G	H	I
UV dose (mJ/cm^2)	pu/un	real inactivation	estimate inactivation	Residuals	Residuals	I	P	n-score
40	1	0.006	0.412	-0.406	-0.879	1	0.04166667	-1.73166
80	1	1.229	0.344	0.885	-0.841	2	0.125	-1.15035
160	1	-0.283	0.208	-0.491	-0.491	3	0.20833333	-0.81222
320	1	0.952	-0.064	1.016	-0.406	4	0.29166667	-0.54852
40	-1	0.515	0.164	0.351	-0.296	5	0.375	-0.31864
80	-1	0.283	0.096	0.187	-0.151	6	0.45833333	-0.10463
160	-1	-0.881	-0.04	-0.841	0.187	7	0.54166667	0.104633
320	-1	-0.003	-0.312	0.309	0.309	8	0.625	0.318639
40	1	0.116	0.412	-0.296	0.332	9	0.70833333	0.548522
80	1	0.676	0.344	0.332	0.351	10	0.79166667	0.812218
160	1	0.057	0.208	-0.151	0.885	11	0.875	1.150349
320	1	-0.943	-0.064	-0.879	1.016	12	0.95833333	1.731664

The plotting for n-score residuals figure was same as that described for table C-3.

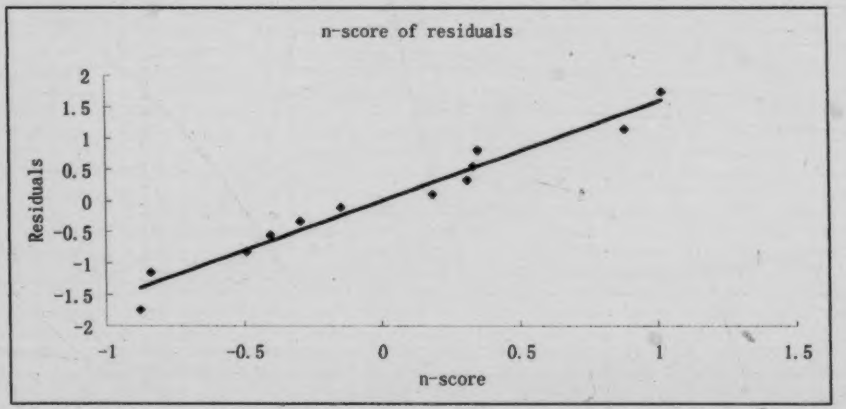

Figure C-2 n-score of residuals plot of ANOVA Direct Taqman® PCR

The curve in figure C-2 is linear, which indicated that the data was normally distributed. ANOVA can be used to analyze.

Table C-6 ANOVA of direct Taqman® PCR to analyze UV inactivation of unpurified and purified Ad41

ANOVA

	df	SS	MS	F	Significance F
Regression	2	0.557926848	0.278963424	0.6010984	0.568813163
Residual	9	4.176804675	0.464089406		
Total	11	4.734731523			

	Coefficients	Standard Error	t Stat	P-value	Lower 95%	Upper 95%	Lower 95.0%	Upper 95.0%	
Intercept	0.3558327	0.345217516	1.030749223	0.3295614	-0.42510359	1.136769	-0.42510359	1.13676896	
UV dose	-0.0016902	0.001833839	-0.92165885	0.3807493	-0.00583861	0.0024583	-0.00583861	0.00245826	nsig
Purification	0.1238839	0.20858663	0.593920755	0.5671914	-0.34797181	0.5957397	-0.34797181	0.59573967	nsig

The upper 95% and lower 95% of UV dose fell between zero, p-value of UV dose which was 0.38 was lager than 0.05, which indicated that the parameter of UV dose did not have a significant effect on direct Taqman® PCR method in analysis of UV inactivation of Ad41. Similarly, the upper 95% and lower 95% of purification fell between zero, p-value of purification which was 0.57 was larger than 0.05, which indicated that the parameter of purification did not have a significant effect on direct Taqman® PCR method in analysis of UV inactivation of Ad41.

Cell culture integrated Taqman® RT-PCR

Table C-7 Data for ANOVA of integrated cell culture Taqman® RT-PCR to analyze UV inactivation of unpurified and purified Ad41

UV dose (mJ/cm²)	pu/un	Real inactivation	Estimated inactivation	Residuals	Residuals	I	P	n-score
40	-1	0.756	0.806	-0.050	-1.114	1	0.017857143	-2.1001655
80	-1	1.077	1.109	-0.032	-0.683	2	0.053571429	-1.6111692
160	-1	1.878	1.715	0.163	-0.330	3	0.089285714	-1.3451666
320	-1	3.113	2.926	0.188	-0.282	4	0.125	-1.1503494
40	-1	0.476	0.806	-0.330	-0.250	5	0.160714286	-0.9915265
80	-1	0.827	1.109	-0.282	-0.244	6	0.196428571	-0.8544474
160	-1	1.470	1.715	-0.244	-0.216	7	0.232142857	-0.7318081
320	-1	3.491	2.926	0.566	-0.092	8	0.267857143	-0.6193058
40	-1	0.557	0.806	-0.250	-0.090	9	0.303571429	-0.5141561
80	-1	0.893	1.109	-0.216	-0.070	10	0.339285714	-0.4144133
160	-1	1.821	1.715	0.107	-0.067	11	0.375	-0.3186394
320	-1	3.054	2.926	0.128	-0.050	12	0.410714286	-0.225708
80	-1	1.199	1.109	0.090	-0.032	13	0.446428571	-0.1346898
160	-1	1.970	1.715	0.256	0.020	14	0.482142857	-0.0447762
320	-1	2.833	2.926	-0.092	0.046	15	0.517857143	0.04477618
40	1	1.408	1.224	0.183	0.090	16	0.553571429	0.13468979
80	1	1.438	1.527	-0.090	0.107	17	0.589285714	0.22570795
160	1	2.065	2.133	-0.067	0.128	18	0.625	0.31863936
320	1	2.229	3.344	-1.114	0.157	19	0.660714286	0.41441333
40	1	1.271	1.224	0.046	0.163	20	0.696428571	0.5141561
160	1	2.542	2.133	0.409	0.183	21	0.732142857	0.61930677
320	1	2.661	3.344	-0.683	0.188	22	0.767857143	0.73180808
40	1	1.155	1.224	-0.070	0.190	23	0.803571429	0.8544474
80	1	1.685	1.527	0.157	0.256	24	0.839285714	0.99152647
320	1	3.923	3.344	0.579	0.409	25	0.875	1.15034938
40	1	1.244	1.224	0.020	0.439	26	0.910714286	1.34516663
80	1	1.717	1.527	0.190	0.566	27	0.946428571	1.61116916
160	1	2.571	2.133	0.439	0.579	28	0.982142857	2.10016549

The plotting for n-score residuals figure was same as that described for table C-3.

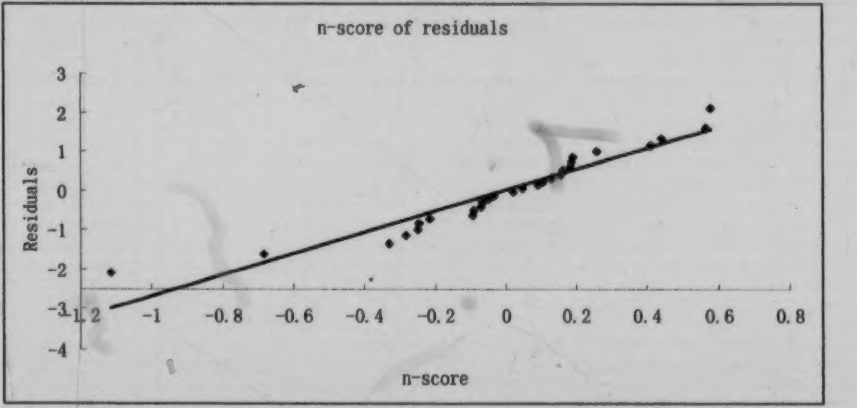

Figure C-3 n-score of residuals Cell culture integrated Taqman® RT-PCR

The curve in figure C-3 is linear, which indicated that the data was normally distributed. ANOVA can be used to analyze.

Table C-8 ANOVA of integrated cell culture Taqman® RT-PCR to analyze UV inactivation of unpurified and purified Ad41

ANOVA

	df	SS	MS	F	nificance F
Regressic	2	18.9642702	9.482135	70.33875	5.41E-11
Residual	25	3.37016753	0.134807		
Total	27	22.3344377			

	Coefficient	standard Errc	t Stat	P-value	Lower 95%	Upper 95%	ower 95.	Upper 95.0%	
Intercept	0.71271226	0.11932703	5.972764	3.09E-06	0.466954	0.958471	0.466954	0.958471	
UV dose	0.0075682	0.00064879	11.66515	1.31E-11	0.006232	0.008904	0.006232	0.008904	Sig
Purificat	0.20899865	0.06975291	2.996272	0.006093	0.06534	0.352657	0.06534	0.352657	Sig

The upper 95% and lower 95% of UV dose fell at one side of zero, p-value of UV dose which was $1.31*10^{-11}$ was much smaller than 0.05, which indicated that the parameter of UV dose had a significant effect on integrated cell culture Taqman® RT-PCR method in analysis of UV inactivation of Ad41. Similarly, the upper 95% and lower 95% of purification fell at one side of zero, p-value of purification which was 0.006 was smaller than 0.05, which indicated that the parameter of purification had a significant effect on integrated cell culture Taqman® RT-PCR method in analysis of UV inactivation of Ad41.

Cell culture integrated Taqman® PCR

Table C-9 Data for ANOVA of integrated cell culture Taqman® RT-PCR to analyze UV inactivation of unpurified and purified Ad41

UV dose (mJ/cm^2)	pu/un	Real inactivation	Estimated inactivation	Residuals	Residuals	I	P	n-score
40	-1	0.896	0.806	0.089	-2.427	1	0.0166667	-2.128045
80	-1	1.068	1.109	-0.041	-1.957	2	0.05	-1.644854
160	-1	1.670	1.715	-0.045	-1.882	3	0.0833333	-1.382994
320	-1	2.068	2.926	-0.857	-1.775	4	0.1166667	-1.191816
40	-1	-0.304	0.806	-1.110	-1.722	5	0.15	-1.036433
80	-1	1.009	1.109	-0.100	-1.281	6	0.1833333	-0.902735
160	-1	1.824	1.715	0.110	-1.228	7	0.2166667	-0.7835
320	-1	2.354	2.926	-0.571	-1.227	8	0.25	-0.67449
40	-1	-0.411	0.806	-1.217	-1.217	9	0.2833333	-0.572968
80	-1	1.068	1.109	-0.041	-1.204	10	0.3166667	-0.47704
160	-1	1.583	1.715	-0.131	-1.110	11	0.35	-0.38532
320	-1	2.098	2.926	-0.827	-1.087	12	0.3833333	-0.296738
80	-1	1.071	1.109	-0.038	-1.009	13	0.4166667	-0.210428
160	-1	1.932	1.715	0.217	-0.966	14	0.45	-0.125661
320	-1	2.098	2.926	-0.827	-0.957	15	0.4833333	-0.041789
40	1	0.732	1.224	-0.492	-0.858	16	0.5166667	0.0417893
80	1	0.301	1.527	-1.227	-0.857	17	0.55	0.1256613
160	1	0.411	2.133	-1.722	-0.827	18	0.5833333	0.2104284
320	1	0.917	3.344	-2.427	-0.827	19	0.6166667	0.2967378
80	1	0.440	1.527	-1.087	-0.571	20	0.65	0.3853205
160	1	0.929	2.133	-1.204	-0.492	21	0.6833333	0.4770404
320	1	1.461	3.344	-1.882	-0.131	22	0.7166667	0.5729675
40	1	0.268	1.224	-0.957	-0.100	23	0.75	0.6744898
80	1	0.518	1.527	-1.009	-0.045	24	0.7833333	0.7835004
160	1	0.851	2.133	-1.281	-0.041	25	0.8166667	0.9027348
320	1	1.387	3.344	-1.957	-0.041	26	0.85	1.0364334
40	1	0.259	1.224	-0.966	-0.038	27	0.8833333	1.1918162
80	1	0.670	1.527	-0.858	0.089	28	0.9166667	1.3829941
160	1	0.905	2.133	-1.228	0.110	29	0.95	1.6448536
320	1	1.568	3.344	-1.775	0.217	30	0.9833333	2.1280452

The plotting for n-score residuals figure was same as that described for table C-3.

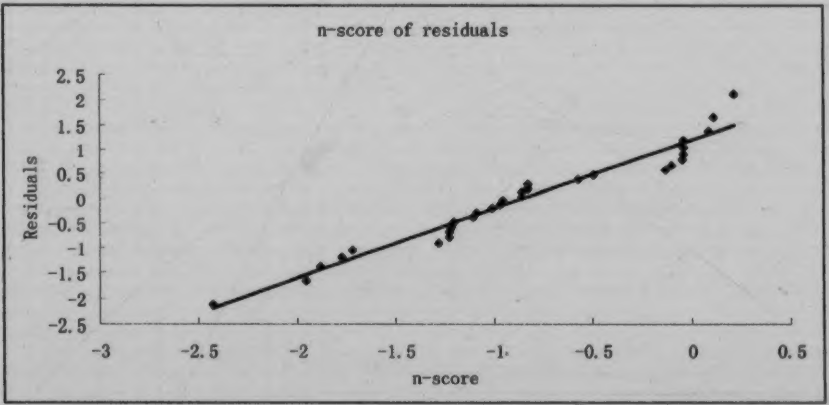

Figure C-4 n-score of residuals Cell culture integrated Taqman® PCR

Table C-10 ANOVA of integrated cell culture Taqman® PCR to analyze UV inactivation of unpurified and purified Ad41

ANOVA

	df	SS	MS	F	ignificance F
Regression	2	10. 33619497	5. 16809749	31. 77654	8. 03927E-08
Residual	27	4. 391246321	0. 16263875		
Total	29	14. 72744129			

	Coefficienitandard Erro		t Stat	P-value	Lower 95%	Upper 95%	Lower 95. 0%	Upper 95. 0%	
Intercept	0. 29502	0. 131097584	2. 25038673	0. 032775	0. 026030242	0. 56401	0. 02603024	0. 56401028	
UV dose (mJ/	0. 004829	0. 000689415	7. 00408005	1. 58E-07	0. 003414153	0. 006243	0. 00341415	0. 00624328	Sig
pu/un	-0. 28033	0. 073629422	-3. 8073548	0. 000735	-0. 43140843	-0. 12926	-0. 4314084	-0. 1292582	Sig

The upper 95% and lower 95% of UV dose fell at one side of zero, p-value of UV dose which was $1.58*10^{-7}$ was much smaller than 0.05, which indicated that the parameter of UV dose had a significant effect on integrated cell culture Taqman® PCR method in analysis of UV inactivation of Ad41. Similarly, the upper 95% and lower 95% of purification fell at one side of zero, p-value of purification which was 0.0007 was smaller than 0.05, which indicated that the parameter of purification had a significant effect on integrated cell culture Taqman® PCR method in analysis of UV inactivation of Ad41.

Cell culture CPE based TCID$_{50}$ and integrated cell culture Taqman® PCR in detection of UV inactivated purified and unpurified Ad41

Table C-11 Data for ANOVA of integrated cell culture Taqman® PCR and cell culture CPE based TCID$_{50}$ to analyze UV inactivation of unpurified and purified Ad41

UV dose (ml/cm^2)	Purification	method	real inactivation	estimate inactivation	Residuals	Residuals	I	P	n-score
40	-1	1	0.896	0.555	0.341	-1.016	1	0.011364	-2.27799
80	-1	1	1.068	0.781	0.288	-0.932	2	0.034091	-1.8238
160	-1	1	1.670	1.232	0.437	-0.702	3	0.056818	-1.58206
320	-1	1	2.068	2.136	-0.067	-0.698	4	0.079545	-1.40814
80	-1	1	1.009	0.781	0.228	-0.688	5	0.102273	-1.26871
160	-1	1	1.824	1.232	0.592	-0.618	6	0.125	-1.15035
320	-1	1	2.354	2.136	0.218	-0.545	7	0.147727	-1.04623
80	-1	1	1.068	0.781	0.288	-0.471	8	0.170455	-0.95237
160	-1	1	1.583	1.232	0.351	-0.379	9	0.193182	-0.86623
320	-1	1	2.098	2.136	-0.037	-0.364	10	0.215909	-0.78608
80	-1	1	1.071	0.781	0.291	-0.343	11	0.238636	-0.7107
160	-1	1	1.932	1.232	0.699	-0.277	12	0.261364	-0.63915
320	-1	1	2.098	2.136	-0.037	-0.268	13	0.284091	-0.57073
40	1	1	0.732	0.351	0.381	-0.178	14	0.306818	-0.50489
80	1	1	0.301	0.577	-0.277	-0.137	15	0.329545	-0.44117
160	1	1	0.411	1.029	-0.618	-0.124	16	0.352273	-0.37919
320	1	1	0.917	1.932	-1.016	-0.100	17	0.375	-0.31864
80	1	1	0.440	0.577	-0.137	-0.092	18	0.397727	-0.25923
160	1	1	0.929	1.029	-0.100	-0.084	19	0.420455	-0.20073
320	1	1	1.461	1.932	-0.471	-0.067	20	0.443182	-0.14291
40	1	1	0.268	0.351	-0.084	-0.059	21	0.465909	-0.08556
80	1	1	0.518	0.577	-0.059	-0.058	22	0.488636	-0.02849
160	1	1	0.851	1.029	-0.178	-0.054	23	0.511364	0.028488
320	1	1	1.387	1.932	-0.545	-0.037	24	0.534091	0.085558
40	1	1	0.259	0.351	-0.092	-0.037	25	0.556818	0.142907
80	1	1	0.670	0.577	0.092	0.011	26	0.579545	0.200731
160	1	1	0.905	1.029	-0.124	0.092	27	0.602273	0.259234
320	1	1	1.568	1.932	-0.364	0.138	28	0.625	0.318639
40	-1	-1	0.770	1.472	-0.702	0.218	29	0.647727	0.379192
80	-1	-1	1.010	1.698	-0.688	0.228	30	0.670455	0.441169
160	-1	-1	2.161	2.149	0.011	0.264	31	0.693182	0.50489
320	-1	-1	3.191	3.053	0.138	0.288	32	0.715909	0.570731
40	-1	-1	0.540	1.472	-0.932	0.288	33	0.738636	0.639147
80	-1	-1	1.000	1.698	-0.698	0.291	34	0.761364	0.710696
160	-1	-1	1.770	2.149	-0.379	0.341	35	0.784091	0.786084
320	-1	-1	2.710	3.053	-0.343	0.351	36	0.806818	0.866231
40	1	-1	1.000	1.268	-0.268	0.361	37	0.829545	0.952371
80	1	-1	2.318	1.494	0.824	0.381	38	0.852273	1.046231
160	1	-1	3.318	1.946	1.372	0.437	39	0.875	1.150349
320	1	-1	4.000	2.849	1.151	0.592	40	0.897727	1.268707
40	1	-1	1.210	1.268	-0.058	0.699	41	0.920455	1.408136
80	1	-1	1.440	1.494	-0.054	0.824	42	0.943182	1.582058
160	1	-1	2.210	1.946	0.264	1.151	43	0.965909	1.823803
320	1	-1	3.210	2.849	0.361	1.372	44	0.988636	2.277988

For purification column, 1 represents with purification, -1 represents without purification; for method column, 1 represents integrated cell culture Taqman® PCR, -1 represents cell culture CPE based TCID$_{50}$. The plotting for n-score residuals figure was same as that described for table C-3.

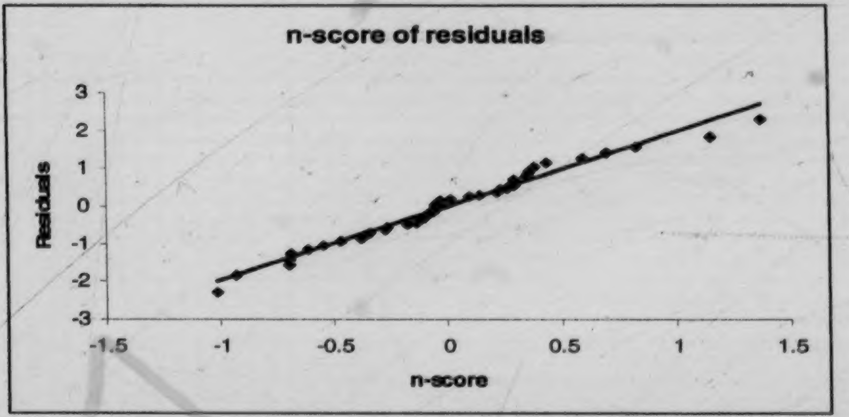

Figure C-5 n-score of residuals Cell culture CPE based $TCID_{50}$ and integrated cell culture Taqman® PCR in detection of UV inactivated purified and unpurified Ad41

Table C-12 ANOVA of integrated cell culture Taqman® PCR and cell culture CPE based $TCID_{50}$ to analyze UV inactivation of unpurified and purified Ad41

ANOVA

	df	SS	MS	F	gnificance F
Regression	3	23.68174851	7.893916	29.28285	3.48E-10
Residual	40	10.78298869	0.269575		
Total	43	34.4647372			

	Coefficien	Standard Error	t Stat	P-value	Lower 95%	Upper 95%	ower 95.0	Upper 95.0
Intercept	0.685752	0.142218432	4.82182	2.09E-05	0.398317	0.973186	0.398317	0.973186
UV dose	0.005646	0.000737785	7.652373	2.35E-09	0.004155	0.007137	0.004155	0.007137
Purificati	-0.10174	0.078514615	-1.29575	0.202488	-0.26042	0.056948	-0.26042	0.056948
method	-0.45846	0.081622547	-5.61687	1.63E-06	-0.62343	-0.2935	-0.62343	-0.2935

The upper 95% and lower 95% of UV dose fell at one side of zero, p-value of UV dose which was $2.35*10^{-9}$ was much smaller than 0.05, which indicated that the parameter of UV dose had a significant effect on UV inactivation of Ad41. The upper 95% and lower 95% of purification fell at two sides of zero, p-value of purification which was 0.202 was greater than 0.05, which indicated that the parameter of purification did not have a significant effect on UV inactivation of Ad41. In addition, the upper 95% and lower 95% of method fell at one side of zero, p-value of UV dose which was $1.63*10^{-6}$ was much smaller than 0.05, which indicated that the parameter of method had a significant effect on UV inactivation of Ad41.

Cell culture CPE based TCID$_{50}$ and integrated cell culture real-time quantitative RT-PCR in detection of UV inactivated purified and unpurified Ad41

Table C-13 Data for ANOVA of integrated cell culture Taqman® RT-PCR and cell culture CPE based TCID$_{50}$ to analyze UV inactivation of unpurified and purified Ad41

UV	Purification	method	Real inactivation	Estimated inactivation	Residuals	Residuals	I	P	n-score
40	-1	-1	0.770	0.865	-0.095	-0.480	1	0.0114	-2.27799
80	-1	-1	1.010	0.446	0.564	-0.095	2	0.0341	-1.8238
160	-1	-1	2.161	1.329	0.832	-0.048	3	0.0568	-1.58206
320	-1	-1	3.191	2.257	0.934	0.355	4	0.0795	-1.40814
40	-1	-1	0.540	0.124	0.416	0.362	5	0.1023	-1.26871
80	-1	-1	1.000	0.438	0.562	0.384	6	0.1250	-1.15035
160	-1	-1	1.770	1.068	0.702	0.416	7	0.1477	-1.04623
320	-1	-1	2.710	2.326	0.384	0.480	8	0.1705	-0.95237
40	-1	1	0.756	-0.016	0.772	0.492	9	0.1932	-0.86623
80	-1	1	1.077	0.299	0.779	0.529	10	0.2159	-0.78608
160	-1	1	1.878	0.928	0.950	0.542	11	0.2386	-0.7107
320	-1	1	3.113	2.187	0.926	0.562	12	0.2614	-0.63915
40	-1	1	0.476	-0.016	0.492	0.564	13	0.2841	-0.57073
80	-1	1	0.827	0.299	0.529	0.565	14	0.3068	-0.50489
160	-1	1	1.470	0.928	0.542	0.572	15	0.3295	-0.44117
320	-1	1	3.491	2.187	1.304	0.594	16	0.3523	-0.37919
40	-1	1	0.557	-0.016	0.572	0.615	17	0.3750	-0.31864
80	-1	1	0.893	0.299	0.594	0.617	18	0.3977	-0.25923
160	-1	1	1.821	0.928	0.893	0.621	19	0.4205	-0.20073
320	-1	1	3.054	2.187	0.867	0.646	20	0.4432	-0.14291
80	-1	1	1.199	0.299	0.901	0.649	21	0.4659	-0.08556
160	-1	1	1.970	0.928	1.042	0.702	22	0.4886	-0.02849
320	-1	1	2.833	2.187	0.646	0.738	23	0.5114	0.028488
40	1	-1	1.000	0.645	0.355	0.765	24	0.5341	0.085558
80	1	-1	2.318	0.960	1.358	0.772	25	0.5568	0.142907
160	1	-1	3.318	1.589	1.729	0.779	26	0.5795	0.200731
320	1	-1	4.000	2.848	1.152	0.832	27	0.6023	0.259234
40	1	-1	1.210	0.645	0.565	0.864	28	0.6250	0.318639
80	1	-1	1.440	0.960	0.480	0.867	29	0.6477	0.379192
160	1	-1	2.210	1.589	0.621	0.893	30	0.6705	0.441169
320	1	-1	3.210	2.848	0.362	0.897	31	0.6932	0.50489
40	1	1	1.408	0.506	0.902	0.901	32	0.7159	0.570731
80	1	1	1.438	0.821	0.617	0.902	33	0.7386	0.639147
160	1	1	2.065	1.450	0.615	0.926	34	0.7614	0.710696
320	1	1	2.229	2.709	-0.480	0.934	35	0.7841	0.786084
40	1	1	1.271	0.506	0.765	0.950	36	0.8068	0.866231
160	1	1	2.542	1.450	1.092	1.042	37	0.8295	0.952371
320	1	1	2.661	2.709	-0.048	1.092	38	0.8523	1.046231
40	1	1	1.155	0.506	0.649	1.121	39	0.8750	1.150349
80	1	1	1.685	0.821	0.864	1.152	40	0.8977	1.268707
320	1	1	3.923	2.709	1.214	1.214	41	0.9205	1.408136
40	1	1	1.244	0.506	0.738	1.304	42	0.9432	1.582058
80	1	1	1.717	0.821	0.897	1.358	43	0.9659	1.823803
160	1	1	2.571	1.450	1.121	1.729	44	0.9886	2.277968

For purification column, 1 represents with purification, -1 represents without purification; for method column, 1 represents integrated cell culture Taqman® RT-PCR, -1 represents cell culture CPE based TCID$_{50}$. The plotting for n-score residuals figure was same as that described for table C-3.

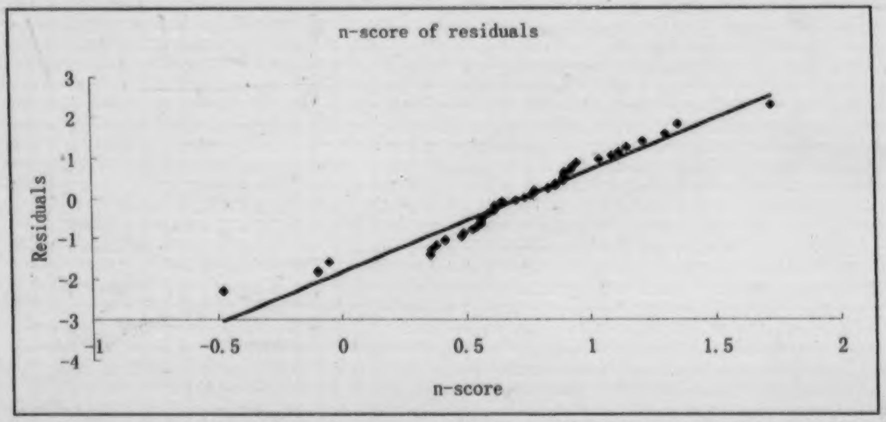

Figure C-6 n-score of residuals Cell culture CPE based $TCID_{50}$ and integrated cell culture real-time quantitative RT-PCR in detection of UV inactivated purified and unpurified Ad41

Table C-14 ANOVA of integrated cell culture Taqman® RT-PCR and cell culture CPE based $TCID_{50}$ to analyze UV inactivation of unpurified and purified Ad41

ANOVA

	df	*SS*	*MS*	*F*	*ignificance F*
Regression	3	33.6562029	11.2187343	76.80986	1.2E-16
Residual	40	5.84234047	0.14605851		
Total	43	39.4985433			

	Coefficients	*Standard Erroi*	*t Stat*	*P-value*	*Lower 95%*	*Upper 95%*	*.ower 95.0%*	*Jpper 95.0%*	
Intercept	0.7412573	0.10041842	7.38168631	5.55E-09	0.538304	0.944211	0.538304	0.944211	
UV dose	0.0078674	0.00053785	14.627474	1.2E-17	0.00678	0.008954	0.00678	0.008954	
Purification	0.260911	0.057772	4.51621886	5.45E-05	0.144149	0.377673	0.144149	0.377673	
method	-0.069717	0.05992091	-1.16349085	0.251524	-0.19082	0.051387	-0.19082	0.051387	nsig

The upper 95% and lower 95% of UV dose fell at one side of zero, p-value of UV dose which was $1.2*10^{-17}$ was much smaller than 0.05, which indicated that the parameter of UV dose had a significant effect on UV inactivation of Ad41. Similarly, the upper 95% and lower 95% of purification fell at one side of zero, p-value of purification which was $5.45*10^{-5}$ was smaller than 0.05, which indicated that the parameter of purification had a significant effect on UV inactivation of Ad41. In addition, the upper 95% and lower 95% of method fell at two sides of zero, p-value of UV dose which was 0.25 was greater than 0.05, which indicated that the parameter of method did not have a significant effect on UV inactivation of Ad41.